Isopedopeptins A-H: Cationic Cyclic Lipodepsipeptides from *Pedobacter cryoconitis* UP508 targeting WHO top-priority carbapenem-resistant bacteria

Christina Nord,[†] Joakim Bjerketorp,[†,‡] Jolanta J. Levenfors,[†,‡] Sha Cao,[§] Adam A. Strömstedt,[^] Bengt Guss,[‖] Rolf Larsson,[▽] Diarmaid Hughes,[§] Bo Öberg,[‡,^] Anders Broberg[†,*]

[†]Department of Molecular Sciences, Uppsala BioCentrum, Swedish University of Agricultural Sciences, P.O. Box 7015, SE-750 07 Uppsala, Sweden

[‡]Ultupharma AB, Södra Rudbecksgatan 13, SE-752 36 Uppsala, Sweden

[§]Department of Medical Biochemistry and Microbiology, Uppsala University, P.O. Box 582, SE-751 23 Uppsala, Sweden

[^]Department of Medicinal Chemistry, Uppsala University, P.O. Box 574, SE-751 23 Uppsala, Sweden

[‖]Department of Biomedical Sciences and Veterinary Public Health, Swedish University of Agricultural Sciences, P.O. Box 7036, SE-750 07 Uppsala, Sweden; Bengt.Guss@slu.se

[▽]Department of Medical Sciences, Uppsala University, SE-751 85 Uppsala, Sweden

*Correspondence: Anders.Broberg@slu.se; Tel.: +46-18-672217

Contents Page

METHODS

General. Optical rotation was measured on a PerkinElmer 341, with samples dissolved in MeOH at room temperature (20°C). UV spectra were recorded on a Hitachi U-2001 spectrophotometer in MeOH at room temperature. ^{1}H and ^{13}C NMR data were acquired in DMSO-d_6 or $CHCl_3$-*d* on a Bruker Avance III 600 MHz NMR spectrometer (Bruker Biospin GmBH, Rheinstetten, Germany) equipped with a 5 mm cryoprobe (^{1}H, ^{13}C, ^{15}N, ^{31}P). Standard pulse sequences supplied by the manufacturer were used for determination of ^{1}H and ^{13}C frequencies and connectivities. For structure analysis, 1D ^{1}H, COSY, TOCSY, DEPT-HSQC, HSQC-TOCSY and HMBC were applied. Chemical shifts were determined relative to internal DMSO-d_5 (δ_C 39.51; δ_H 2.50) or internal chloroform (δ_C 77.23; δ_H 7.27). HR-ESIMS and MSMS were performed on a maXis Impact Q-TOF MS (Bruker Daltonic GmbH, Bremen, Germany) connected to an Agilent 1290 Infinity II UHPLC (Agilent, Palo Alto, CA, USA). Preparative HPLC was run on a Gilson 306/306 pump system (Gilson Inc., Middleton, WI, USA) with a Gilson 119 UV/vis detector monitoring at 210 nm and fractions were collected with a Gilson 204 fraction collector, in polypropylene 2.2 mL square well plates (VWR, Radnor, PA, USA). HPLC gradient grade MeCN (Sigma-Aldrich, St. Louis, MO, USA) and deionized filtered water (Millipore, Billerica, MA, USA) were used for preparation of HPLC and UHPLC solvents.

Isolation and identification of *Pedobacter cryoconitis* UP508. The bacterial strain UP508 was isolated from a soil sample collected at the esker Kronåsen, at Ultuna, Uppsala, Sweden (59°49'07.2"N, 17°39'55.6"E), by pressing a sterile 50 mL centrifuge tube into the soil surface. Approximately 4 g of the soil sample was vortexed thoroughly with 40 mL of sterile PBS and the mixture was allowed to settle for ten minutes. Then, 1 mL of the supernatant was mixed with 9 mL of sterile PBS in a 15-mL centrifuge tube. From this dilution, 0.1 mL was spread onto NBCA isolation plates [Difco Nutrient Broth, 1g/L (Becton Dickinson: BD), Bacto Casamino Acids, 1g/L (BD), Bacto Agar, 15g/L (Saveen & Werner), cycloheximide 100 mg/L, nystatin 10 mg/L, in deionized water] supplemented with 20 mg/L of ampicillin (AMP), kanamycin (KAN) and nalidixic acid (NAL). The plates were then incubated at 20°C for approximately one week in darkness. Selected bacterial

colonies were restreaked on Vegetable Peptone Broth Agar (VPA) comprising one third strength Vegetable Peptone Broth (VPB10), 10g/L (Oxoid) and Bacto Agar, 15g/L (Saveen & Werner) in deionized water, and one of the purified strains was denoted UP508. The strain was afterwards maintained as deep-frozen (-70°C) cell stocks and transferred to VPA plates prior to culturing.

The isolate UP508 was found to be closest related to *P. cryoconitis* A37 (≥99%) by sequencing the 16S rRNA gene. In short, colony PCR amplification of the 16S rRNA gene was performed with the universal bacterial primers 27F (AGAGTTTGATCMTGGCTCAG) and 1492R (TACGGYTACCTTGTTACGACTT) followed by PCR-purification (QIAquick PCR purifications kit, QIAGEN) and sequencing of the PCR-products (EZ-sequencing, Macrogen). The resulting DNA sequencing chromatograms were manually trimmed and assembled using the Geneious R8 software (Biomatters Ltd., Auckland, New Zealand). The resulting sequence was then submitted to an online Nucleotide BLAST search (https://blast.ncbi.nlm.nih.gov/Blast.cgi) against 16S rRNA sequences (Bacteria and Archeae) to retrieve the closest possible identity of the isolate.

Culture Conditions and Metabolite Sampling. *P. cryoconitis* UP508 was cultivated in half strength Vegetable Peptone Broth [VPB15, 15 g VPB (Oxoid Ltd) in 1 L deionised water]. Initially, one 150-mL culture in a 500-mL E-flask was studied, and for production of larger amounts of metabolites, the isolate was cultured in half strength VPB (14 cultures × 300 mL in 1 L Erlenmeyer flasks). The cultures were started by transferring a loop (10 µL) of 24-48 h-old bacterial colonies grown on VPA plates. Cultures were incubated on a rotary shaker (130 rpm) for 7 d at 20 °C in darkness. To collect extracellular metabolites sterile nylon mesh bags containing a polymeric resin, Sepabeads® SP850 (Mitsubishi Chemical Co., Tokyo, Japan), were submerged in actively growing cultures, approximately 16 to 24 hours after inoculation (approximately 8 g of resin per bag for 150-mL and 15 g per bag for 300-mL cultures).

Isolation of compounds 1–8. The resin bag from the 150-mL culture of *P. cryoconitis* UP508 was washed with de-ionized water, extracted with 2 × 10 mL MeOH and 2 × 10 mL MeCN under sonication, and the pooled extract was dried in a vacuum centrifuge. The dried extract was dissolved

in 1 mL 50% MeCN, centrifuged and then fractionated by preparative reversed-phase HPLC (1 mL injected, Hypersil Gold column, 21 × 100 mm, 5 μm) using a gradient of MeCN in water (10–95% in 10 min, 95% for 10 min, 0.2% formic acid, 10 mL/min), and 2-mL fractions were collected. The collected fractions were subjected to bioassays and UHPLC-MS analysis. Many fractions, including fractions 23–25 (**1** and **2**), were subjected to another round of chromatography on the same column, solvents and flow-rate, and for **1** and **2** the gradient was 20–90% MeCN in 10 min, followed by 90% for 10 min, which gave ca 0.4 and 0.5 mg of **1** and **2**, respectively, in semi-pure form. For isolation of more of each compound, the isolation procedure was improved and used on many batches of culture extracts. The description below is representative for the procedure, but the yield of the different compounds differed between batches.

Adsorbent bags from 14 cultures of *P. cryoconitis* UP508 (each 300 mL in 1-L E-flasks) were extracted with 2 × 300 mL MeOH (0.2% formic acid) and 2 × 300 mL MeCN (0.2% formic acid) under sonication, and the combined extract was dried under reduced pressure. The extract was dissolved in 15 mL 50% MeCN (aq), centrifuged (15 000 rpm, 5 min) and fractionated (HPLC1) on preparative reversed-phase HPLC (14 × 1 mL injected, Luna Omega column, 21 × 100 mm, 5 μm) using a gradient of MeCN in water (15–50% in 15 min, 50-95% in 2 min, 95% for 4 min, 0.2% formic acid), and 2-mL fractions were collected. The following antibacterial fractions were collected and pooled based on results from bioassays and UHPLC-MS analysis (as below): 57–59 (**2**), 60–65 (**1**, **3**, and **4**), 66–70 (**5**–**7**), and 71–75 (**8**). Compounds **1**–**8** were purified further (HPLC2) using the same column, solvents and flow-rate, but with gradient 20–40% MeCN in 17 min followed by a hold at 40% MeCN (for compounds **1**, **3**–**8**), or with gradient 15–65% MeCN in 17 min, followed by a hold at 65% MeCN (**2**). As guided by UHPLC-MS, fractions containing compounds **1**–**8** were pooled and dried. The compounds were further purified (HPLC3) on the same column, solvents and flow-rate, with gradient 20-37.5% MeCN in 17 min (**1** and **3**), or 20-40% MeCN in 17 min (**2** and **4**), or 20-75% MeCN in 17 min (**5**), or 20–80% MeCN in 17 min (**6** and **7**), or 20–35% MeCN in 25 min, 37.5–42.5% in 8 min, 42.5–75% in 6 min (**8**). Fractions were analysed by UHPLC-MS, pooled, dried and weighed, which resulted in 7.95 mg of **5**, 5.49 mg of **6**, 3.87 mg of **7**, and 5.35 mg of **8**. Compounds

1-**4** were subjected to one final round of chromatography on the same column, solvents and flow-rate, with gradient 17.5–40% MeCN in 17 min (**1**, **3** and **4**), or 20–37.5% MeCN in 17 min (**2**). After UHPLC-MS, fractions with the individual compounds were pooled, dried and weighed, to give 0.66 mg of **1**, 1.28 mg of **2**, 1.97 mg or **3**, and 0.70 mg of **4**.

In Vitro **Bioassay of chromatographic fractions.** Antimicrobial activity of chromatographic fractions was assayed according to an earlier described protocol ("Microtiter plate assay 2"),[1] which is based on inhibition of cell growth or spore germination in microtiter plates. The following organisms were used for the bioassays: *Escherichia coli* LMG15862, *Acinetobacter baumannii* LMG1041^T, *Enterobacter cloacae* LMG2783^T, *Klebsiella pneumoniae* LMG20218, *Pseudomonas aeruginosa* LMG6395, *Staphylococcus aureus* LMG15975, *Candida albicans* H-29 and *Aspergillus fumigatus* J7. The bacterial isolates originated from the Belgian Co-ordinated Collections of Micro-organisms, Gent, Belgium, whereas the origin of the strains of the yeast *Candida albicans* and the fungus *Aspergillus fumigatus* Fres., was as previously described.[2] In short, aliquots of HPLC fractions were transferred to 96-well microtiter plates and the solvent was evaporated in a fume-hood overnight. Cell suspensions (all bacterial strains and *C. albicans*) or spore suspensions (*A. fumigatus*), 100 μL at a concentration of 10^4 cells/spores per mL in VPB for bacteria, malt extract (ME) for *A. fumigatus*, and yeast extract-malt extract medium (ISP2[3]) for *C. albicans*, were added to the wells and incubated at 37 °C in the dark for 16 to 24 h. The effect on the bacterial/fungal growth was estimated visually according to the following scale: 3 - full growth inhibition, 2 - intermediate growth inhibition, 1 - weak growth inhibition, 0 - no growth inhibition. Positive controls were cell/spore suspensions only, and sterile medium was used as negative control.

UHPLC-MS and UHPLC-MSMS analysis. Culture extracts and fractions from preparative reversed-phase HPLC were analyzed by UHPLC-MS on a reversed-phase column (2.1 × 50 mm, 1.5

[1] Thaning, C., Welch, C. J., Borowicz, J. J., Hedman, R., and Gerhardson, B. (2001) Suppression of *Sclerotinia sclerotiorum* apothecial formation by the soil bacterium *Serratia plymuthica*: identification of a chlorinated macrolide as one of the causal agents. *Soil Biol. Biochem. 33*, 1817–26.
[2] Levenfors, J. J., Hedman, R., Thaning, C., Gerhardson, B., Welch, C. J. (2004) Broad-spectrum antifungal metabolites produced by the soil bacterium *Serratia plymuthica* A 153. *Soil. Biol. Biochem*. *36*, 677−685.
[3] Shirling, E. B. and Gottlieb, D. (1966) Methods for characterization of *Streptomyces* species. *Int. J. Syst. Bacteriol. 16,* 313–340.

μm, Accucore Vanquish, Thermo Scientific) using a gradient of MeCN in water, both with 0.2% formic acid (10–95% MeCN in 3 min, 95% MeCN for 1.2 min, at 0.9 mL/min). The MS was operated in positive mode with scanning of *m/z* 50–1500, and the mass spectra were calibrated against sodium formate clusters.

Before MSMS analysis of compound **1**–**8**, each compound (ca 100 μg) was treated with 300 μL 1% NaOMe in MeOH for 20 min at room temperature, and the reaction was stopped by the addition of 30 μL 2 M HCl (aq). The samples were analysed by UHPLC-MS as above, but with the gradient 30–60% MeCN in 3 min (0.9 mL/min), and MSMS was run in automatic precursor selection mode with 22 eV fragmentation energy.

Advanced Marfey's analysis.[4,5] Samples of compound **1**–**8** (2 × 100 μg each) were hydrolysed in 6 M HCl (aq) at 120°C, in evacuated glass ampoules, for 17 h and 45 h, respectively. The ampoules were opened and the solutions dried under N_2 in plastic 1.5-mL tubes. Each sample was then treated with 36 μL 1 M $NaHCO_3$ and 180 μL L-FDLA (10 mg/mL acetone) for 1 h in 40°C, and then 20 μL 2 M HCl (aq) was added. Following dilution with 500 μL MeOH, the samples (2 μL injected) were analysed by UHPLC-MS on the same column as above, using MeCN/H_2O with 0.2% formic acid, but with the gradient 30–60% MeCN in 6 min at 0.9 mL/min. Extracted-ion chromatograms corresponding the $[M+H]^+$ ions of the FDLA derivatives of Asp, OHVal, Val, Phe, DAPA, Thr, ABA, DABA and Leu were constructed and compared with corresponding chromatograms obtained by analysing D/L-FDLA derivatives of commercial reference amino acids. To evaluate possible racemization of amino acids during the hydrolysis, selected samples were hydrolysed in 6 M HCl in H_2O/D_2O (1:1), and then derivatized and analysed as above.

[4] Harada, K., Fujii, K., Mayumi, T., Hibino, Y., Suzuki, M., Ikai, Y., and Oka, H. (1995) Constituent Amino Acids in Peptide --- Advanced Marfey's Method. *Tetrahedron Lett. 36*, 1515-1518.
[5] Fujii, K., Ikai, Y., Mayumi, T., Oka, H., Suzuki, M., and Harada, K. (1997) A Nonempirical Method Using LC/MS for Determination of the Absolute Configuration of Constituent Amino Acids in a Peptide: Elucidation of Limitations of Marfey's Method and of Its Separation Mechanism. *Anal. Chem. 69*, 3346-3352.

Mosher's ester analysis.[6] A sample of **1** (6 mg) was hydrolysed in 300 μL 6 M HCl (aq), in an evacuated glass ampoule, at 120°C for 6 h. The ampoule was opened and the sample was dried under N_2 in a 1.5-mL plastic tube. The sample was dissolved in H_2O (0.5 mL) and extracted with EtOAc (2 × 0.5 mL). The combined EtOAc extracts were split into two equal portions in 1.5-mL HPLC vials, and the samples were dried under N_2. After dissolving each sample in 600 μL dry pyridine-d_5, one of the two samples obtained from **1** was treated with 5 μL (*R*)-MTPA-Cl and the other sample with 5 μL (*S*)-MTPA-Cl. The reactions were kept at room temperature for 6 h and were then analysed by NMR at 30°C without any further purification. Additionally, the samples were dried under N_2 and then analysed by NMR in $CHCl_3$-*d*.

*Isopedopeptin A (**1**)*: off-white solid; $[\alpha]_D^{20}$ –66° (c 0.3 in methanol); UV (MeOH) λ_{max} ($\log_{10}$ ε) 240 (4.0); ^{1}H NMR (DMSO-d_6, 600 MHz), see Table S1; ^{13}C NMR (DMSO-d_6, 150 MHz), see Table S1; ESI-QTOFMS *m/z* 566.3243 $[M + 2H]^{2+}$ (calcd for $C_{53}H_{88}N_{12}O_{15}^{2+}$ 566.3241).

*Isopedopeptin B (**2**)*: off-white solid; $[\alpha]_D^{20}$ –58° (c 0.2 in methanol); UV (MeOH) λ_{max} ($\log_{10}$ ε) 240 (4.1); ^{1}H NMR (DMSO-d_6, 600 MHz), see Table S2; ^{13}C NMR (DMSO-d_6, 150 MHz), see Table S2; ESI-QTOFMS *m/z* 559.3169 $[M + 2H]^{2+}$ (calcd for $C_{52}H_{86}N_{12}O_{15}^{2+}$ 559.3163).

*Isopedopeptin C (**3**)*: off-white solid; $[\alpha]_D^{20}$ –68° (c 0.3 in methanol); UV (MeOH) λ_{max} ($\log_{10}$ ε) 240 (4.0); ^{1}H NMR (DMSO-d_6, 600 MHz), see Table S3; ^{13}C NMR (DMSO-d_6, 150 MHz), see Table S3; ESI-QTOFMS *m/z* 572.3246 $[M + 2H]^{2+}$ (calcd for $C_{54}H_{88}N_{12}O_{15}^{2+}$ 572.3241).

*Isopedopeptin D (**4**)*: off-white solid; $[\alpha]_D^{20}$ –62° (c 0.2 in methanol); UV (MeOH) λ_{max} ($\log_{10}$ ε) 240 (3.9); ^{1}H NMR (DMSO-d_6, 600 MHz), see Table S4; ^{13}C NMR (DMSO-d_6, 150 MHz), see Table S4; ESI-QTOFMS *m/z* 551.3194 $[M + 2H]^{2+}$ (calcd for $C_{52}H_{86}N_{12}O_{14}^{2+}$ 551.3188).

[6] Dale, J. A. and Mosher, H. S. (1973) Nuclear magnetic resonance enantiomer reagents. Configurational correlation via nuclear magnetic resonance chemical shifts of diastereomericmandelate, O-methylmandelate, and α-methoxy-α-trifluorophenylacetate (MTPA) esters. *J. Am. Chem. Soc. 95,* 512-519.

*Isopedopeptin E (**5**)*: off-white solid; $[\alpha]_D^{20}$ –36° (c 0.3 in methanol); UV (MeOH) λ_{max} ($\log_{10}$ ε) 240 (3.8); ^{1}H NMR (DMSO-d_6, 600 MHz), see Table S5; ^{13}C NMR (DMSO-d_6, 150 MHz), see Table S5; ESI-QTOFMS *m/z* 558.3275 $[M + 2H]^{2+}$ (calcd for $C_{53}H_{88}N_{12}O_{14}^{2+}$ 558.3266).

*Isopedopeptin F (**6**)*: off-white solid; $[\alpha]_D^{20}$ –32° (c 0.05 in methanol); UV (MeOH) λ_{max} ($\log_{10}$ ε) 240 (3.8); ^{1}H NMR (DMSO-d_6, 600 MHz), see Table S6; ^{13}C NMR (DMSO-d_6, 150 MHz), see Table S6; ESI-QTOFMS *m/z* 580.3401 $[M + 2H]^{2+}$ (calcd for $C_{55}H_{92}N_{12}O_{15}^{2+}$ 580.3397).

Isopedopeptin G (7): off-white solid; $[\alpha]_D^{20}$ –49° (c 0.1 in methanol); UV (MeOH) λ_{max} ($\log_{10}$ ε) 240 (4.0); ^{1}H NMR (DMSO-d_6, 600 MHz), see Table S7; ^{13}C NMR (DMSO-d_6, 150 MHz), see Table S7; ESI-QTOFMS *m/z* 571.3356 $[M + 2H]^{2+}$ (calcd for $C_{55}H_{90}N_{12}O_{14}^{2+}$ 571.3345).

*Isopedopeptin H (**8**)*: off-white solid; $[\alpha]_D^{20}$ –56° (c 0.2 in methanol); UV (MeOH) λ_{max} ($\log_{10}$ ε) 240 (4.0); ^{1}H NMR (DMSO-d_6, 600 MHz), see Table S8; ^{13}C NMR (DMSO-d_6, 150 MHz), see Table S8; ESI-QTOFMS *m/z* 571.3348 $[M + 2H]^{2+}$ (calcd for $C_{55}H_{90}N_{12}O_{14}^{2+}$ 571.3345).

Minimal Inhibitory Concentration (MIC) against the primary panel of microorganisms. The MIC for compounds **1**–**8** was measured by means of a broth micro-dilution method in 96-wells microtiter plates with the addition of *E. coli* LMG15862, *A. baumannii* LMG1041^T, *E. cloacae* LMG2783^T, *K. pneumoniae* LMG20218, *P. aeruginosa* LMG6395, *S. aureus* LMG15975, *C. albicans* H-29 and *A. fumigatus* J7*,* as test organisms. The test media were AM3 Broth (BD Difco Ltd) mixed with phosphate buffered saline (PBS, Amresco LLC, Solon, USA) in 1:4 ratio (*E. coli*, *A. baumannii, E. cloacae*, *K. pneumoniae* and *P. aeruginosa*), AM3 Broth mixed with PBS in 1:1 ratio (*S. aureus*), ME (*A. fumigatus*) and ISP2 (*C. albicans*). Prior to MIC determination, the cell concentration of tested bacterial/fungal pathogens was adjusted to ≅ 4×10^5 CFU/mL (acceptable range $2 – 6 \times 10^5$ CFU/mL). Cell concentration was confirmed by colony counting after diluting and plating the respective bacterial pathogen on VPA plates [VPA, 10 g Vegetable Peptone Broth (Oxoid Ltd., Basingstoke,UK), 15 g Bacto Agar (Difco Ltd, Tyrone) in 1 L deionised water] directly after each of MIC-tests. The cells of *C. albicans* were plated on ISP2 agar plates [ISP2, 15 g Bacto Agar (Difco Ltd) in 1 L deionised water] and respectively spores of *A. fumigatus* were plated on MEA plates.

Plates were, subsequently, incubated at 37 °C in the dark, and viable colonies counted after 16 to 24 h. To estimate MIC values (concentration range between 0.05 and 50 μg/mL), solutions of the tested compounds (100, 10 and 1 and if needed 0.1 μg/mL in MeOH) were dispensed into wells of microtiter plate(s) and the solvent was evaporated in a fume-hood. Subsequently, suspensions of pathogen cells in the appropriate medium were dispensed to the wells of microtiter plates and the growth of pathogens were observed after 16 to 20 h of incubation at 37 °C in the dark. Positive controls were the respective pathogen cells suspended in untreated sterile media without addition of compounds(s) and negative controls were the media only. MIC values were defined as the lowest concentration of each compound with no visible growth of pathogen. All MIC tests were performed in triplicate and repeated at least twice.

MIC determination for compound 2 against an extended panel of bacterial strains.

Compound **2** was evaluated against a panel of Gram-negative bacteria (Hughes strain collection), including: *A. baumannii* ATCC 19606, wild-type; BM4454, multidrug-resistant clinical isolate; BM4652, efflux-defective derivative of BM4454; CH9622, colistin-resistant clinical isolate; *E. coli* ATCC 25922, wild-type; CH3130, efflux-defective Δ*tolC* mutant isogenic to ATCC 25922; D22, a drug-hypersensitive *lpxC* mutant of *E. coli*; CH3491, multidrug-resistant clinical isolate; CH9623 and CH9624, colistin-resistant clinical isolates carrying *mcr-1*; *K. pneumoniae* ATCC 13833, wild-type; 1161486, wild-type; 1161486a, Δ*tolC* mutant isogenic to 1161486; CH3498, multidrug-resistant clinical isolate; CH9625 and CH9626, colistin-resistant clinical isolates; *P. aeruginosa* PAO1, wild-type; PAO750, efflux-defective mutant isogenic to PAO1. The *in vitro* antimicrobial activity of each compound was determined by measuring the MIC value using the broth micro-dilution technique in cation-adjusted Mueller-Hinton II broth (Becton-Dickinson, 212322) according to EUCAST and CLSI guidelines. Each compound prepared in MHII medium was dispensed into a 96-well round-bottomed microtiter plate to give final assay concentrations from 64 μg/mL down to 0.25 μg/mL (two-fold dilution series in 10 wells, plus two control wells: medium control with no bacteria or compound, and growth control with bacteria added but no compound). Bacteria were prepared from fresh colonies grown on non-selective MHII agar, then suspended in saline to 0.5 McFarland (≅ 1.5 ×

10^8 CFU/mL) with turbidity assessed using a Sensititre Nephelometer (Trek Diagnostics Systems Ltd, UK). 50 μL of this bacterial suspension was transferred to 10 mL of MHII broth to give a final bacterial concentration ≅ 5×10^5 CFU/mL (acceptable range $3 – 7 \times 10^5$ CFU/mL). 50 μL of bacterial suspension was pipetted into each well (except the medium control well, where 50 μL MHII was pipetted). Final volume in each well was 100 μL. Plates were covered and incubated without shaking for 18-20 h at 35 °C ± 2 °C. MIC was read visually, as complete inhibition of growth by the unaided eye, using the medium-only wells as the control. Each compound was assayed at least in duplicate. Additionally, the MIC for compound **2** against clinical carbapenem-resistant strains of *A. baumannii* (A219 and A250), *E. coli* (EC4129 and EC4163) and *P. aeruginosa* (PS826 and PS992), was determined at the Public Health Agency of Sweden (according to EUCAST recommendations).

***In vitro* Cytotoxicity Determination.** *In vitro* cytotoxicity was determined by a fluorometric microculture cytotoxicity assay,[7] based on hydrolysis of fluorescein diacetate to fluorescein by cells with intact plasma membranes. In short, HepG2 cells (hepatocellular carcinoma cells, ATCC), in Eagle's Minimum Essential Medium (ATCC) supplemented with 10 % fetal bovine serum, penicillin/streptomycin (100 U/100 μg/mL) and 2 mM L-glutamine, were seeded in 384-well assay plates at a density of 1000 cells/well. The cells were incubated over night at 37°C and compounds in 10 mM DMSO were added, to obtain final concentrations 64 μM – 0.25 μM in two-fold dilutions. After incubation for 72 h at 37°C, the cells were pelleted and washed. Fluorescein diacetate was added (1 μL, 0.5 mg/mL) and the fluorescence [485 nm(exc)/530 nm(em.)] was measured after 50 min at 37°C. Bortezomib (2 μM) was used as positive control and dose response testing of doxorubicin (top concentration 2 μM) was performed repeatedly to follow assay performance over time. Cytotoxicity was assessed after 72 h with cell survival presented as survival index (SI, %) defined as fluorescence in test wells in percent of control cultures with blank values subtracted. Criteria for a successful assay include a signal-to-noise ratio in control cultures >10, CV <30% and a

[7] Lindhagen, E., Nygren, P., and Larsson, R. (2008) The fluorometric microculture cytotoxicity assay. *Nat. Protoc*. *3*, 1364-69.

positive control (Bortezomib) SI of <5%. The half maximal inhibitory concentration (IC_{50}) was determined from log concentration-effect curves using non-linear regression analysis.

Frequency of resistance (FoR). For the determination of the FoR, the MIC of compound **2** was first evaluated on solid MH-agar medium prepared in 35 mm diameter plates. Each plate contained 4 mL agar with the appropriate amount of compound. Bacterial cultures were grown and prepared as described for the MIC assay. 13 μL of bacterial culture diluted to 0.5 MacFarland was inoculated into 1 mL 0.9% NaCl resulting in ~2 × 10^6 CFU/mL. 5 μL of this bacterial suspension was spotted onto the surface of each agar plate (~10^4 CFU/spot). Plates were sealed and incubated at 37°C for 18–20 hours. Agar MIC was recorded according to CLSI guidelines as the lowest concentration of antimicrobial agent that completely inhibits growth from these spots, disregarding a single colony or a faint haze caused by the inoculum. Then 9 cm plates were prepared with 25 mL MHII agar medium containing 4 × or 8 × solid MIC concentrations of test compounds and seeded with 100 μL of a bacterial preparation, concentrated by centrifugation from overnight cultures and resuspended in 0.9% NaCl, corresponding to 10^8 CFU and 10^9 CFU per plate, and spread on the agar using 4–5 glass beads of 4 mm diameter. Since CFU were evaluated using the McFarland turbidity standard, the exact CFU number plated was evaluated by plating of serial dilutions of each inoculum preparation on MHII agar plates. Plates were incubated at 37°C and colonies were counted at 24 h and 48 h post-plating. The frequencies of resistance were then calculated by counting the number of validated resistant colonies growing on antibiotic preparations divided by the evaluated number of CFU in the inoculum.

Hemolysis assay. Compounds were evaluated for hemolytic activity using red blood cells from heparinized human blood. Red blood cells (RBC) were washed three times in Tyrode buffer (130 mM NaCl, 4 mM KCl, 2.8 mM NaOAc, 1 mM $MgCl_2$, 10 mM HEPES, 10 mM glucose, 1 mM $CaCl_2$, adjusted to pH 7.4) and resuspended in the same buffer. Final concentrations in the hemolysis assay were: 100 μM compound, 1% DMSO, and 50% RBC, assayed in a 200 μL volume in a microtiter plate. The mixture was incubated at 37 °C for 45 min with shaking (250 rpm). After incubation, RBCs were removed by centrifugation (1000 × g for 10 min), 100 μL clear plasma was transferred to a fresh microtiter plate, and the amount of hemoglobin measured using a spectrophotometer at 540 nm. The

complete lysis control contained 2% Triton X-100 (in Tyrode buffer) instead of compound; the negative control contained Tyrode buffer but no compound. Percent hemolysis was calculated as: [Abs compound] - [Abs negative control] / [Abs complete lysis control] - [Abs negative control] × 100. Values greater than 1% hemolysis at 100 μM were regarded as a red flag.

Bacterial membrane permeabilization assay. Liposomes were manufactured and permeabilization assayed as described previously.[8] Briefly, dry lipid films of *E. coli* polar lipid extract were formed on round-bottom flask walls. This was achieved by dissolving lipids in chloroform and evaporating the solvent under agitation and nitrogen gas flow, followed by incubation in vacuum chamber. Lipid films were re-suspended by 30 min stirring (*E. coli*) at 55°C in an aqueous solution of 100 mM 5(6)-carboxyfluorescein in 10 mM Tris buffer (set to pH 7.4 at 37°C). Suspensions were subjected to repeated extrusion through a 100 nm pore size polycarbonate membrane in order to reduce multilamellar structures and polydispersity. Un-trapped carboxyfluorescein was removed by gel filtration. Membrane permeability was measured by monitoring carboxyfluorescein efflux from the liposomes to the external low concentration environment, resulting in loss of self-quenching and an increased fluorescence signal. The 96-well plates were prepared with a 2-fold serial dilution of the samples in Tris buffer, as well as negative controls (background) and 0.16% Triton X-100 (maximum leakage). The plates were pre-heated to incubation temperature (37°C) and administered a liposome suspension, to a final lipid concentration of 10 μM in 200 μL. The effects of each sample concentration on the liposome system were monitored for 45 min, at which point the leakage increment had largely subsided. Results shown represent the mean from four experiments with standard deviations and are expressed as percent of total leakage generated with Triton X-100 and subtraction of the baseline value. The EC_{50}-values, fixed at 50% of total leakage, are calculated (where applicable) from a variable slope sigmoidal dose-response curve for the leakage percentage as a function of the sample concentration (log10).

[8] Strömstedt, A. A., Kristiansen, P. E., Gunasekera, S., Grob, N., Skjeldal, L., and Göransson, U. (2016) Selective membrane disruption by the cyclotide kalata B7: complex ions and essential functional groups in the phosphatidylethanolamine binding pocket. *Biochim. Biophys. Acta 1858*, 1317-1327.

Table S1. ^{1}H and ^{13}C NMR-data (600 and 150 MHz, resp) for compound **1** (DMSO-d_6, 30°C)

Pos.	^{13}C	^{1}H	Mult (*J*, Hz)
3OHFA			
1	167.6	-	-
2	39.4	2.69	dd (13.8, 3.5)
		2.17	dd (13.8, 4.1)
3	70.7	4.97	m
4	31.2	1.49	m
5	26.1	1.20	obsc
6	28.6	1.21	obsc
7	25.0	1.20	obsc
8	38.0	1.12	obsc
9	27.0	1.49	obsc
10	22.1	0.84	d (6.6)
11	22.1	0.84	d (6.6)
DAPA1			
NH	-	8.57	d (9.1)
1	170.8	-	-
2	50.6	4.73	obsc
3	43.9	3.12	dd (13.1, 5.4)
		2.97	dd (13.1, 4.1)
Leu			
NH	-	8.89	br s
1	173.1	-	-
2	52.8	4.33	obsc
3	39.1	1.65	m
		1.46	m
4	24.0	1.65	obsc
5	22.2	0.88	d (6.2)
6	22.2	0.84	d (6.1)
DABA			
NH	-	8.65	d (9.3)
1	168.0	-	-
2	49.5	4.64	ddd (9.3, 7.0, 7.0)
3	29.2	1.82	m
4	35.4	2.75	m
		2.61	m
ABA			
NH	-	10.22	br s
1	165.4	-	-
2	132.6	-	-
3	114.1	5.57	q (7.3)
4	12.5	1.77	d (7.3)
Thr			
NH	-	8.42	d (7.6)
1	169.4	-	-
2	59.5	4.20	dd (7.8, 2.3)
3	65.0	4.35	dq (2.5, 6.5)
4	20.4	1.22	d (6.5)
DAPA2			
NH	-	8.18	d (8.7)
1	169.1	-	-
2	53.2	4.22	ddd (8.7, 8.7, 5.7)
3	40.6	3.04	dd (13.1, 5.7)
		2.87	obsc
Phe			
NH	-	7.26	d (9.0)
1	171.5	-	-
2	53.5	4.76	obsc
3	37.6	2.89	obsc
		2.72	obsc
4	137.2	-	-
5/9	129.2	7.34	m
6/8	127.6	7.21	m
7	125.8	7.15	m
3OHVal			
NH	-	8.59	d (9.6)
1	169.4	-	-
2	58.0	4.72	obsc
3	70.6	-	-
4	26.4	1.05	s
5	26.5	0.92	s
Asp			
NH	-	8.52	d (9.6)
1	173.9	-	-
2	48.4	4.74	obsc
3	40.5	2.84	dd (16.1, 4.5)
		2.23	d (16.1, 3.8)
4	174.4	-	-

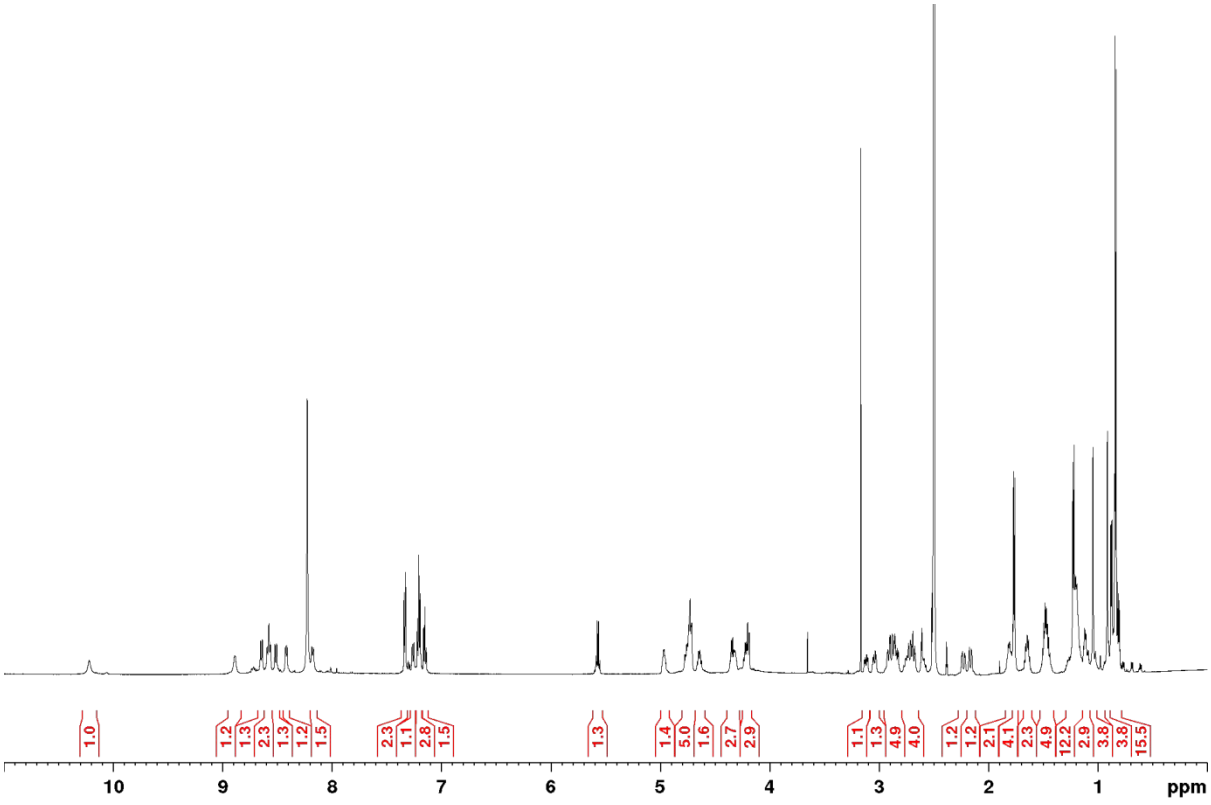

Figure S1. ^{1}H-NMR spectrum of compound **1** (DMSO-d_6, 600 MHz, 298 K).

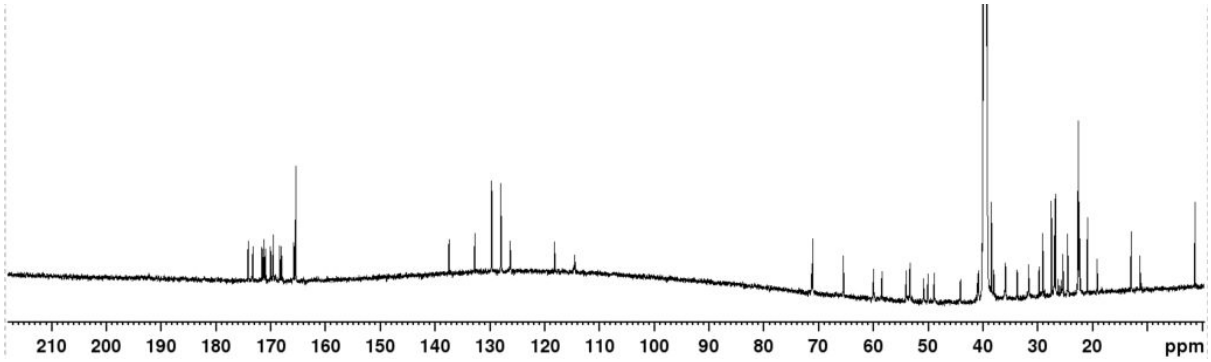

Figure S2. ^{13}C-NMR spectrum of compound **1** (DMSO-d_6, 600 MHz, 298 K).

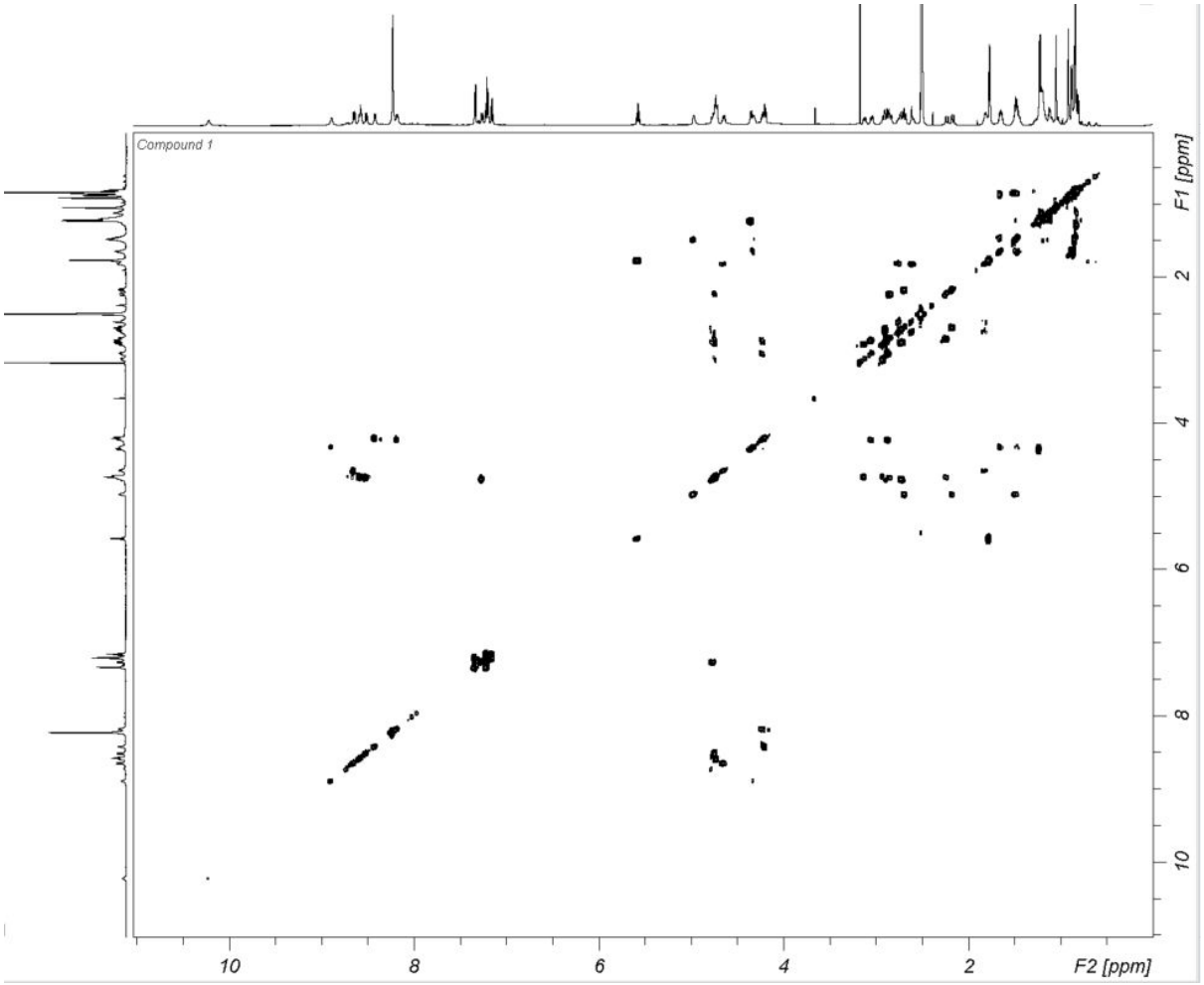

Figure S3. COSY spectrum of compound **1** (DMSO-d_6, 600 MHz, 298 K).

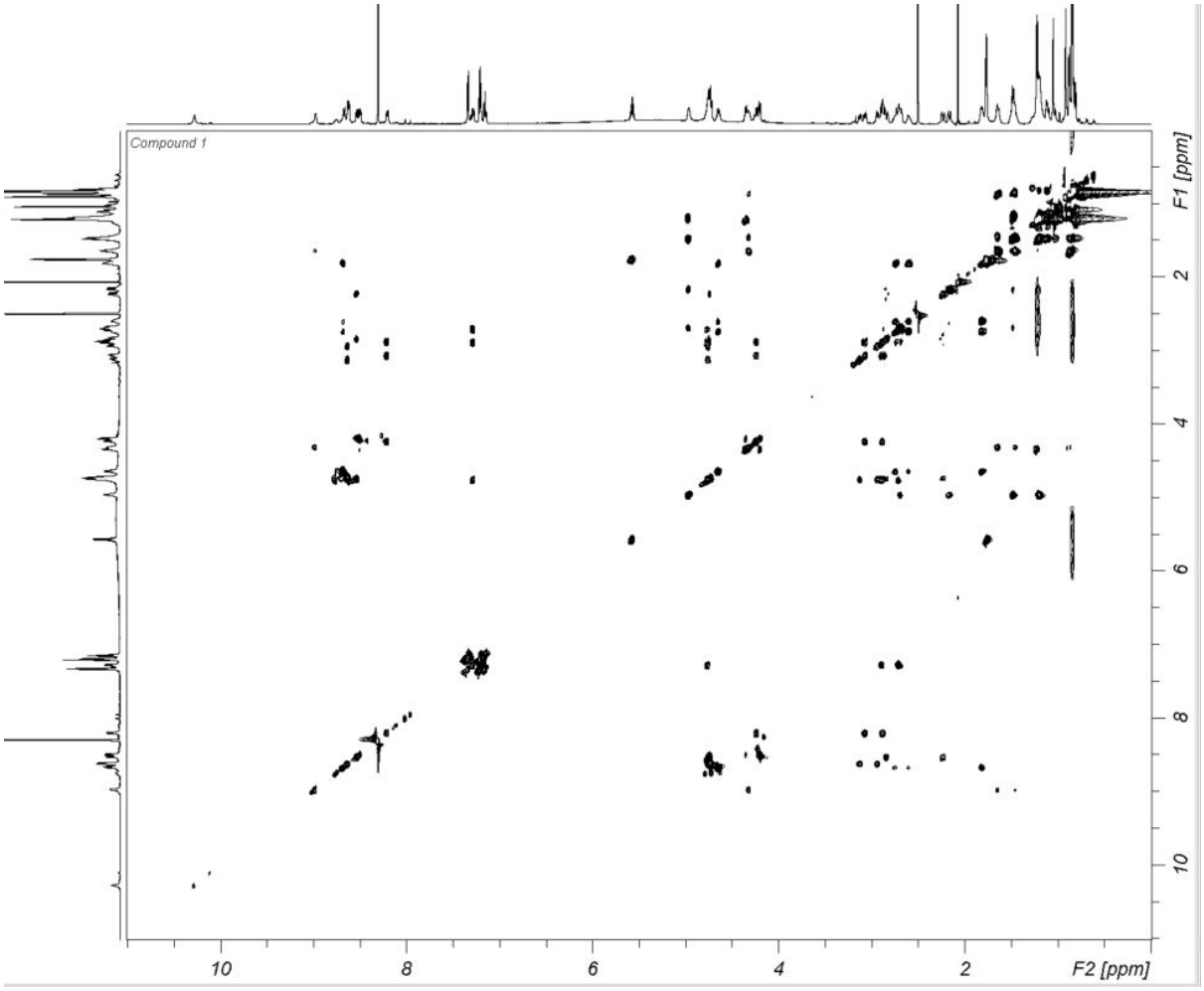

Figure S4. TOCSY spectrum of compound **1** (DMSO-d_6, 600 MHz, 298 K).

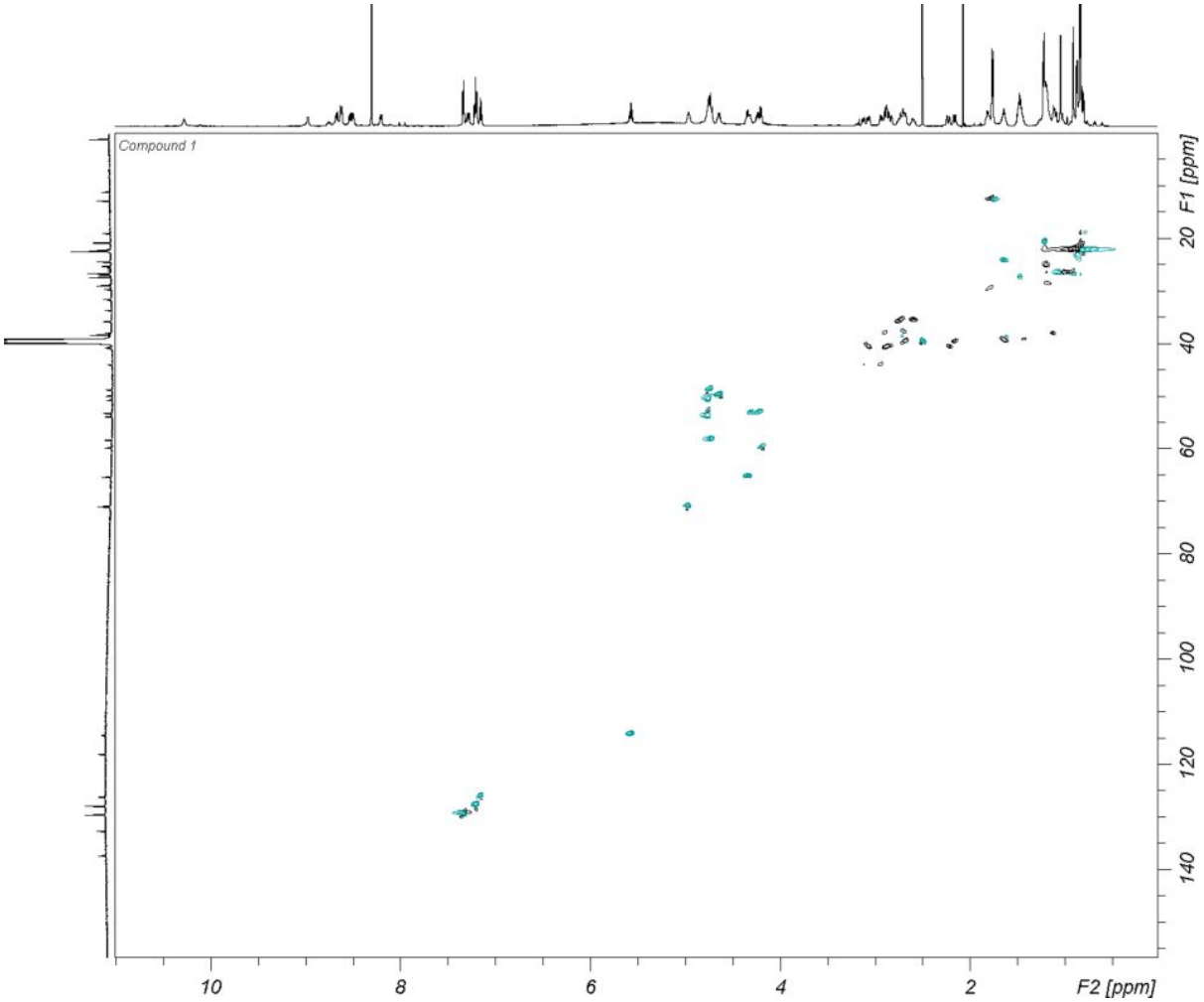

Figure S5. HSQC spectrum of compound **1** (DMSO-d_6, 600 MHz, 298 K).

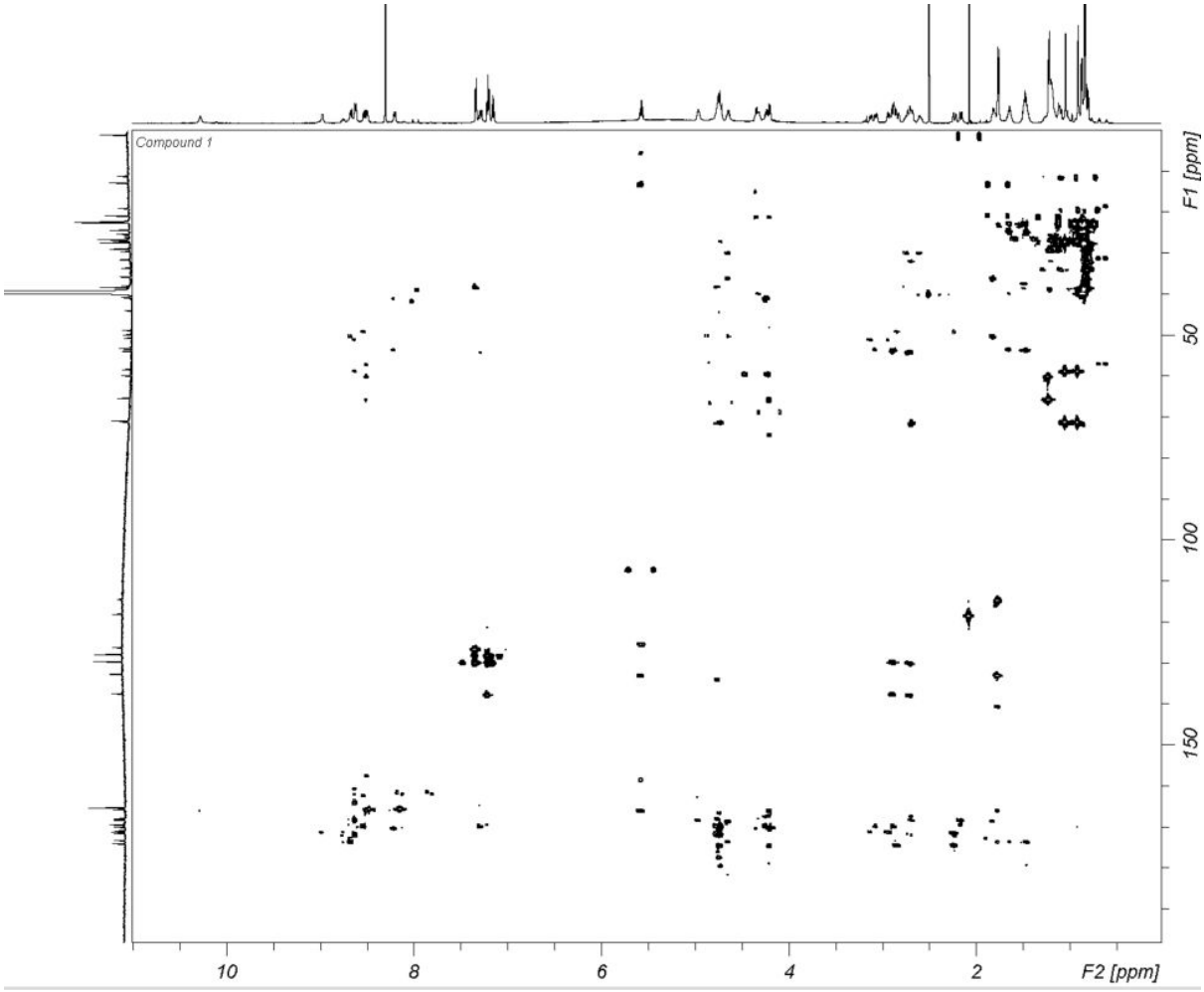

Figure S6. HMBC spectrum of compound **1** (DMSO-d_6, 600 MHz, 298 K).

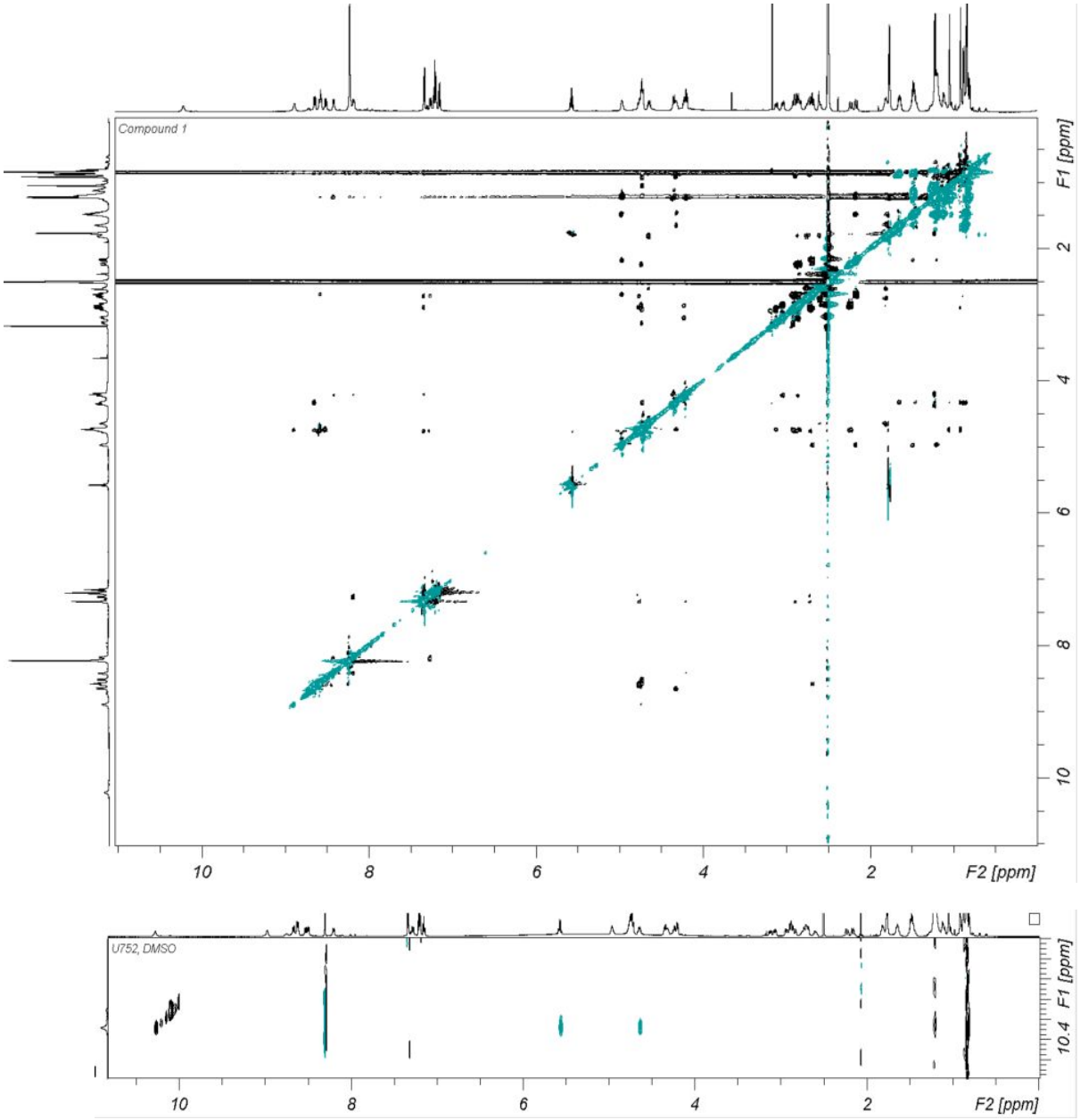

Figure S7. ROESY spectrum of compound **1** (DMSO-d_6, 600 MHz, 298 K). Top: Full spectrum. Bottom: Expansion showing the correlation between ABA-NH (10.22 ppm) and the ABA-CH_3 (5.57 ppm) and the DABA-H-2 (4.64 ppm).

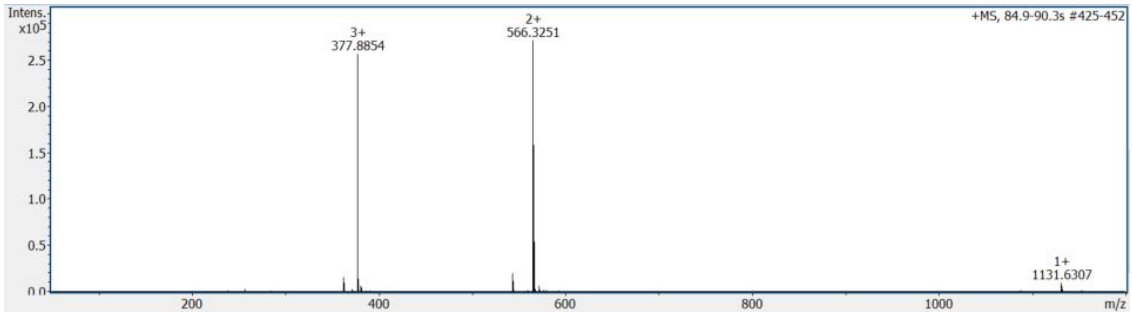

Figure S8. HRMS spectrum of compound **1**.

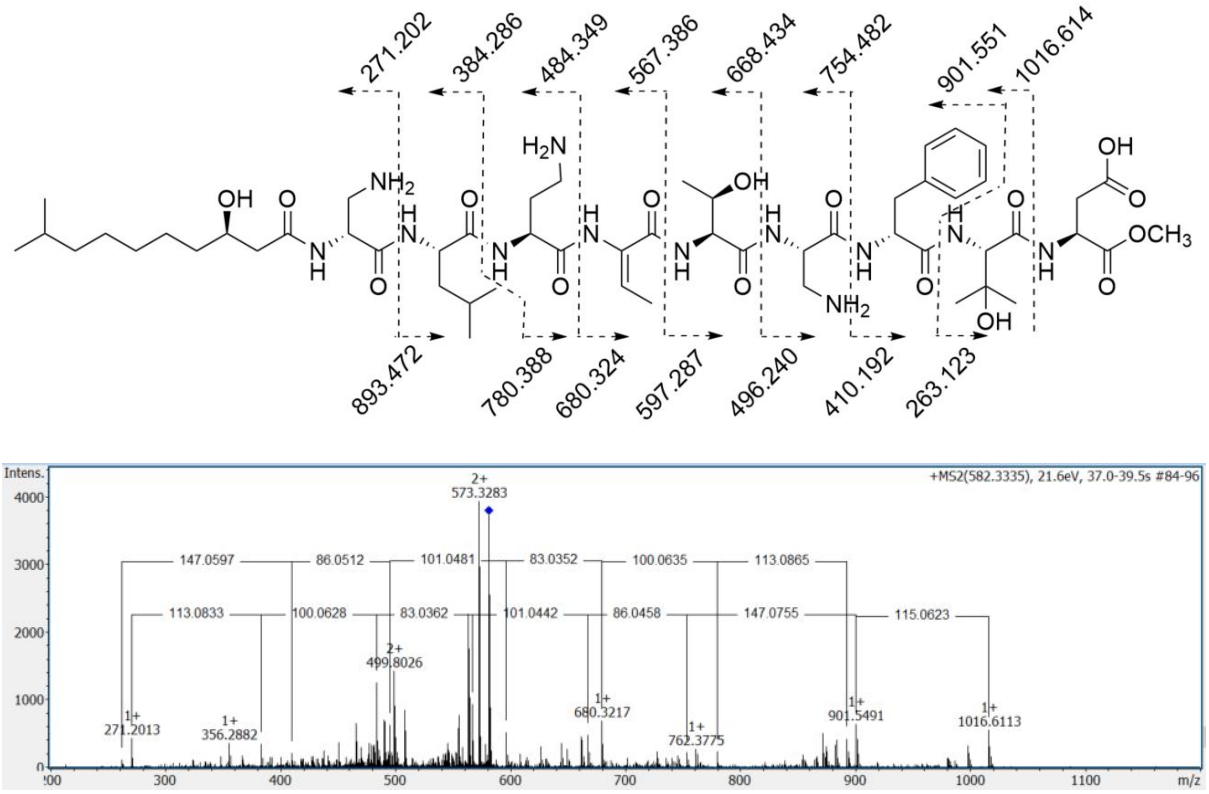

Figure S9. MSMS spectrum of compound **1** after ring-opening with NaOMe in MeOH. Mass differences between Y-series ions (top) and B-series ions (bottom) are shown in the mass spectrum. Theoretical m/z-values for the observed B- and Y-series ions are shown in the structure on top.

Table S2. ^{1}H and ^{13}C NMR-data (600 and 150 MHz, resp) for compound **2** (DMSO-d_6, 30°C)

Pos.	^{13}C	^{1}H	Mult (*J*, Hz)
3OHFA			
1	168.1	-	-
2	39.6	2.68	dd (13.7, 4.1)
		2.19	br d (13.7)
3	70.9	4.97	m
4	31.2	1.49	m
5	24.9	1.20	obsc
6	28.3	1.21	obsc
7	28.3	1.21	obsc
8	30.8	1.21	obsc
9	21.7	1.26	obsc
10	22.2	0.85	t (7.1)
DAPA1			
NH	-	8.53	d (8.7)
1	170.4	-	-
2	49.8	4.80	m
3	43.2	3.18	m
		3.02	m
Leu			
NH	-	8.97	br s
1	173.2	-	-
2	53.0	4.33	obsc
3	39.2	1.65	m
		1.48	m
4	24.1	1.66	obsc
5	22.2	0.89	d (6.9)
6	22.2	0.85	d (6.0)
DABA			
NH	-	8.65	d (9.2)
1	n.d.	-	-
2	49.6	4.63	ddd (7.6, 7.5, 7.5)
3	29.1	1.81	m
4	35.6	2.73	m
		2.61	m
ABA			
NH	-	10.23	br s
1	165.6	-	-
2	133.0	-	-
3	114.4	5.58	q (7.3)
4	12.7	1.77	d (7.3)
Thr			
NH	-	8.42	d (7.1)
1	169.8	-	-
2	59.6	4.20	dd (7.7, 2.0)
3	65.1	4.35	obsc
4	20.5	1.23	d (7.1)
DAPA2			
NH	-	8.26	d (8.7)
1	169.0	-	-
2	52.2	4.28	ddd (8.5, 8.5, 7.7)
3	40.0	3.13	m
		2.89	obsc
Phe			
NH	-	7.3	d (8.6)
1	171.2	-	-
2	53.7	4.76	obsc
3	37.5	2.89	obsc
		2.72	obsc
4	137.2	-	-
5/9	129.2	7.34	m
6/8	127.6	7.21	m
7	125.9	7.16	m
3OHVal			
NH	-	8.60	d (9.8)
1	169.3	-	-
2	58.1	4.70	d (9.8)
3	71.3	-	-
4	26.4	1.05	s
5	26.6	0.91	s
Asp			
NH	-	8.49	d (9.6)
1	171.7	-	-
2	48.5	4.75	obsc
3	40.6	2.84	dd (15.8, 4.7)
		2.25	br d (15.8)
4	173.8	-	-

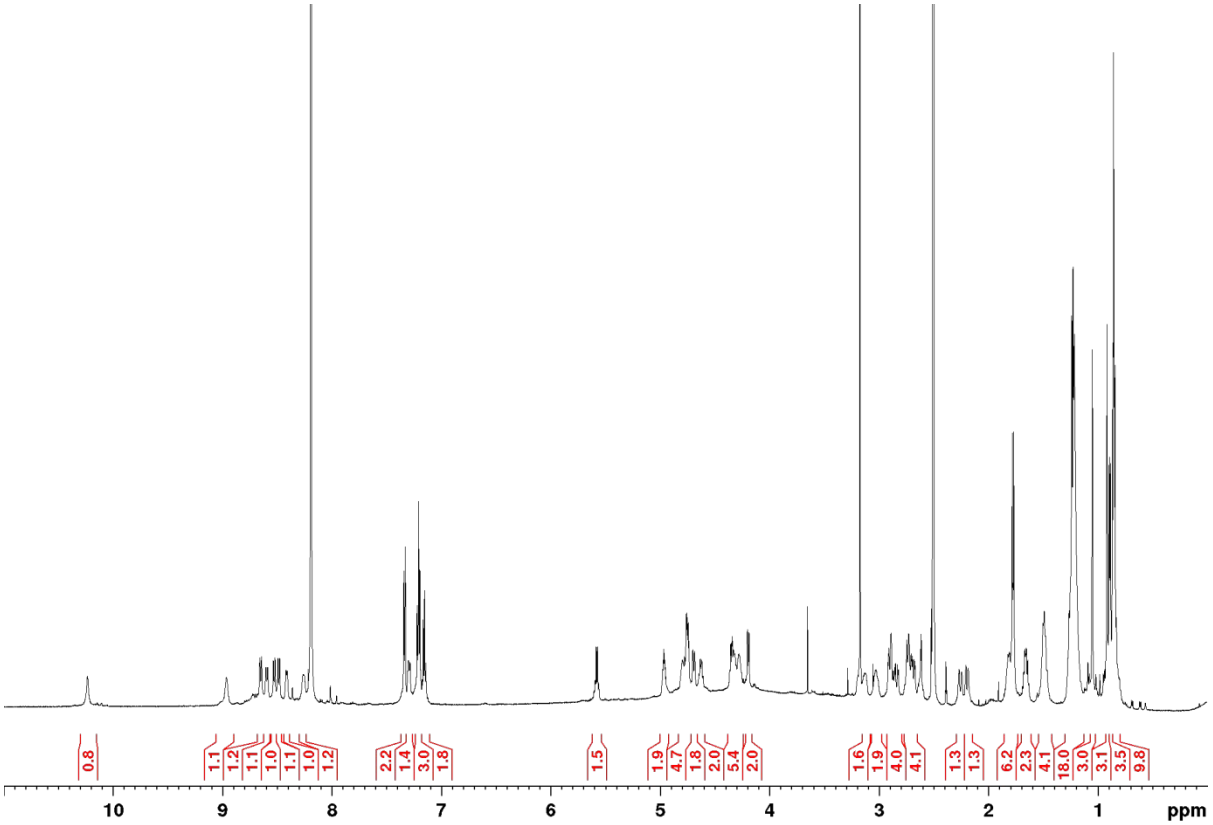

Figure S10. ^{1}H-NMR spectrum of compound **2** (DMSO-d_6, 600 MHz, 298 K).

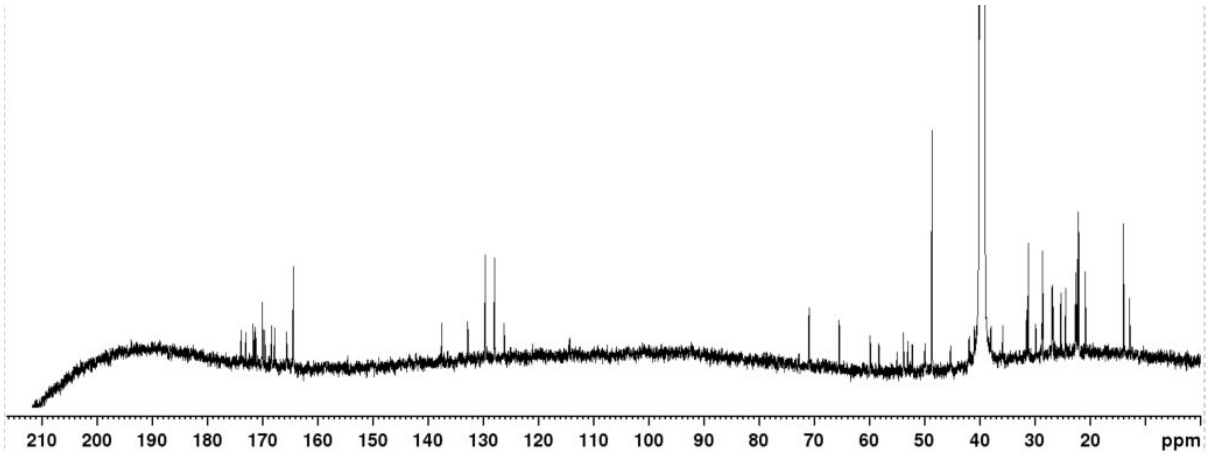

Figure S11. ^{13}C-NMR spectrum of compound **2** (DMSO-d_6, 150 MHz, 298 K).

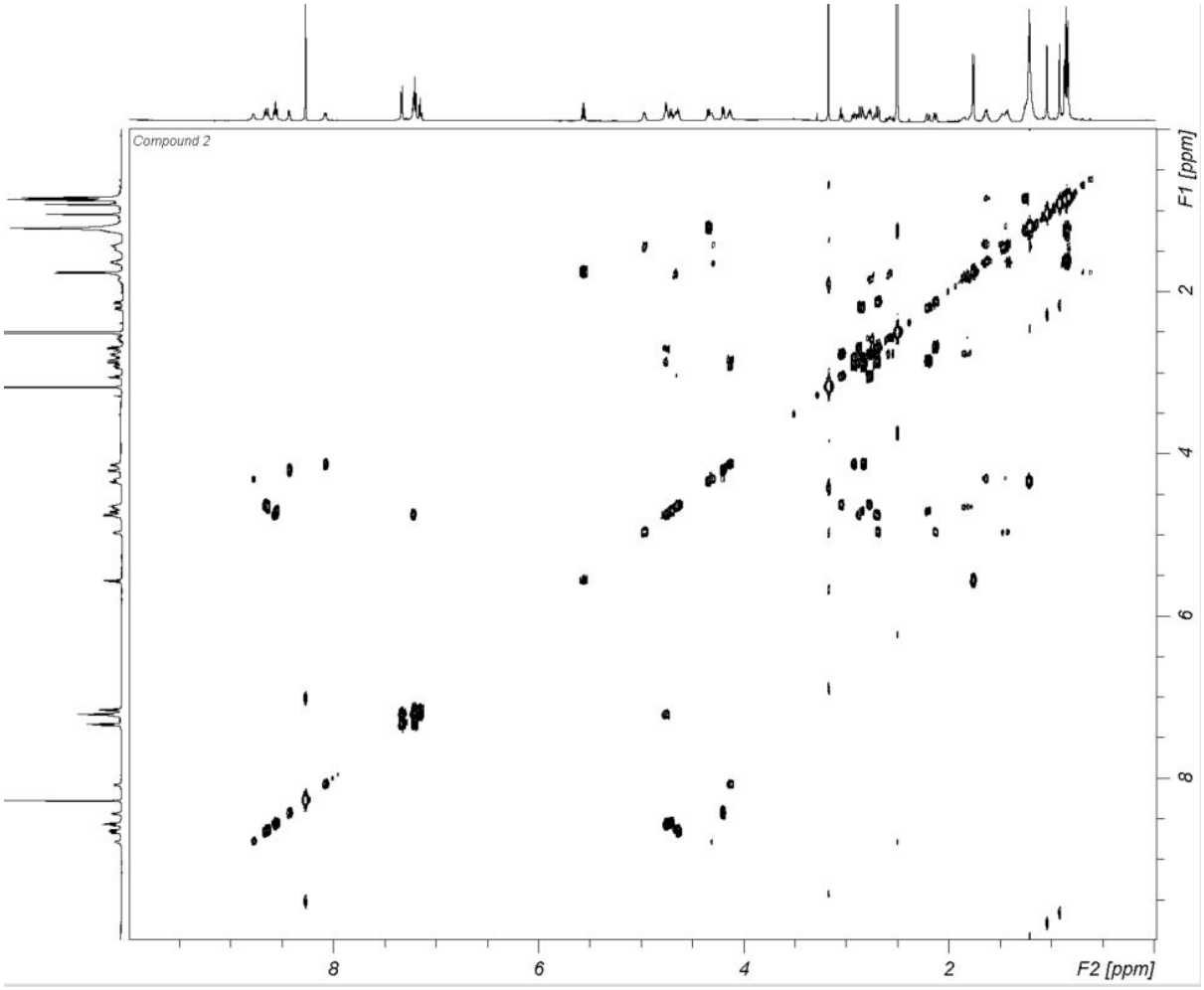

Figure S12. COSY spectrum of compound **2** (DMSO-d_6, 600 MHz, 298 K).

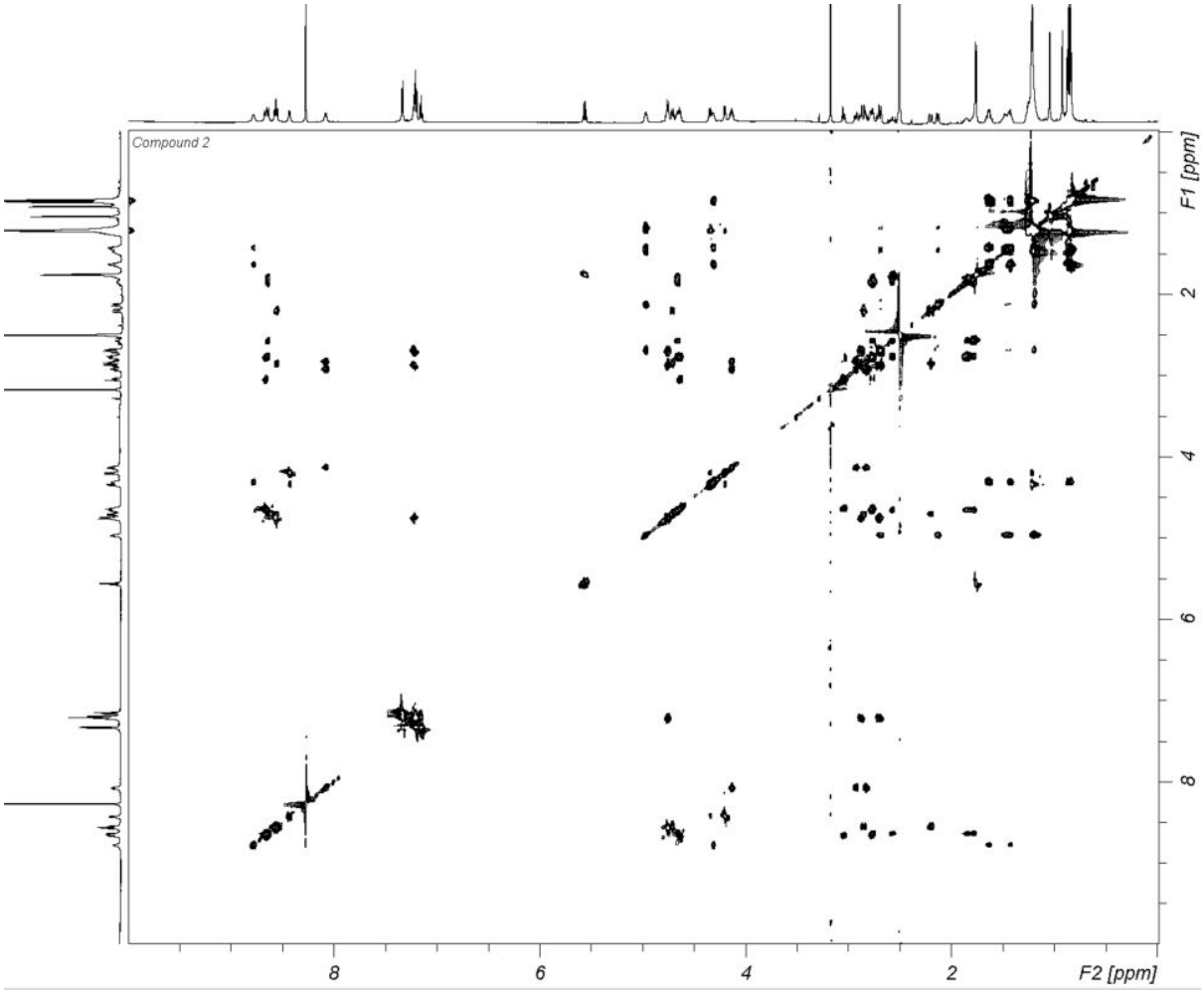

Figure S13. TOCSY spectrum of compound **2** (DMSO-d_6, 600 MHz, 298 K).

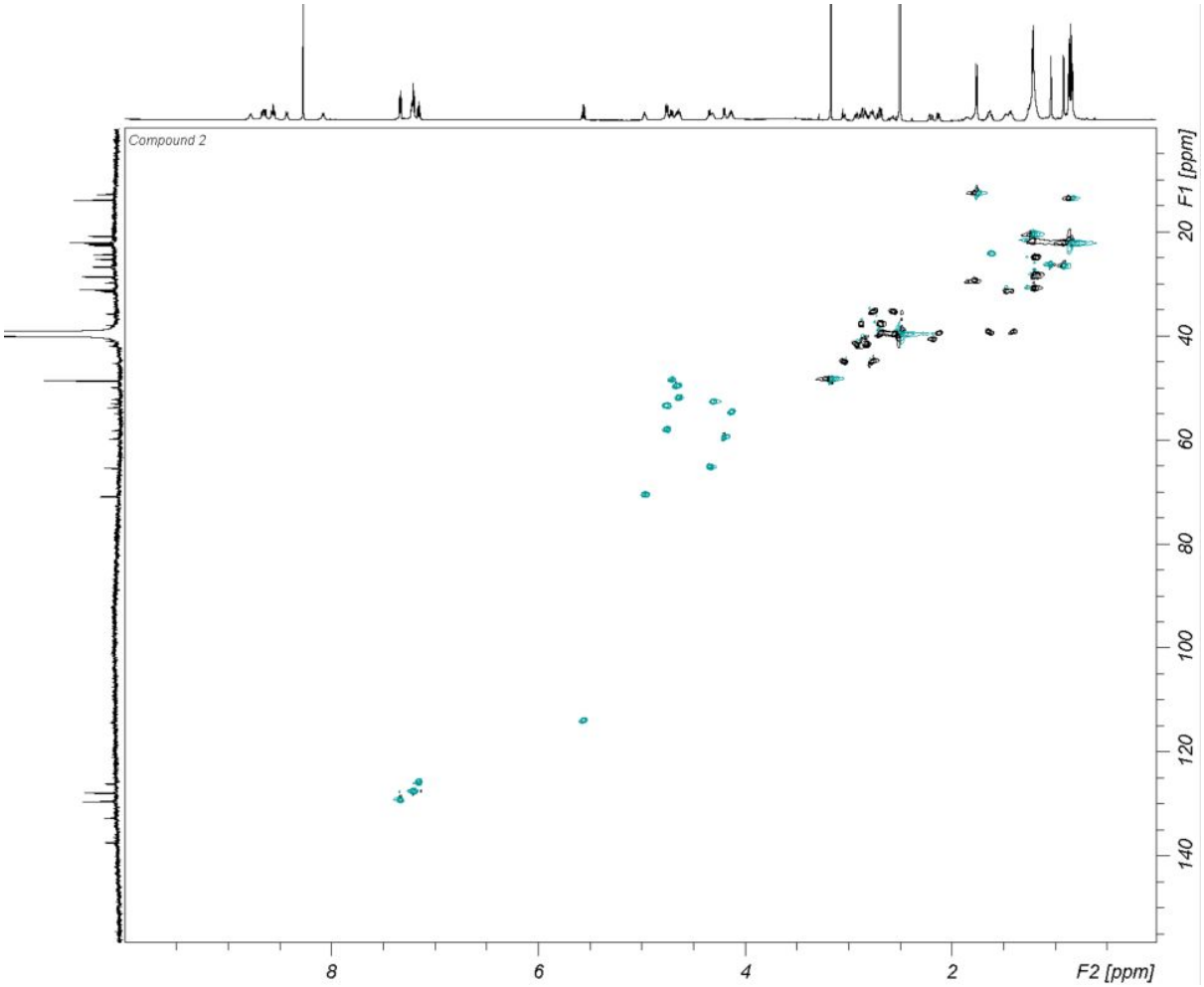

Figure S14. HSCQ spectrum of compound **2** (DMSO-d_6, 600 MHz, 298 K).

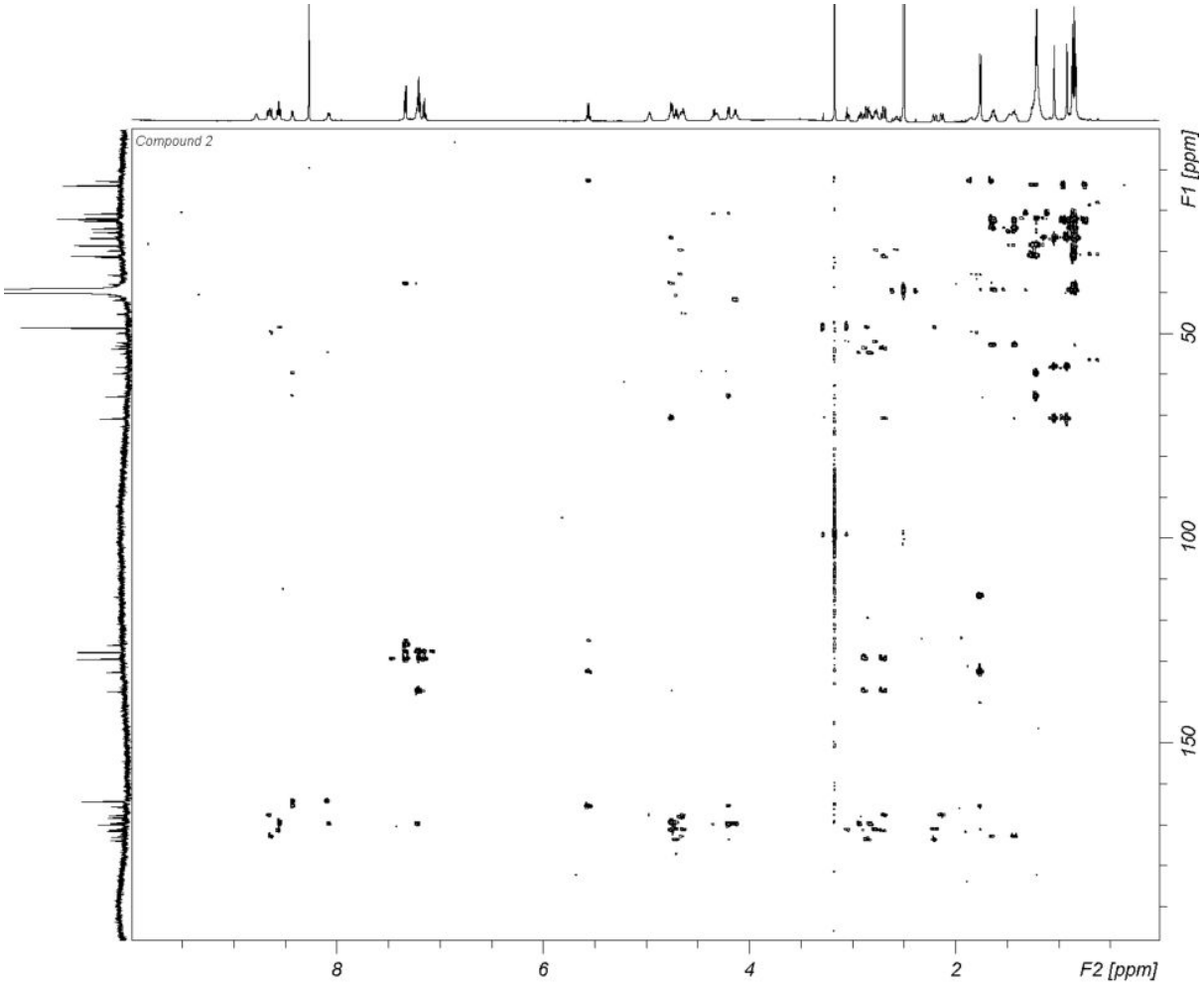

Figure S15. HMBC spectrum of compound **2** (DMSO-d_6, 600 MHz, 298 K).

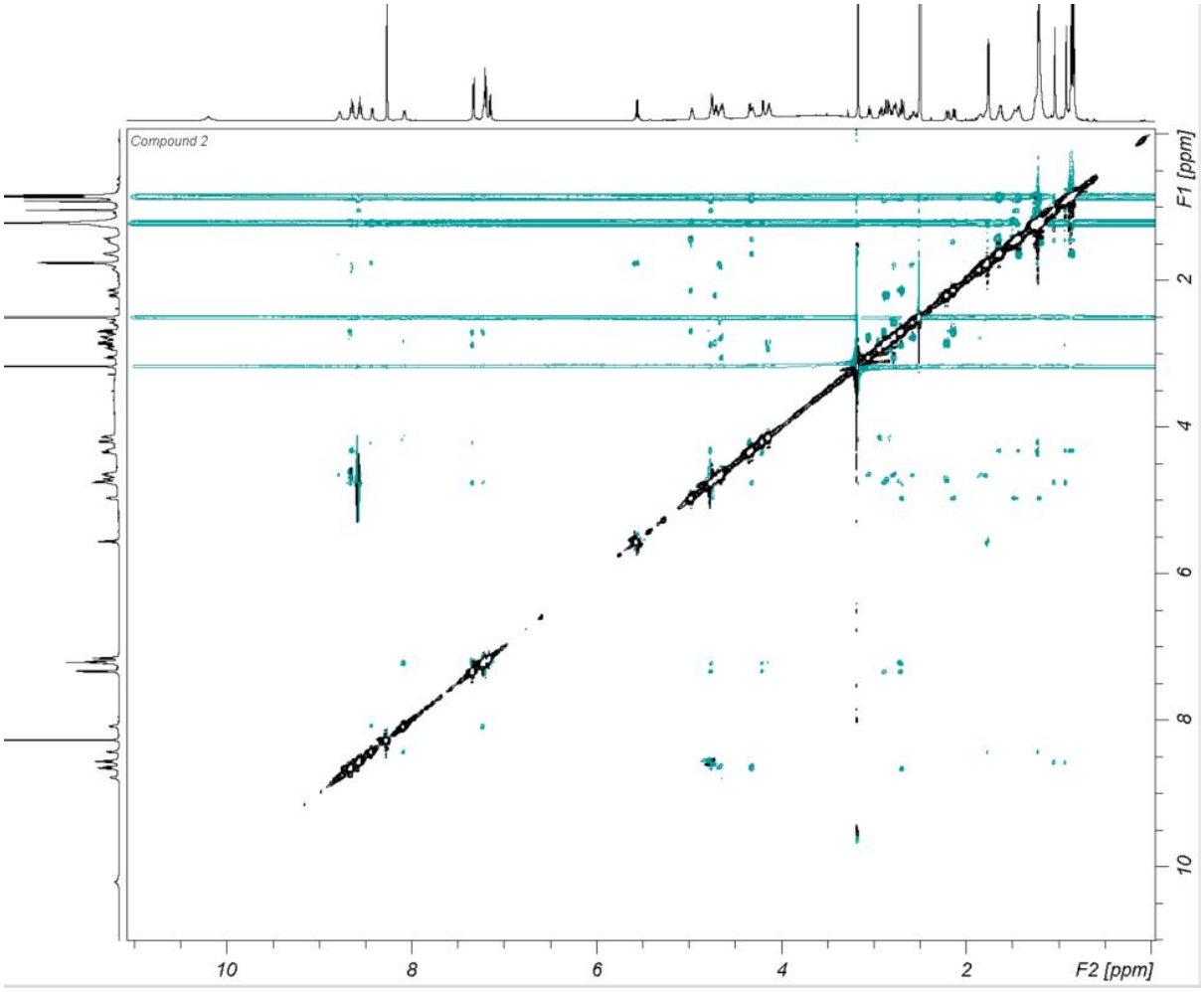

Figure S16. ROESY spectrum of compound **2** (DMSO-d_6, 600 MHz, 298 K).

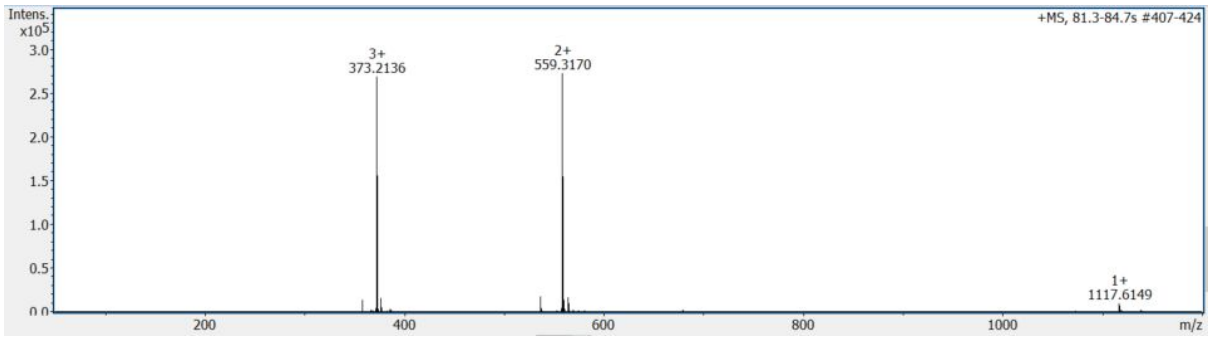

Figure S17. HRMS spectrum of compound **2**.

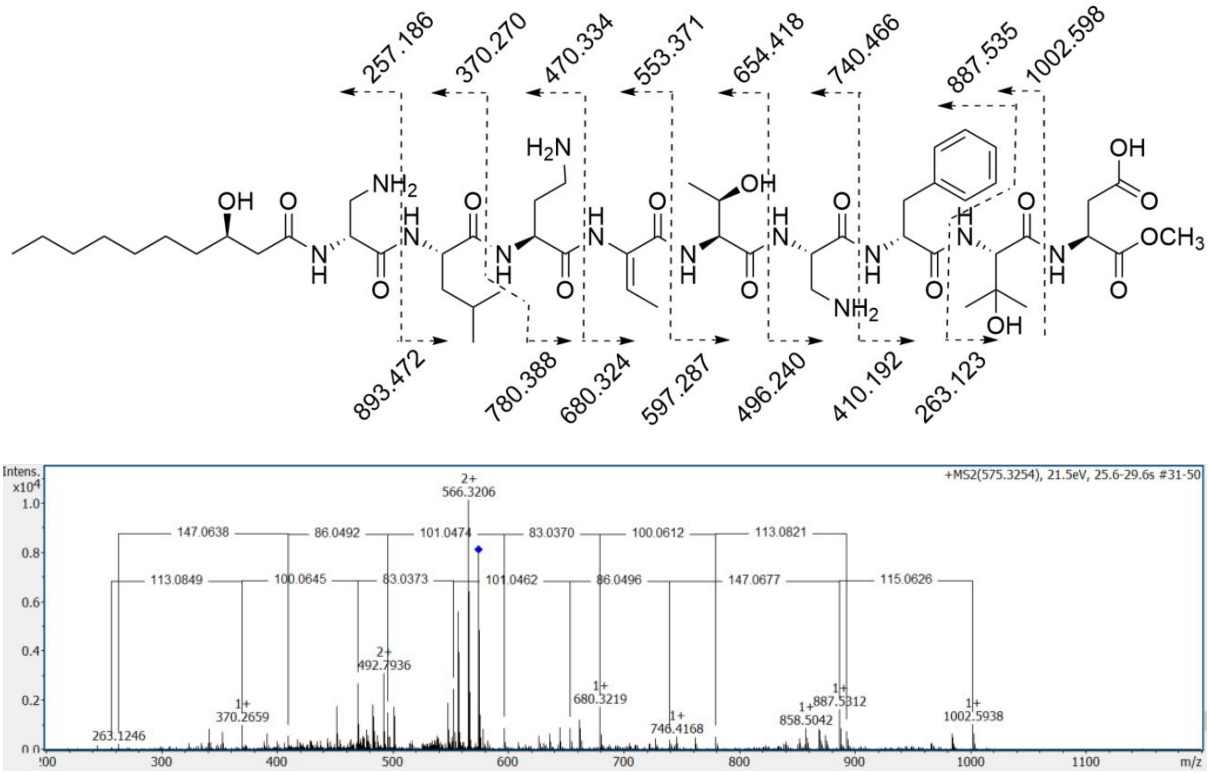

Figure S18. MSMS spectrum of compound **2** after ring-opening with NaOMe in MeOH. Mass differences between Y-series ions (top) and B-series ions (bottom) are shown in the mass spectrum. Theoretical m/z-values for the observed B- and Y-series ions are shown in the structure on top.

Table S3. ^{1}H and ^{13}C NMR-data (600 and 150 MHz, resp) for compound **3** (DMSO-d_6, 30°C)

Pos.	^{13}C	^{1}H	Mult (*J*, Hz)
3OHFA			
1	167.8	-	-
2	38.8	2.64	obsc
		2.24	obsc
3	70.7	4.95	m
4	29.3	2.34	ddd (14.6, 7.3, 7.3)
		2.22	obsc
5	123.9	5.29	m (10.8)
6	132.1	5.40	m (10.8)
7	26.4	1.98	m
8	28.4	1.29	obsc
9	28.0	1.25	obsc
10	30.8	1.24	obsc
11	21.7	1.26	obsc
12	13.6	0.86	t (6.9)
DAPA1			
NH	-	8.51	d (9.0)
1	170.6	-	-
2	50.4	4.76	obsc
3	43.4	3.18	dd (13.1, 6.0)
		2.96	dd (13.1, 3.8)
Leu			
NH	-	8.91	br s
1	173.3	-	-
2	52.8	4.34	obsc
3	39.2	1.64	obsc
		1.47	m
4	24.1	1.64	obsc
5	21.9	0.88	d (6.1)
6	22.0	0.86	d (5.7)
DABA			
NH	-	8.61	d (9.5)
1	167.9	-	-
2	49.5	4.64	ddd (9.5, 7.2, 7.2)
3	29.3	1.81	m
4	35.5	2.74	m
		2.61	m
ABA			
NH	-	10.26	br s
1	165.6	-	-
2	132.6	-	-
3	114.1	5.57	q (7.2)
4	12.5	1.77	d (7.2)
Thr			
NH	-	8.43	d (7.7)
1	169.3	-	-
2	59.5	4.20	dd (7.7, 2.3)
3	65.0	4.35	obsc
4	20.5	1.22	d (6.5)
DAPA2			
NH	-	8.17	d (8.6)
1	169.4	-	-
2	53.1	4.23	ddd (8.6, 8.6, 5.8)
3	40.0	3.13	m
		2.89	obsc
Phe			
NH	-	7.29	d (8.9)
1	169.5	-	-
2	53.5	4.76	obsc
3	37.5	2.89	dd (13.6, 4.3)
		2.72	dd (13.6, 10.2)
4	137.2	-	-
5/9	129.2	7.33	m
6/8	127.6	7.21	m
7	125.8	7.15	m
3OHVal			
NH	-	8.53	d (10.0)
1	171.1	-	-
2	58.9	4.72	d (10.0)
3	70.8	-	-
4	26.5	1.05	s
5	26.5	0.90	s
Asp			
NH	-	8.53	d (9.6)
1	170.5	-	-
2	48.4	4.74	obsc
3	40.6	2.83	dd (16.0, 4.7)
		2.23	obsc
4	173.8	-	-

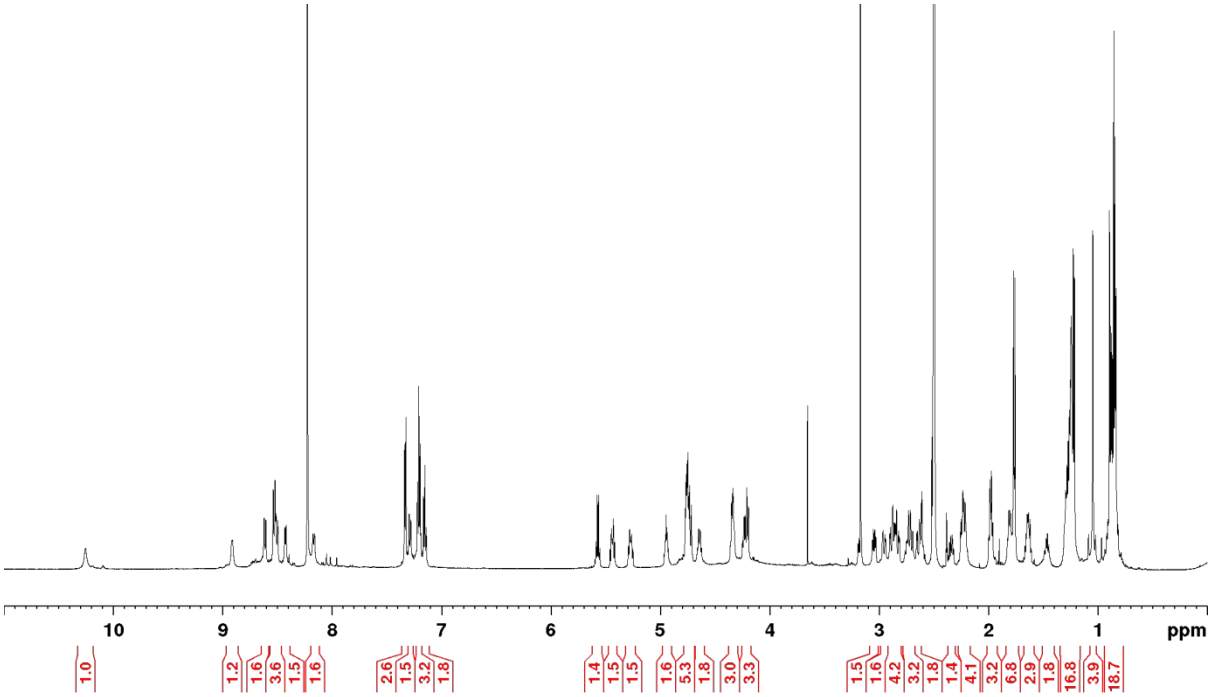

Figure S19. ^{1}H-NMR spectrum of compound **3** (DMSO-d_6, 600 MHz, 298 K).

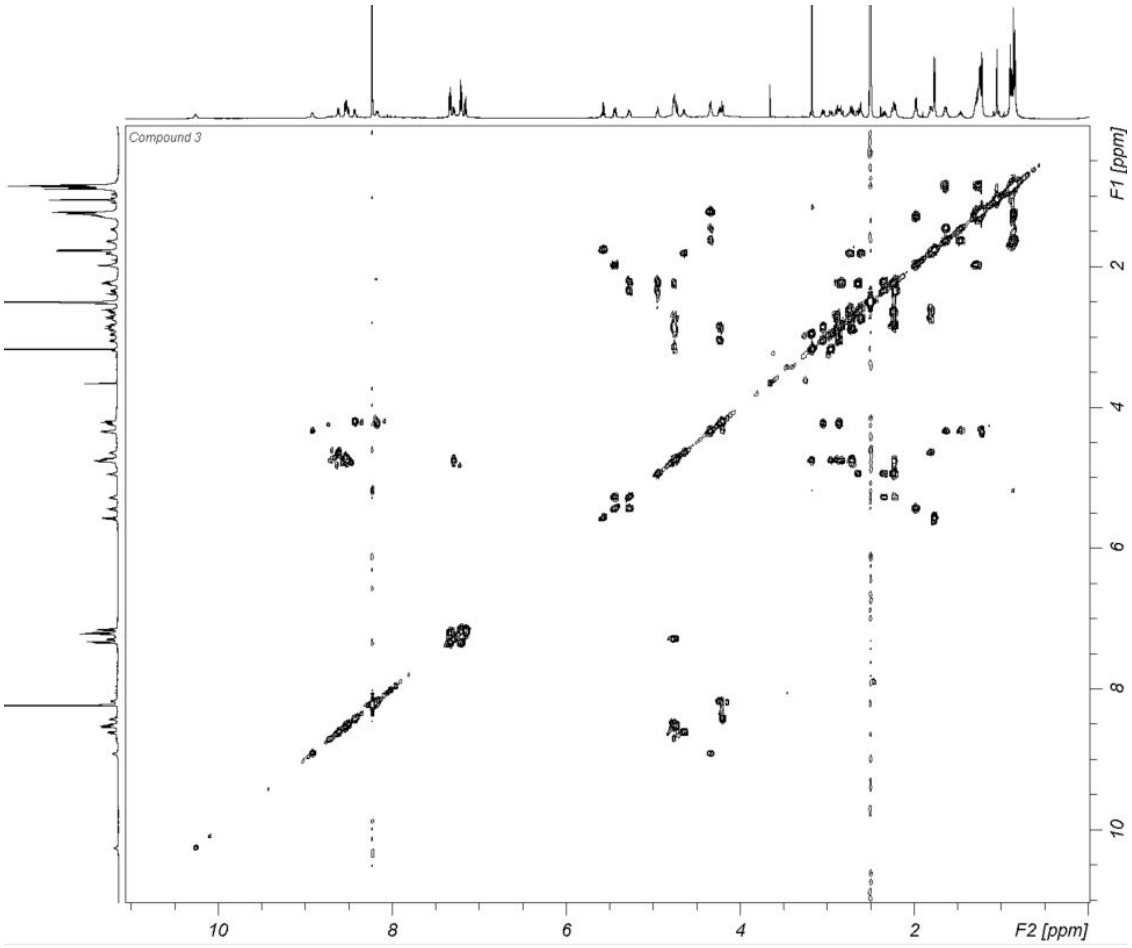

Figure S20. COSY spectrum of compound **3** (DMSO-d_6, 600 MHz, 298 K).

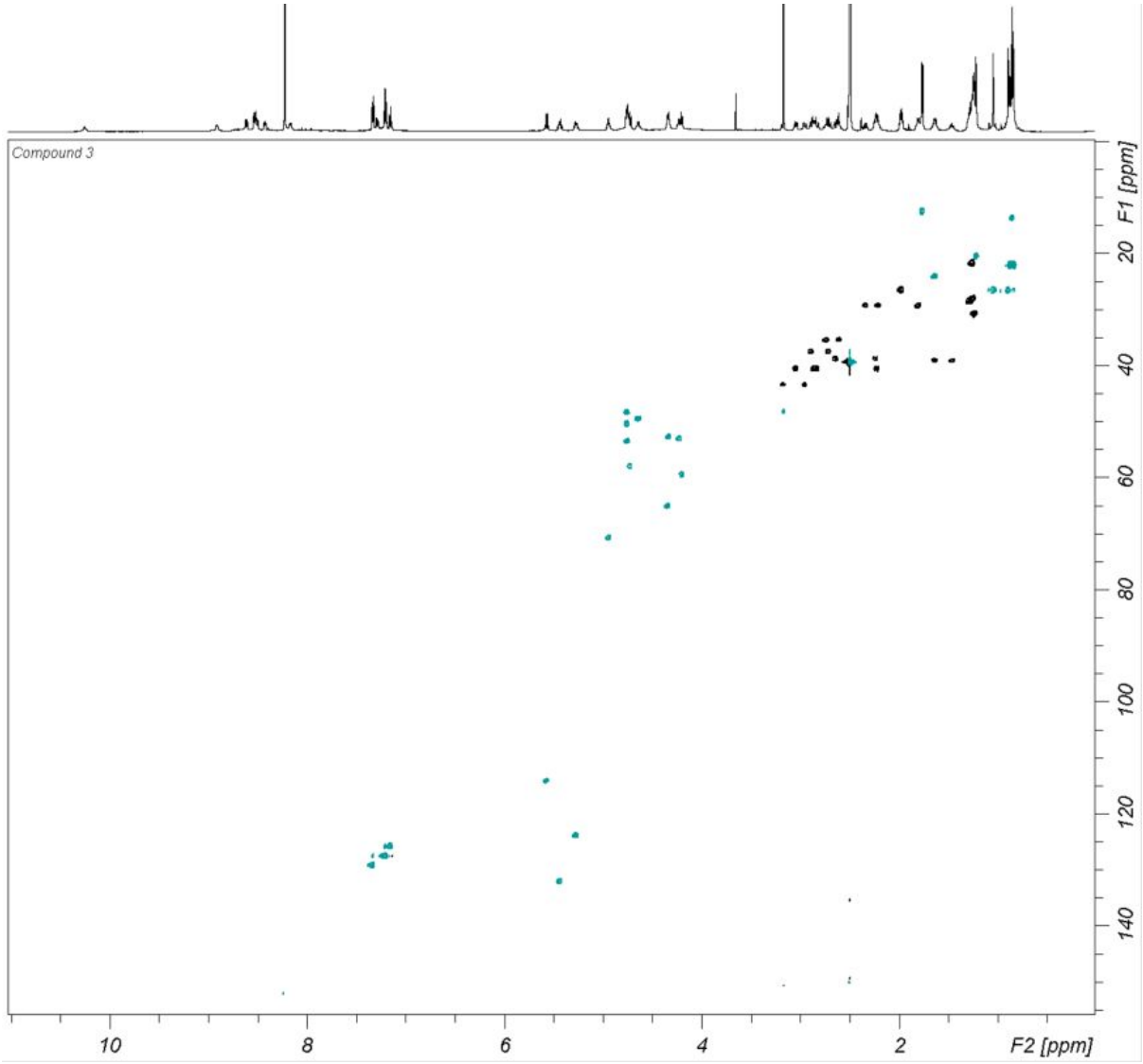

Figure S21. HSQC spectrum of compound **3** (DMSO-d_6, 600 MHz, 298 K).

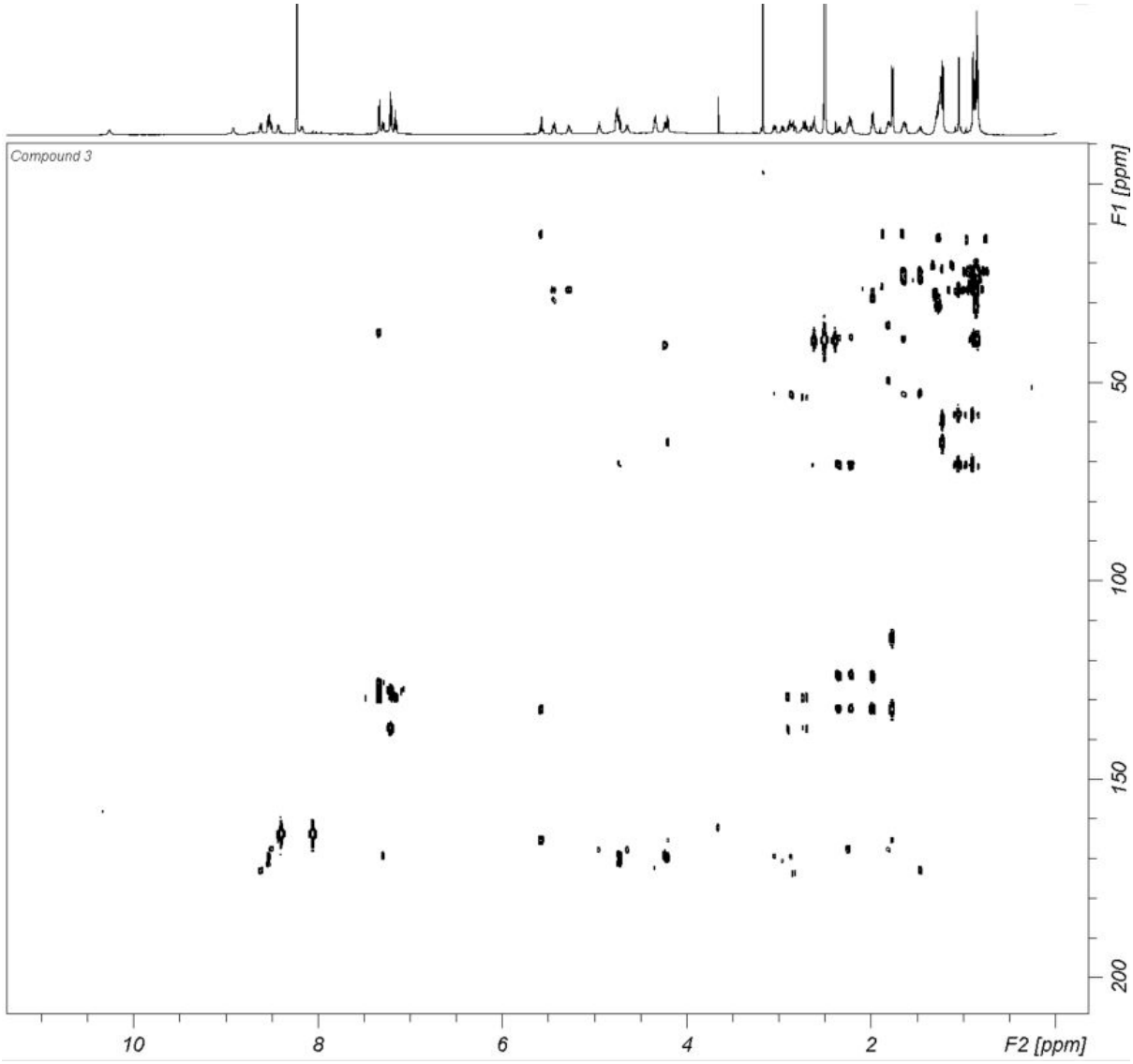

Figure S22. HMBC spectrum of compound **3** (DMSO-d_6, 600 MHz, 298 K).

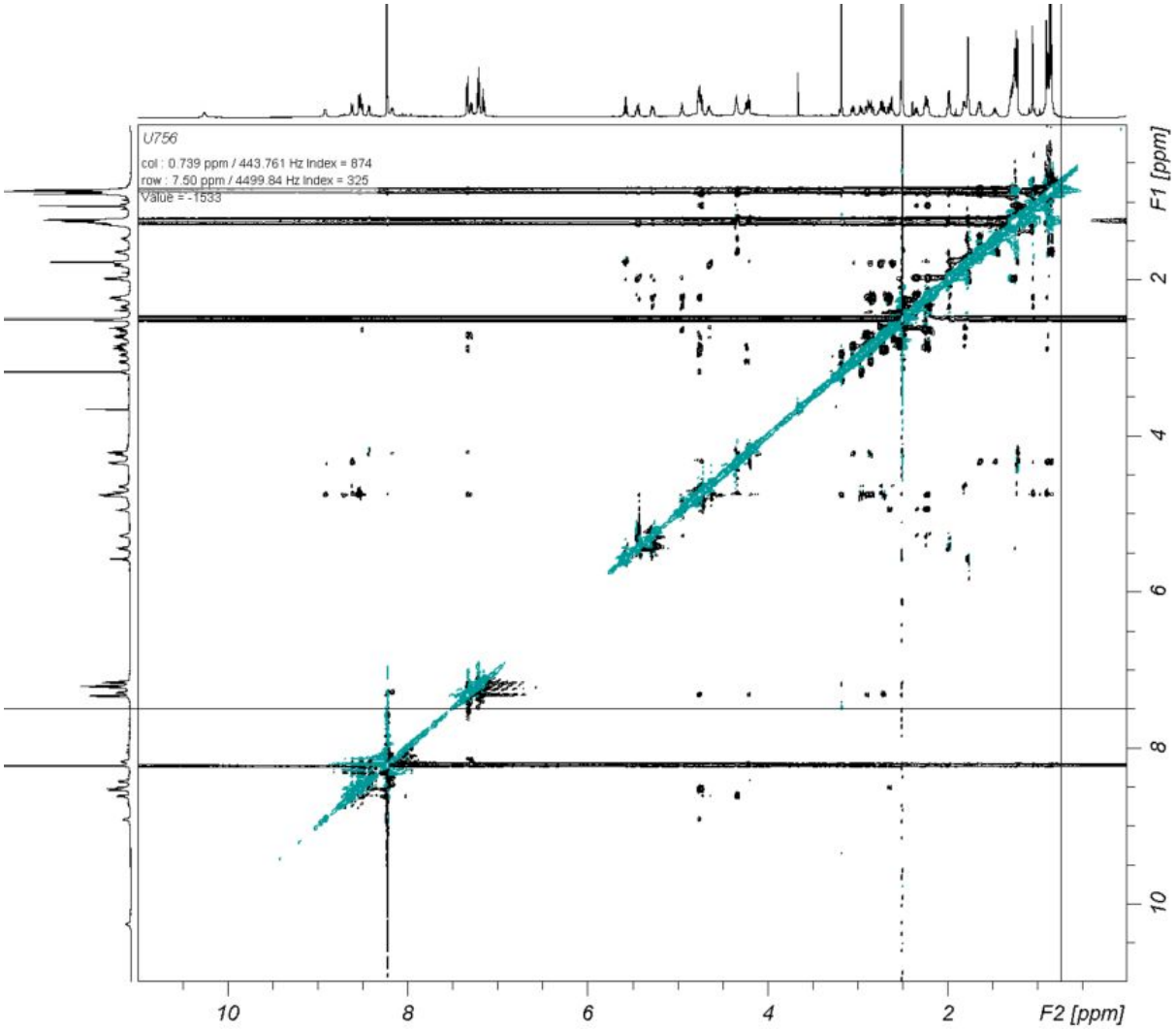

Figure S23. ROESY spectrum of compound **3** (DMSO-d_6, 600 MHz, 298 K).

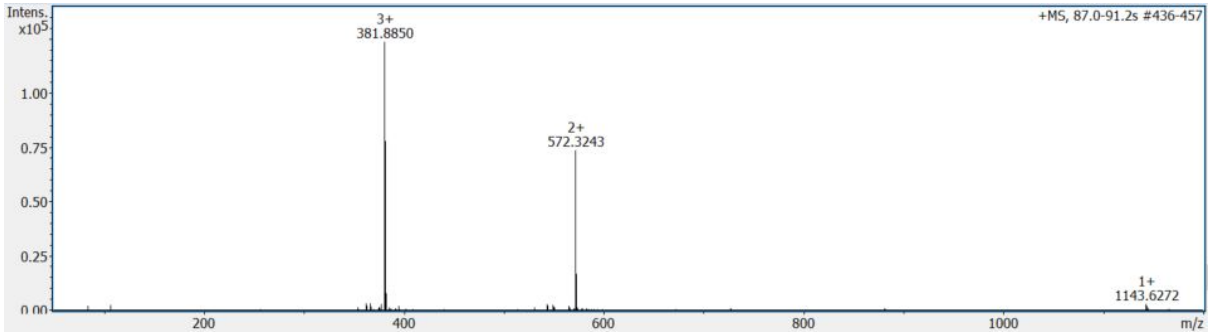

Figure S24. HRMS spectrum of compound **3**.

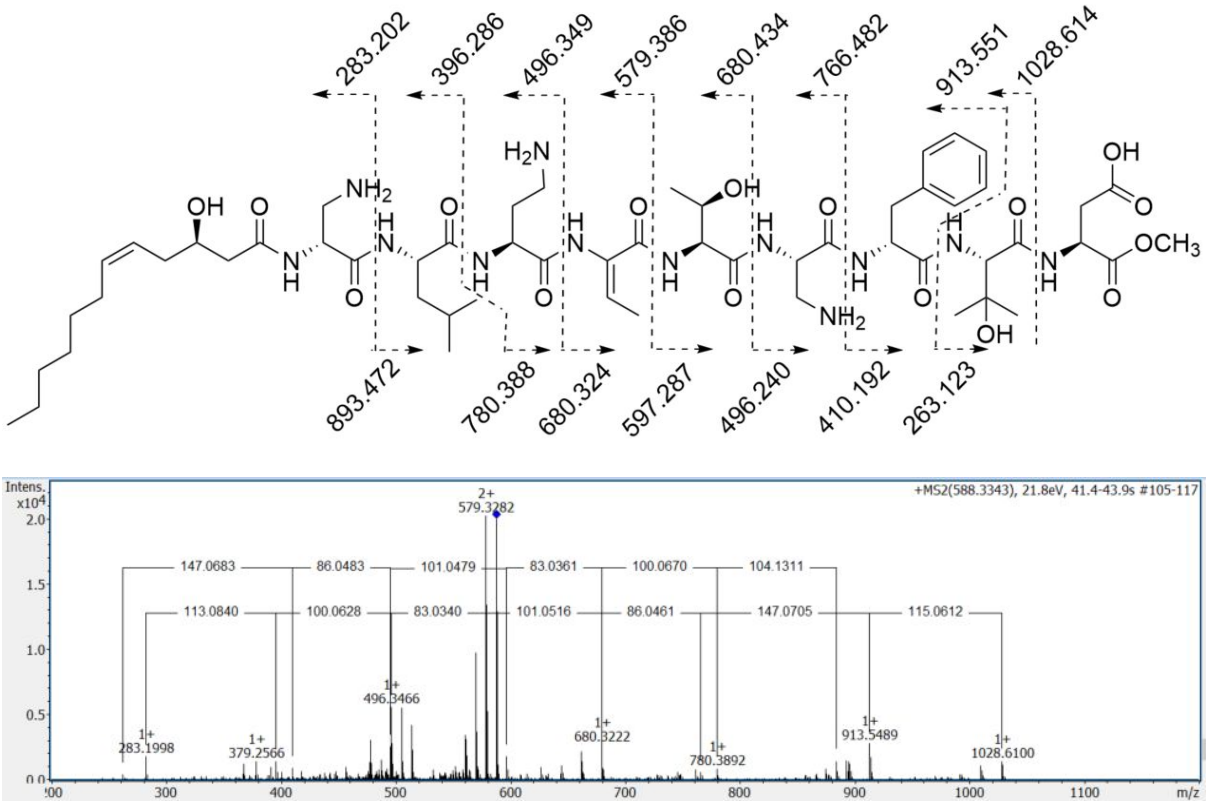

Figure S25. MSMS spectrum of compound **3** after ring-opening with NaOMe in MeOH. Mass differences between Y-series ions (top) and B-series ions (bottom) are shown in the mass spectrum. Theoretical m/z-values for the observed B- and Y-series ions are shown in the structure on top.

Table S4. ^{1}H and ^{13}C NMR-data (600 and 150 MHz, resp) for compound **4** (DMSO-d_6, 30°C)

Pos.	^{13}C	^{1}H	Mult (*J*, Hz)
3OHFA			
1	167.6	-	-
2	39.4	2.70	obsc
		2.16	dd (13.6, 3.2)
3	70.6	4.95	m
4	31.2	1.45	m
5	28.0	1.20	obsc
6	28.0	1.20	obsc
7	28.0	1.20	obsc
8	30.8	1.20	obsc
9	21.5	1.24	obsc
10	13.5	0.85	t (7.1)
DAPA1			
NH	-	8.65	d (9.8)
1	170.4	-	-
2	50.3	4.77	m
3	44.0	3.19	dd (13.5, 5.5)
		2.94	dd (13.5, 3.7)
Leu			
NH	-	8.91	br d (4.4)
1	173.0	-	-
2	53.0	4.28	m
3	39.2	1.64	m
		1.50	m
4	24.0	1.70	m
5	22.2	0.91	d (6.4)
6	22.2	0.86	d (6.6)
DABA			
NH	-	8.67	d (9.6)
1	168.1	-	-
2	49.4	4.63	m
3	29.0	1.82	obsc
4	35.4	2.73	obsc
		2.61	obsc
ABA			
NH	-	10.23	br s
1	165.4	-	-
2	132.4	-	-
3	114.3	5.58	q (7.3)
4	12.5	1.77	d (7.3)
Thr			
NH	-	8.44	d (7.7)
1	169.7	-	-
2	59.5	4.20	dd (7.7, 2.3)
3	65.0	4.35	dq (2.5, 6.5)
4	20.4	1.23	d (6.5)
DAPA2			
NH	-	8.18	d (8.7)
1	169.2	-	-
2	53.4	4.24	ddd (8.7, 8.7, 5.4)
3	40.6	3.05	dd (13.1, 5.4)
		2.87	dd (13.1, 9.0)
Phe			
NH	-	7.20	d (9.0)
1	171.1	-	-
2	53.3	4.76	obsc
3	37.8	2.83	dd (13.1, 5.1)
		2.72	obsc
4	136.9	-	-
5/9	129.1	7.30	m
6/8	127.6	7.20	m
7	125.8	7.15	m
Val			
NH	-	8.60	d (9.7)
1	169.8	-	-
2	56.2	4.60	dd (9.7, 7.2)
3	30.5	1.79	obsc
4	17.7	0.69	d (6.8)
5	18.6	0.61	d (6.8)
Asp			
NH	-	8.48	d (9.8)
1	n.d.	-	-
2	48.5	4.73	ddd (9.8, 4.2, 4.2)
3	40.7	2.83	obsc
		2.22	dd (15.6, 4.2)
4	174.6	-	-

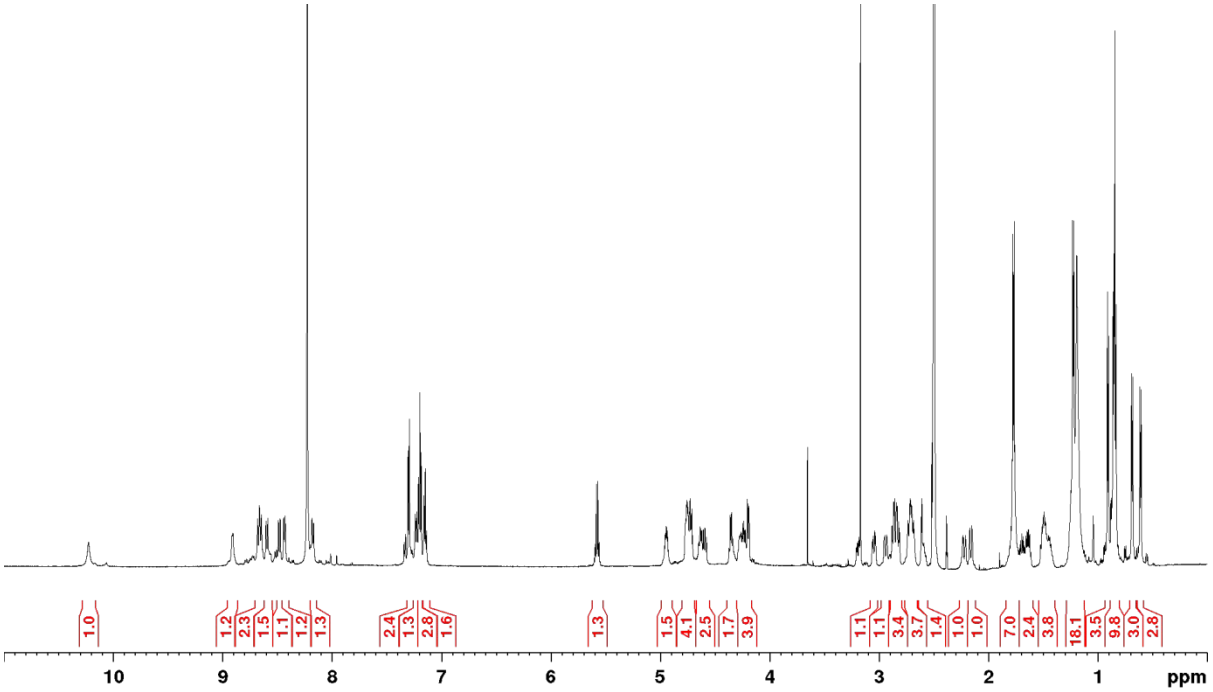

Figure S26. ^{1}H-NMR spectrum of compound **4** (DMSO-d_6, 600 MHz, 298 K).

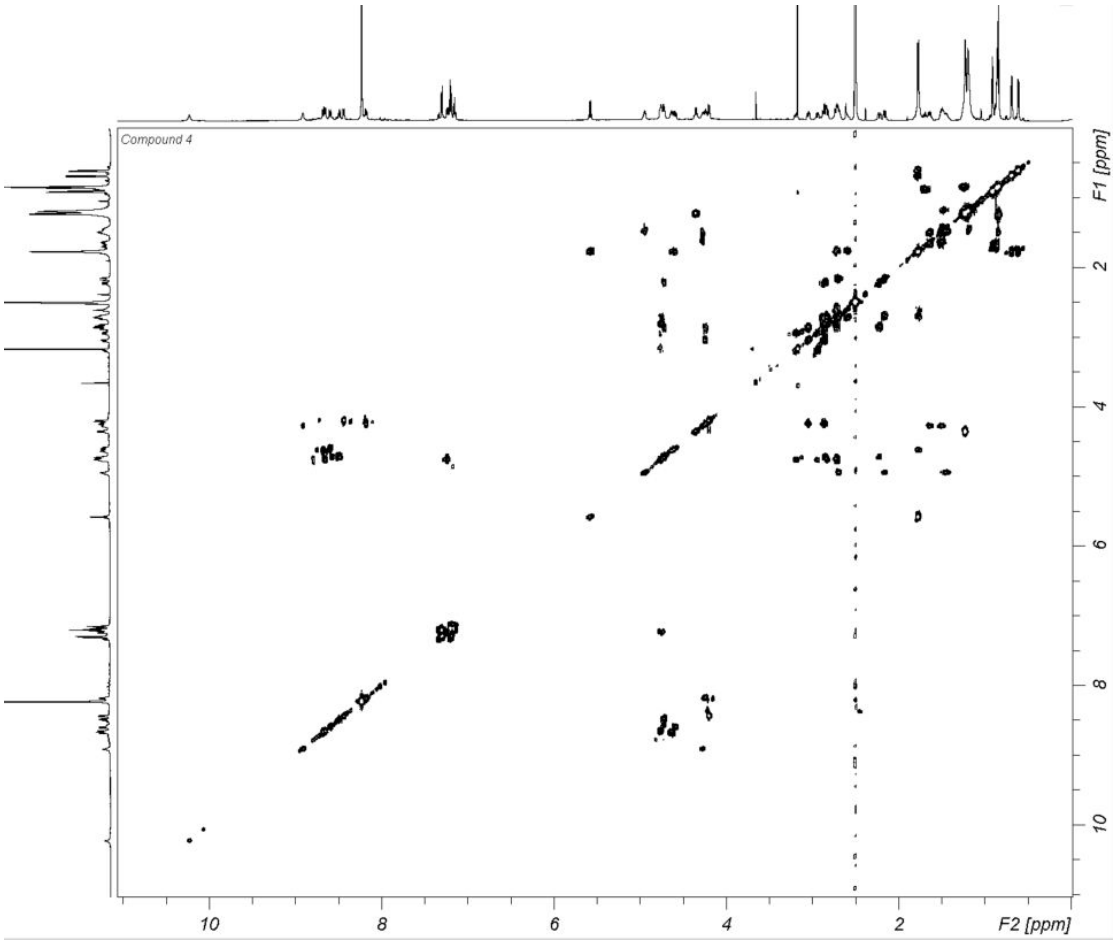

Figure S27. COSY spectrum of compound **4** (DMSO-d_6, 600 MHz, 298 K).

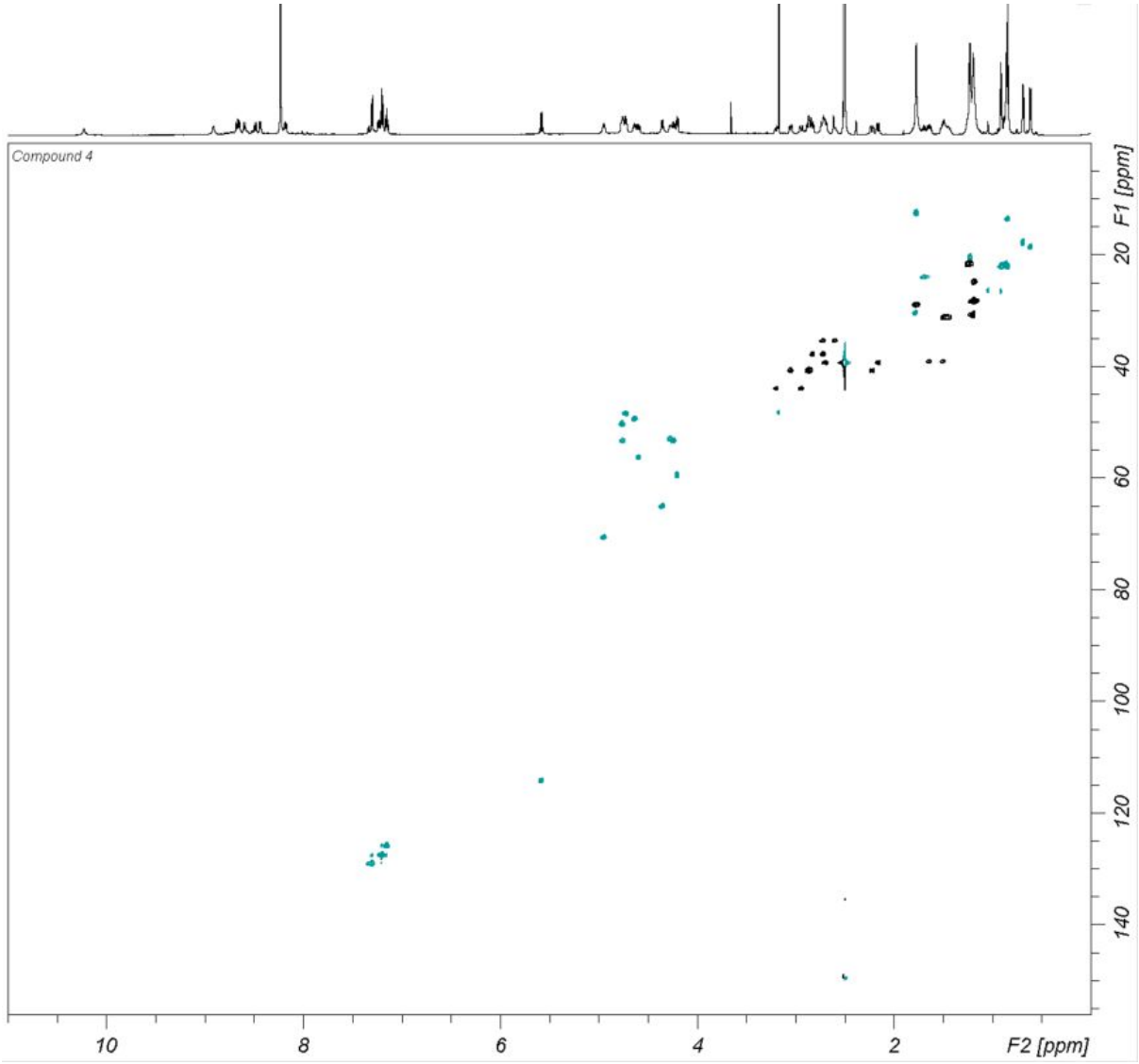

Figure S28. HSQC spectrum of compound **4** (DMSO-d_6, 600 MHz, 298 K).

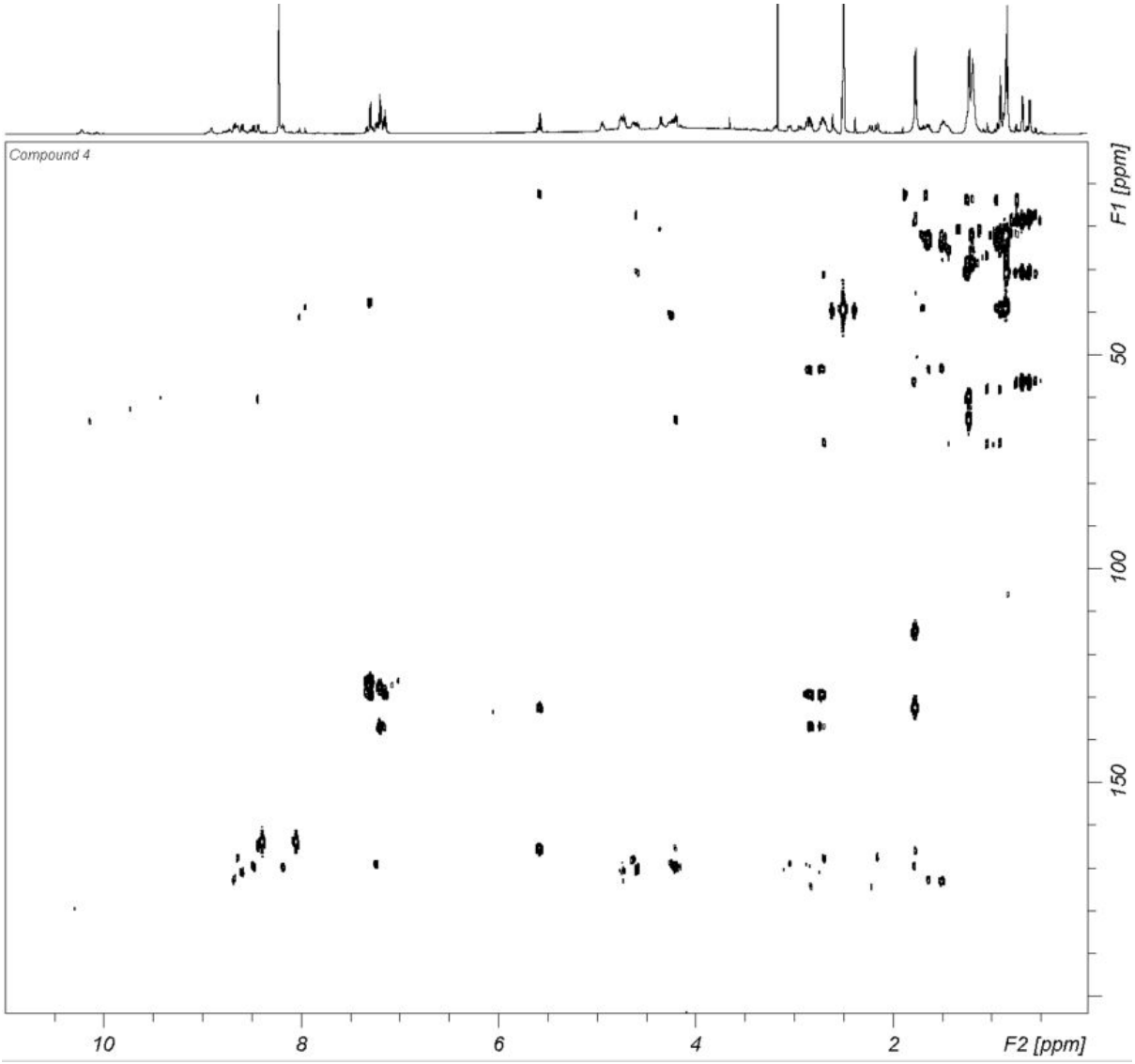

Figure S29. HMBC spectrum of compound **4** (DMSO-d_6, 600 MHz, 298 K).

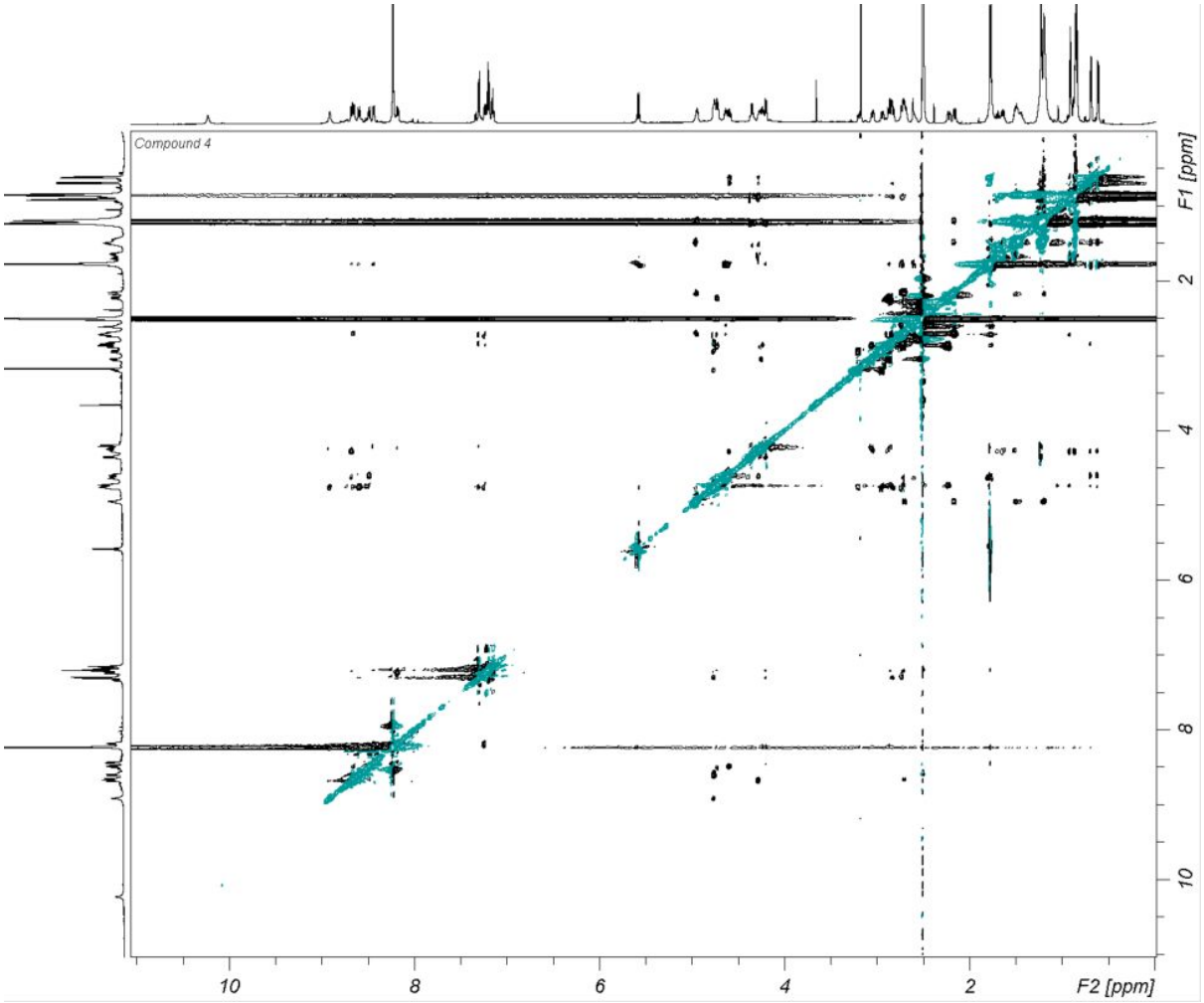

Figure S30. ROESY spectrum of compound **4** (DMSO-d_6, 600 MHz, 298 K).

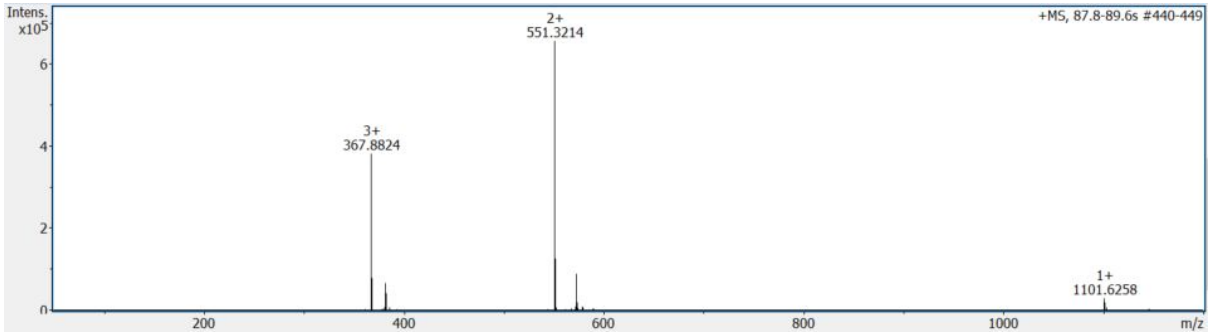

Figure S31. HR-MS spectrum of compound **4**.

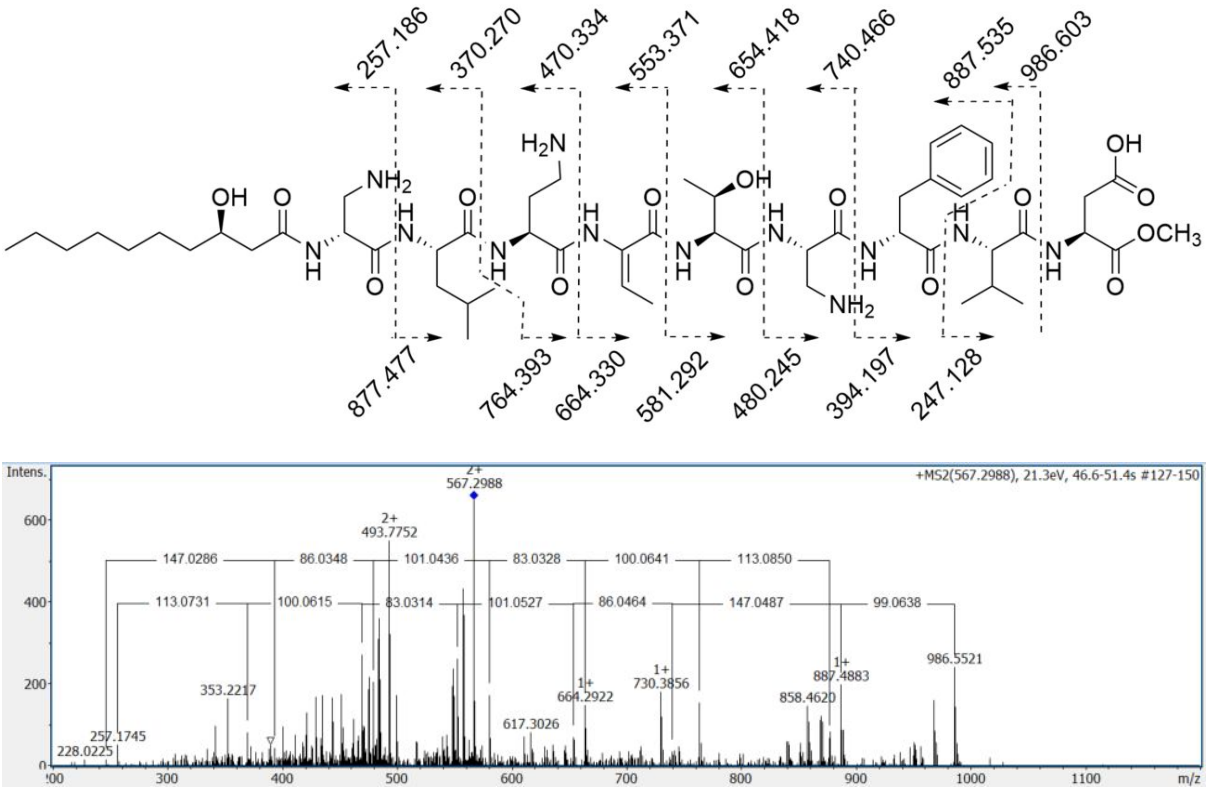

Figure S32. MSMS spectrum of compound **4** after treatment with NaOMe in MeOH. Mass differences between Y-series ions (top) and B-series ions (bottom) are shown in the mass spectrum. Theoretical m/z-values for the observed B- and Y-series ions are shown in the structure on top.

Table S5. ^{1}H and ^{13}C NMR-data (600 and 150 MHz, resp) for compound **5** (DMSO-d_6 30°C)

Pos.	^{13}C	^{1}H	Mult (*J*, Hz)
3OHFA			
1	168.2	-	-
2	39.4	2.69	dd (13.6, 4.1)
		2.15	dd (13.6, 3.0)
3	70.6	4.94	m
4	31.3	1.46	obsc
5	26.2	1.19	obsc
6	28.8	1.19	obsc
7	24.9	1.19	obsc
8	38.0	1.10	m
9	27.0	1.47	obsc
10	22.2	0.83	d (6.6)
11	22.2	0.83	d (6.6)
DAPA1			
NH	-	8.66	d (8.4)
1	169.0	-	-
2	48.4	4.72	obsc
3	44.3	3.18	br d (13.1)
		2.91	br d (13.1)
Leu			
NH	-	8.86	br s
1	172.9	-	-
2	52.9	4.27	m
3	39.2	1.64	m
		1.50	obsc
4	24.0	1.69	m
5	22.1	0.91	d (6.5)
6	21.8	0.86	d (6.5)
DABA			
NH	-	8.67	d (9.3)
1	168.1	-	-
2	49.5	4.63	m
3	29.1	1.77	obsc
4	35.5	2.73	obsc
		2.60	obsc
ABA			
NH	-	10.20	br s
1	165.5	-	-
2	132.8	-	-
3	114.4	5.58	q (7.3)
4	12.5	1.77	d (7.3)
Thr			
NH	-	8.42	d (7.7)
1	169.7	-	-
2	59.6	4.20	dd (7.7, 2.3)
3	65.1	4.35	dq (2.3, 6.4)
4	20.5	1.23	d (6.4)
DAPA2			
NH	-	8.16	d (9.2)
1	169.4	-	-
2	53.9	4.22	m
3	41.0	3.01	br d (13.1)
		2.86	obsc
Phe			
NH	-	7.22	obsc
1	170.7	-	-
2	53.3	4.76	obsc
3	37.9	2.82	dd (13.3, 5.0)
		2.72	obsc
4	137.0	-	-
5/9	129.1	7.30	m
6/8	127.6	7.20	m
7	125.8	7.15	m
Val			
NH	-	8.59	d (9.5)
1	170.3	-	-
2	56.3	4.60	dd (9.5, 7.2)
3	30.5	1.78	obsc
4	17.7	0.69	d (6.9)
5	18.6	0.62	d (6.9)
Asp			
NH	-	8.49	d (9.8)
1	n.d.	-	-
2	48.4	4.72	obsc
3	40.8	2.87	obsc
		2.22	dd (15.7, 4.0)
4	n.d.	-	-

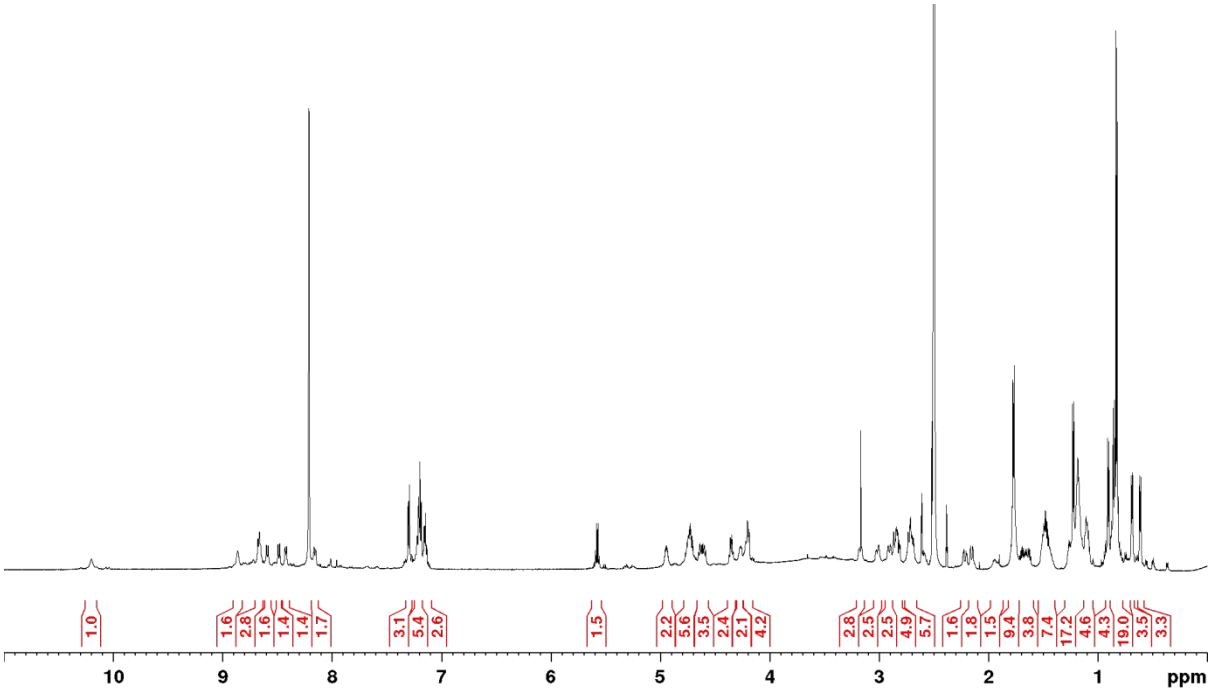

Figure S33. ^{1}H-NMR spectrum of compound **5** (DMSO-d_6, 600 MHz, 298 K).

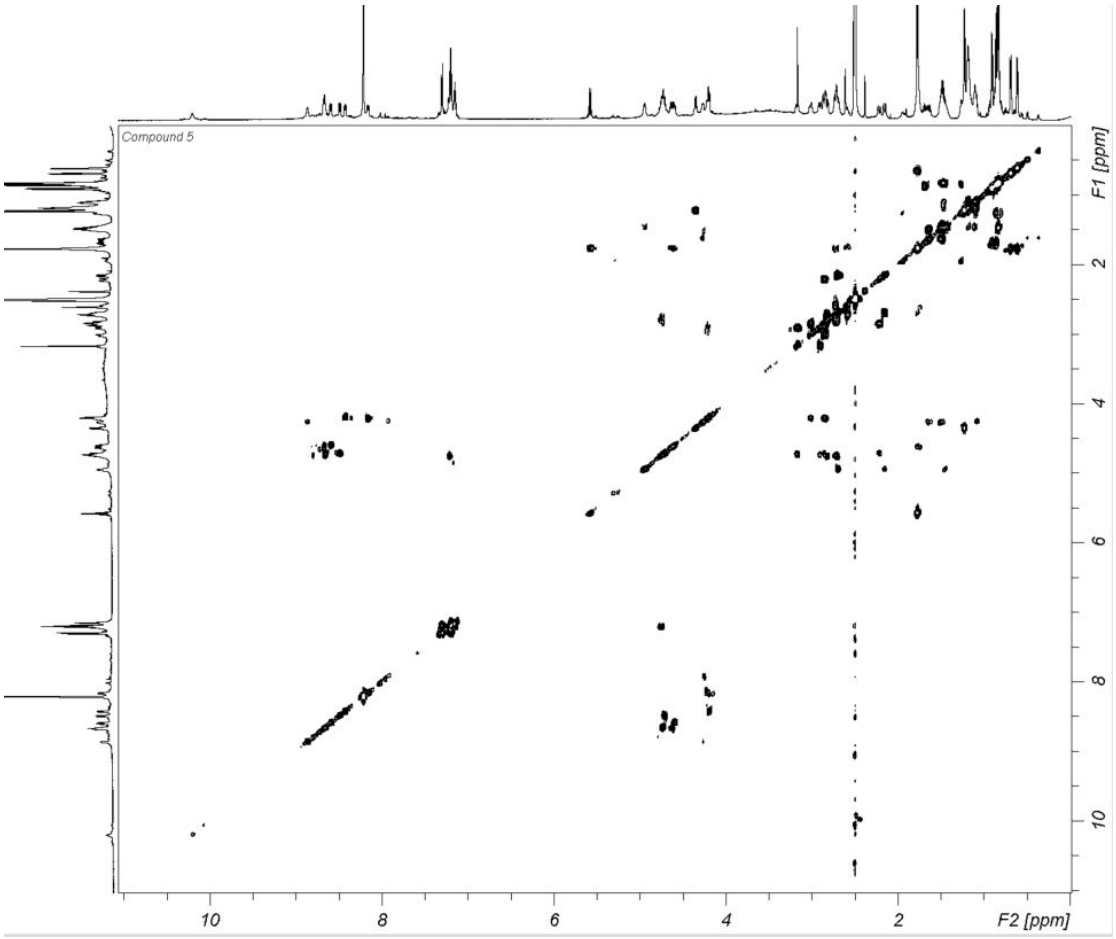

Figure S34. *COSY spectrum of compound* ***5*** *(DMSO-d_6, 600 MHz, 298 K).*

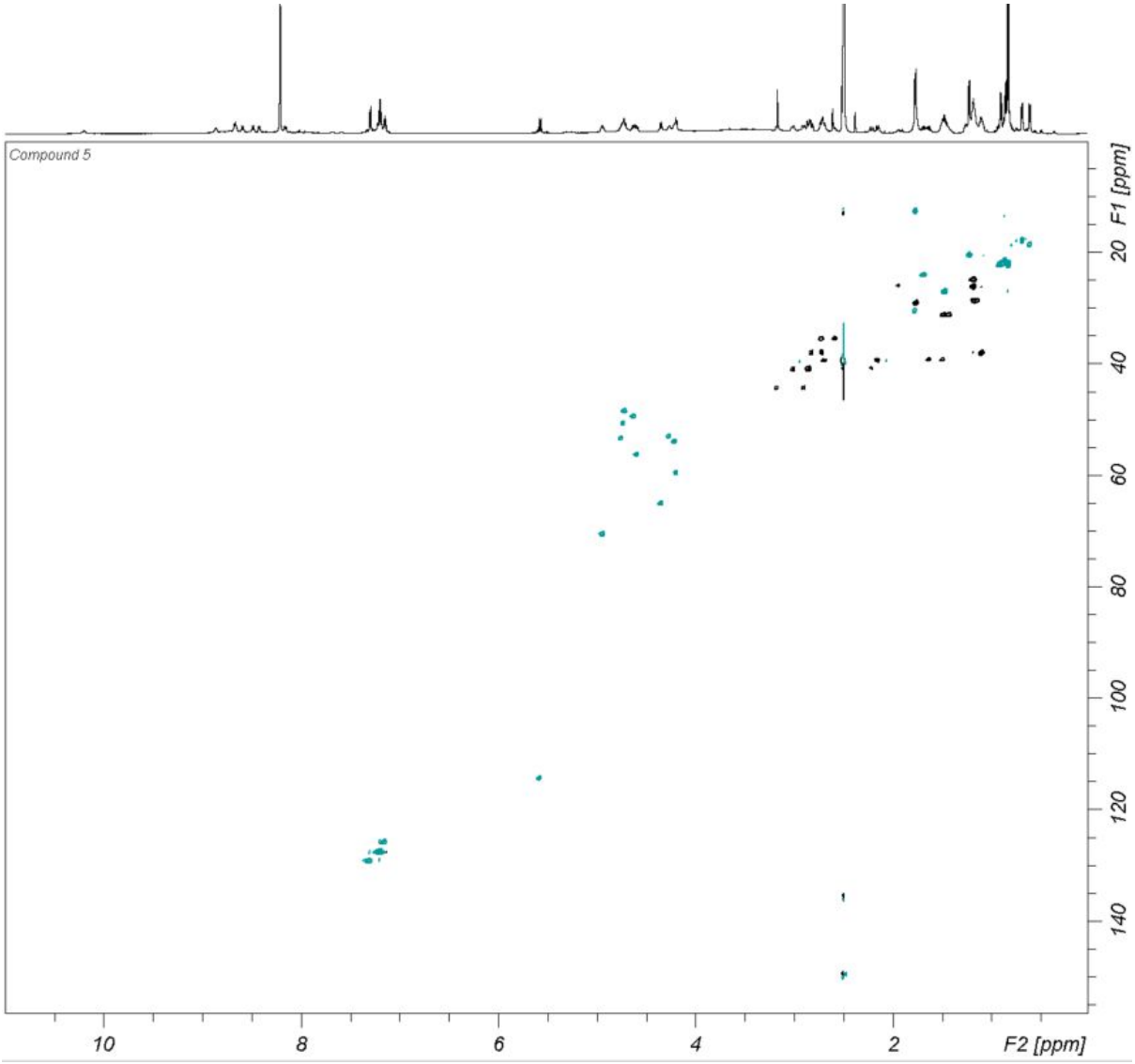

Figure S35. HSQC spectrum of compound **5** (DMSO-d_6, 600 MHz, 298 K).

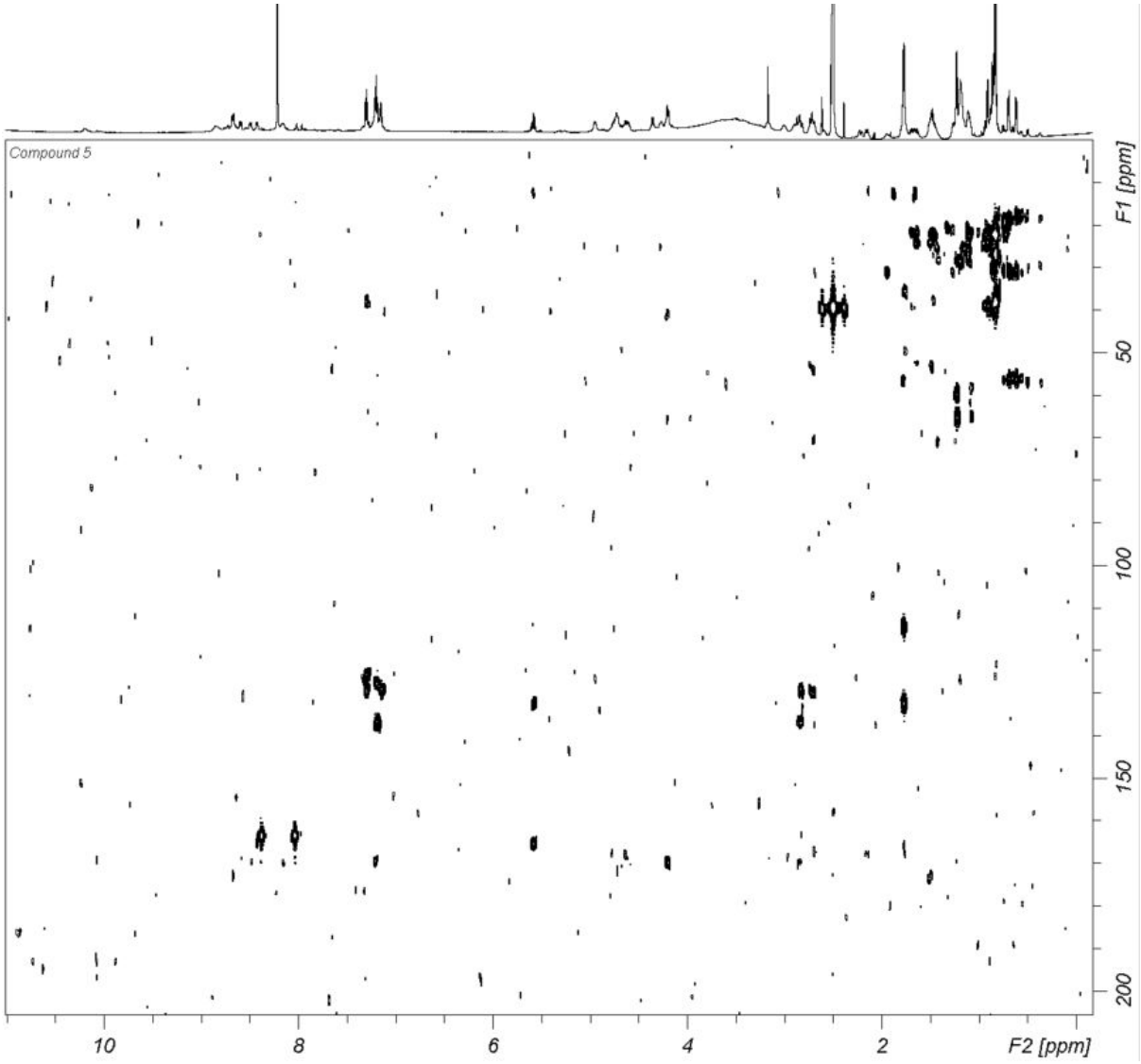

Figure S36. HMBC spectrum of compound **5** (DMSO-d_6, 600 MHz, 298 K).

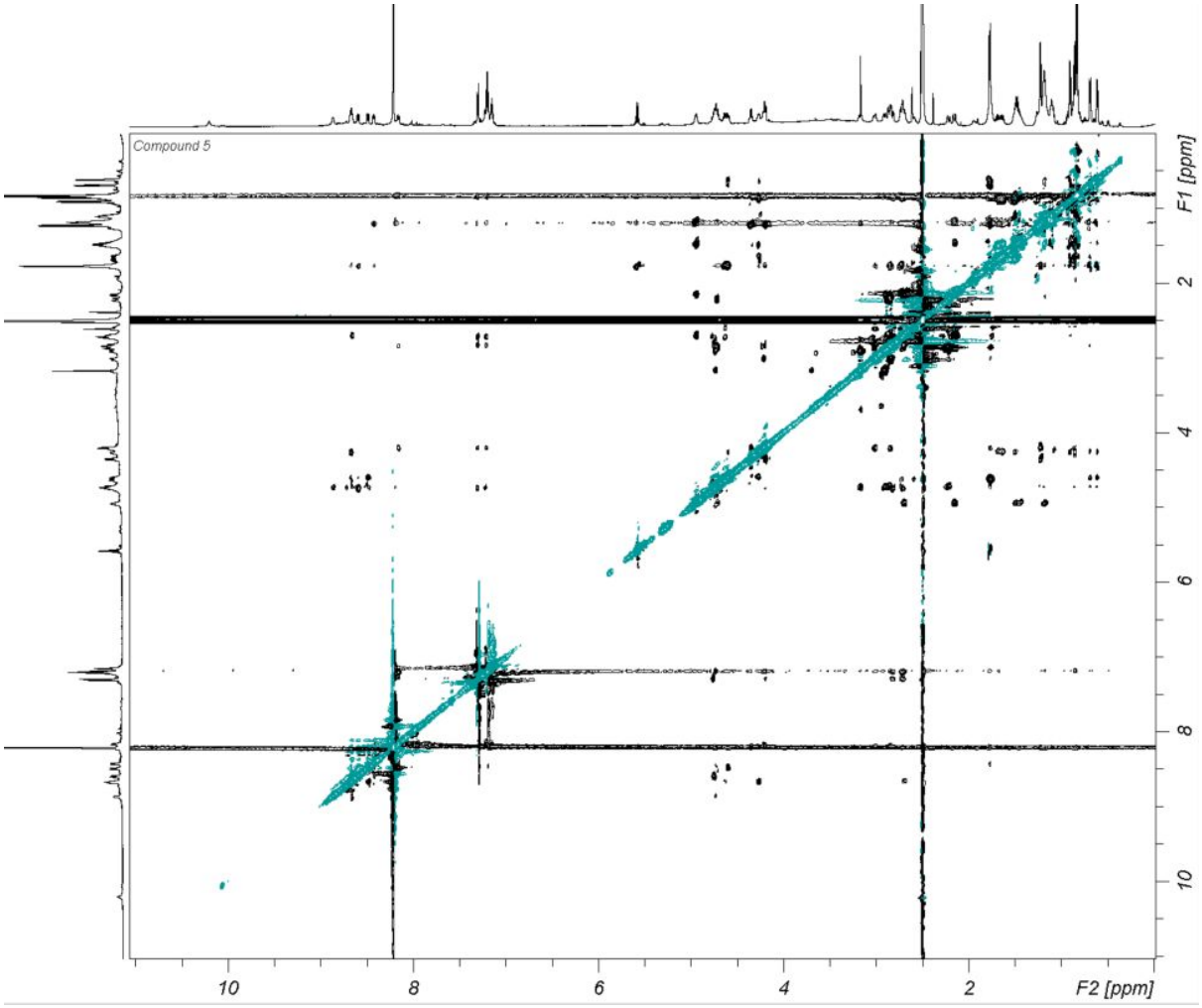

Figure S37. ROESY spectrum of compound **5** (DMSO-d_6, 600 MHz, 298 K).

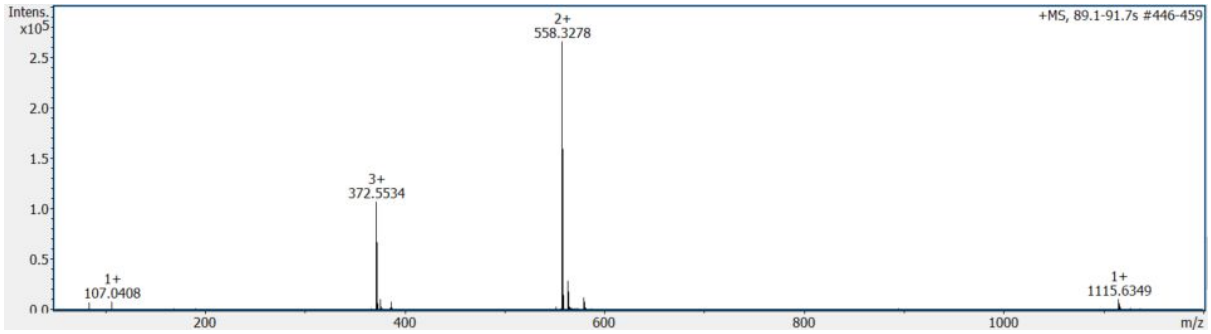

Figure S38. HRMS spectrum of compound **5**.

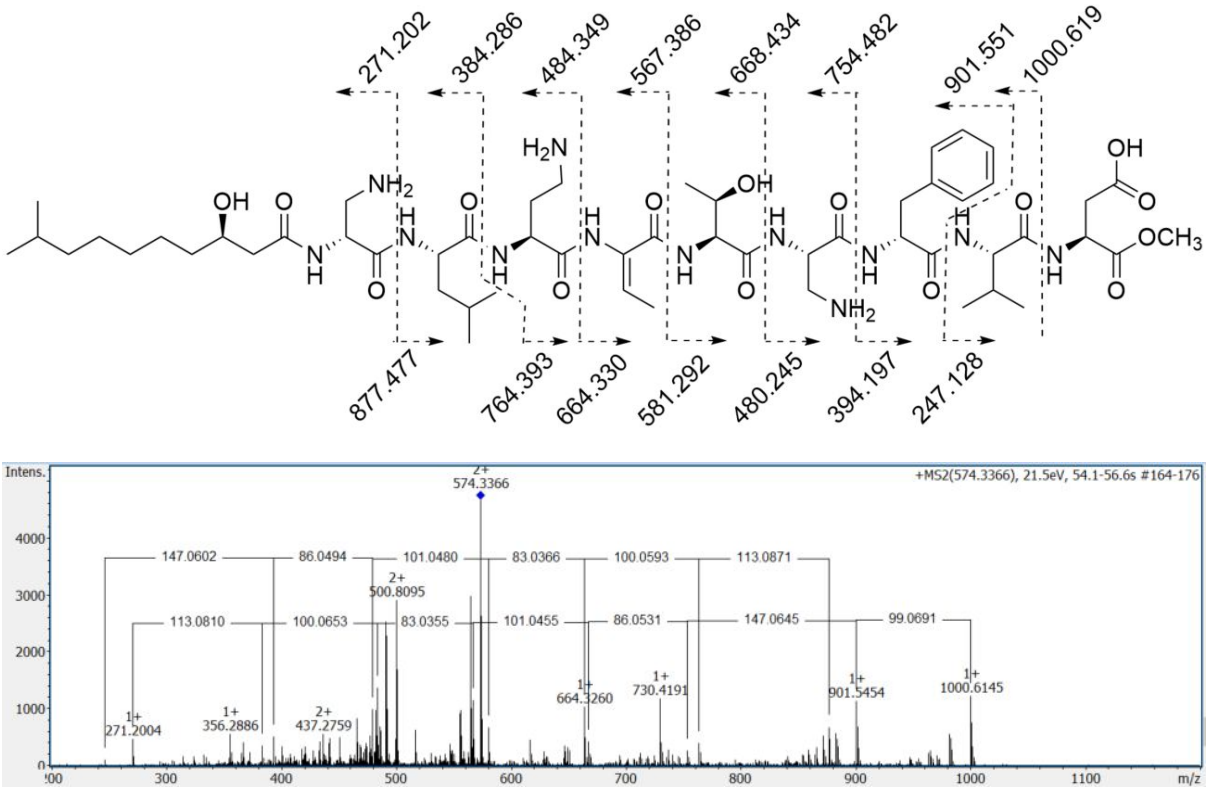

Figure S39. MSMS spectrum of compound **5** after treatment with NaOMe in MeOH. Mass differences between Y-series ions (top) and B-series ions (bottom) are shown in the mass spectrum. Theoretical m/z-values for the observed B- and Y-series ions are shown in the structure on top.

Table S6. ^{1}H and ^{13}C NMR-data (600 and 150 MHz, resp) for compound **6** (DMSO-d_6, 30°C)

Pos.	^{13}C	^{1}H	Mult (*J*, Hz)
3OHFA			
1	167.7	-	-
2	39.4	2.69	obsc
		2.12	dd (13.3, 3.2)
3	70.5	4.96	m
4	31.1	1.47	obsc
		1.44	obsc
5	26.4	1.21	obsc
6	28.7	1.20	obsc
7	28.7	1.20	obsc
8	28.7	1.20	obsc
9	25.0	1.20	obsc
10	38.1	1.13	m
11	27.0	1.49	m
12	22.2	0.85	d (6.7)
13	22.2	0.85	d (6.7)
DAPA1			
NH	-	8.68	d (8.9)
1	171.4	-	-
2	51.9	4.63	ddd (8.9, 4.7, 4.7)
3	45.0	3.04	dd (13.1, 4.7)
		2.77	obsc
Leu			
NH	-	8.78	br s
1	172.8	-	-
2	52.6	4.32	obsc
3	39.2	1.63	obsc
		1.42	m
4	24.1	1.62	obsc
5	22.0	0.87	d (6.4)
6	22.3	0.83	d (6.5)
DABA			
NH	-	8.63	d (9.7)
1	168.4	-	-
2	49.5	4.66	m
3	29.5	1.84	m
		1.79	m
4	35.4	2.76	obsc
		2.57	ddd (11.3, 4.5, 4.5)
ABA			
NH	-	10.21	br s
1	165.4	-	-
2	132.7	-	-
3	113.9	5.56	q (7.3)
4	12.5	1.76	d (7.3)
Thr			
NH	-	8.44	d (7.9)
1	170.0	-	-
2	59.4	4.20	dd (7.9, 2.3)
3	65.1	4.34	dq (2.3, 6.5)
4	20.5	1.22	d (6.5)
DAPA2			
NH	-	8.06	d (8.5)
1	170.1	-	-
2	54.7	4.13	ddd (8.5, 8.5, 5.1)
3	41.6	2.91	obsc
		2.84	obsc
Phe			
NH	-	7.23	obsc
1	171.6	-	-
2	53.4	4.76	ddd (9.9, 9.9, 4.3)
3	37.6	2.88	obsc
		2.70	obsc
4	137.1	-	-
5/9	129.3	7.33	m
6/8	127.6	7.20	m
7	125.9	7.15	m
OHVal			
NH	-	8.55	d (9.7)
1	169.6	-	-
2	57.9	4.77	d (9.6)
3	70.6	-	-
4	26.5	1.04	s
5	26.6	0.92	s
Asp			
NH	-	8.57	d (9.7)
1	172.3	-	-
2	48.3	4.70	ddd (9.7, 3.8, 3.8)
3	40.6	2.85	m
		2.20	d (16.0, 3.8)
4	173.4	-	-

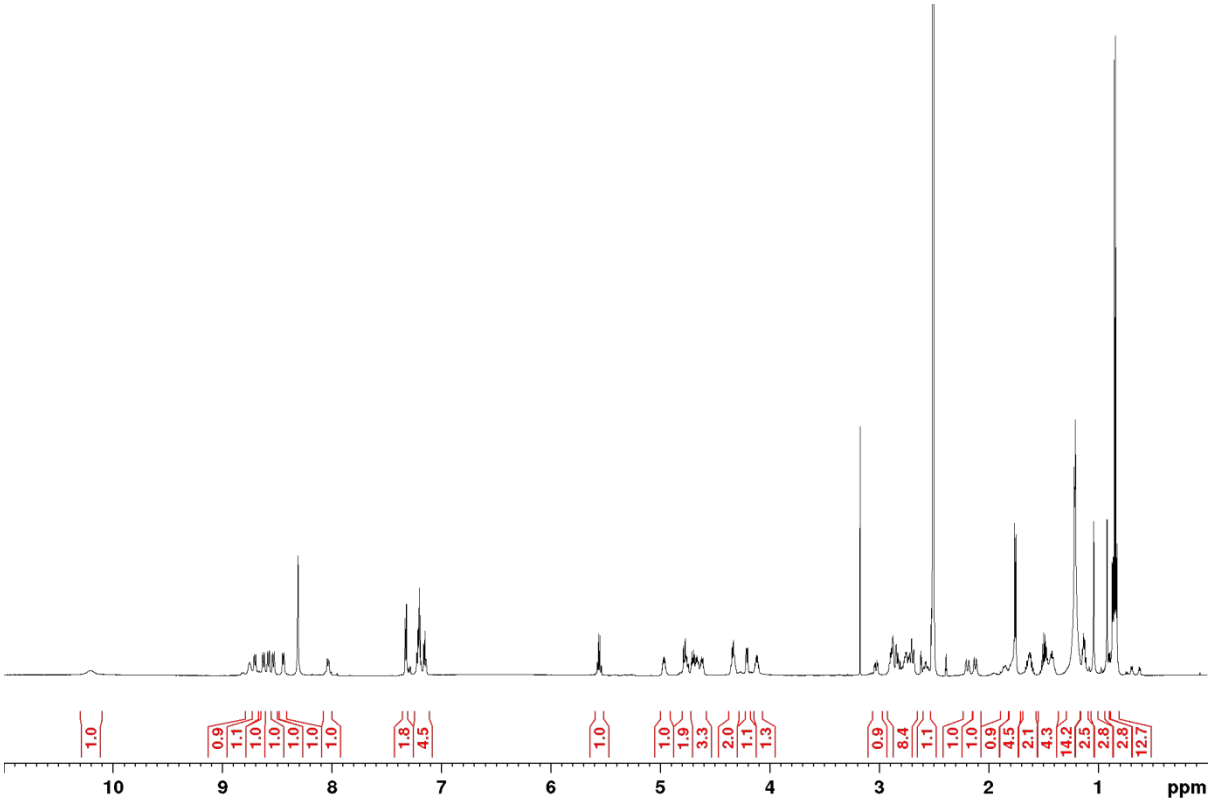

Figure S40. ^{1}H-NMR spectrum of compound **6** (DMSO-d_6, 600 MHz, 298 K).

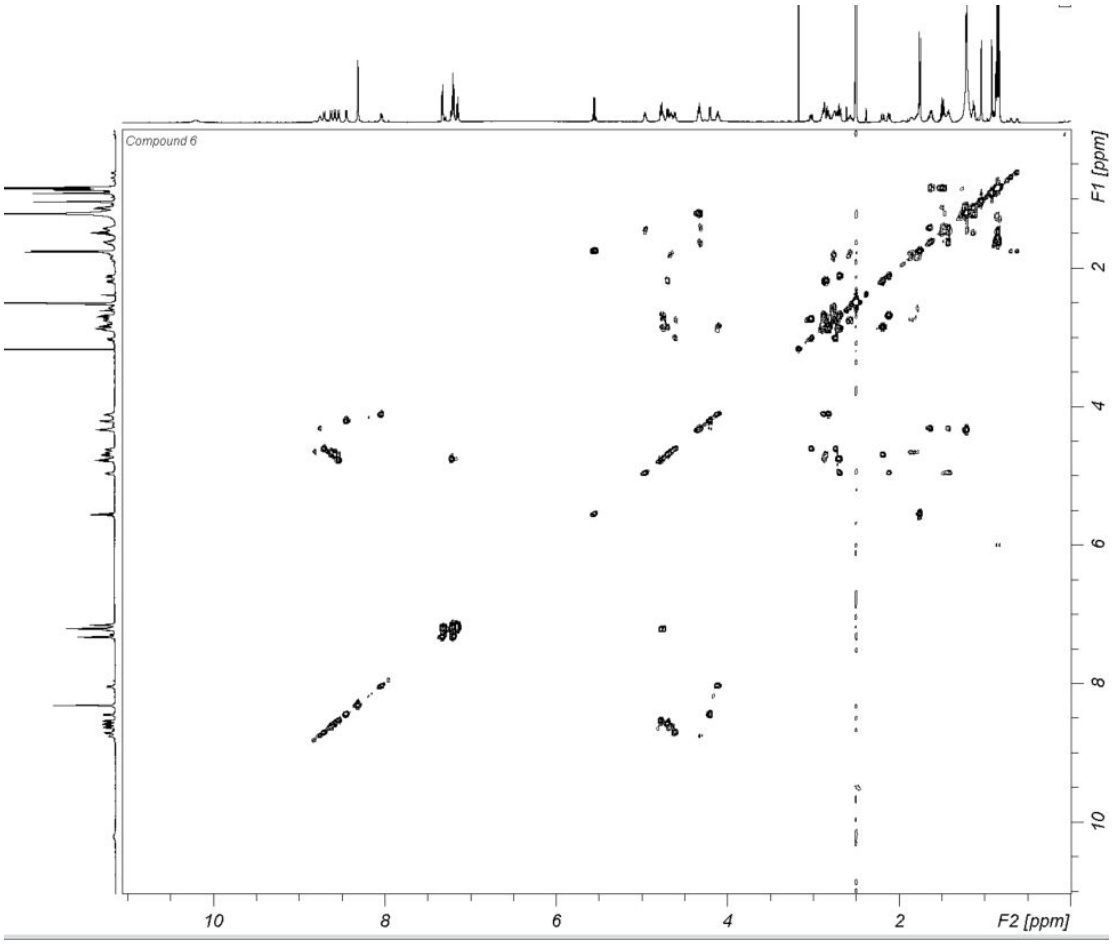

Figure S41. COSY spectrum of compound **6** (DMSO-d_6, 600 MHz, 298 K).

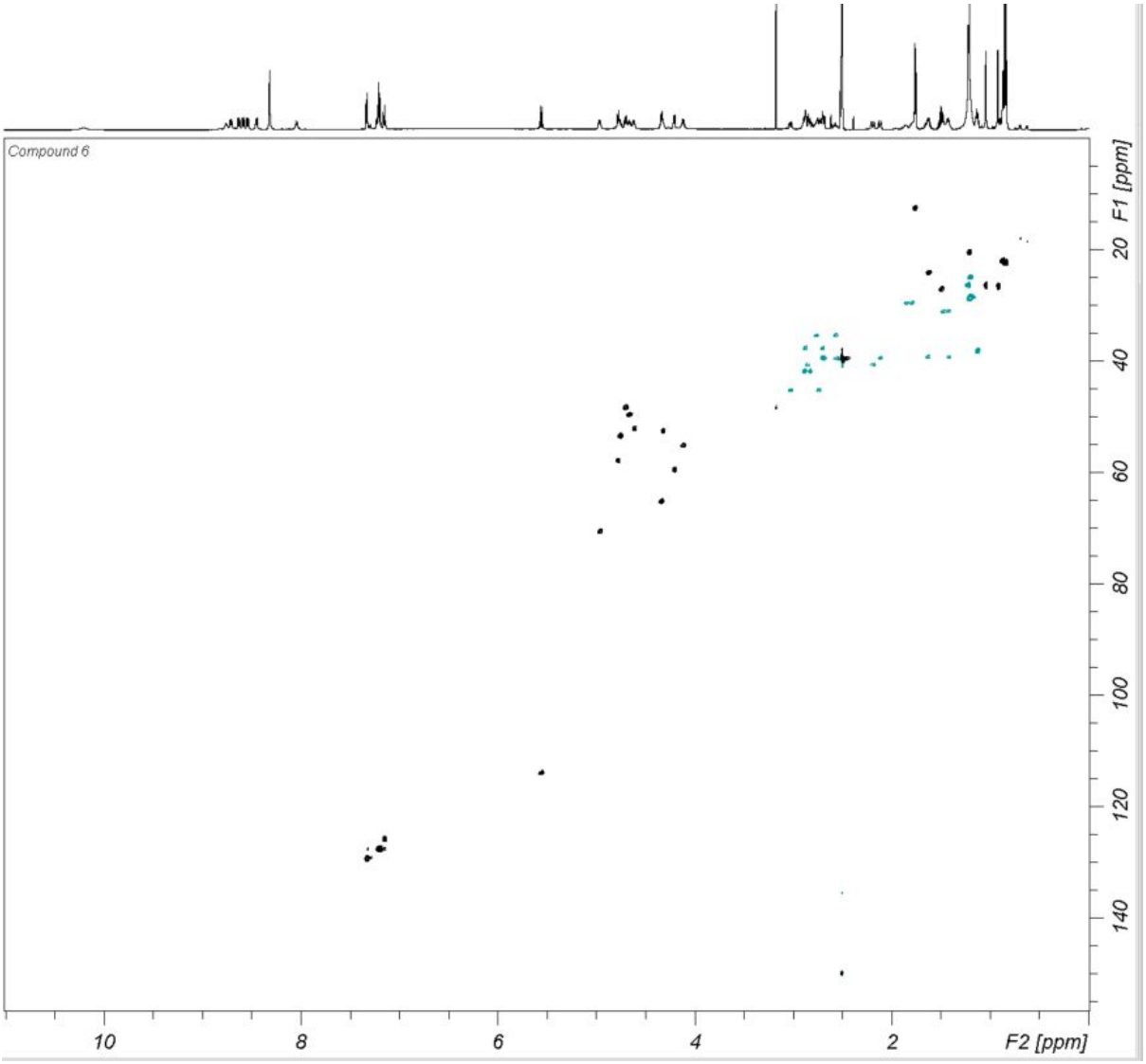

Figure S42. HSQC spectrum of compound **6** (DMSO-d_6, 600 MHz, 298 K).

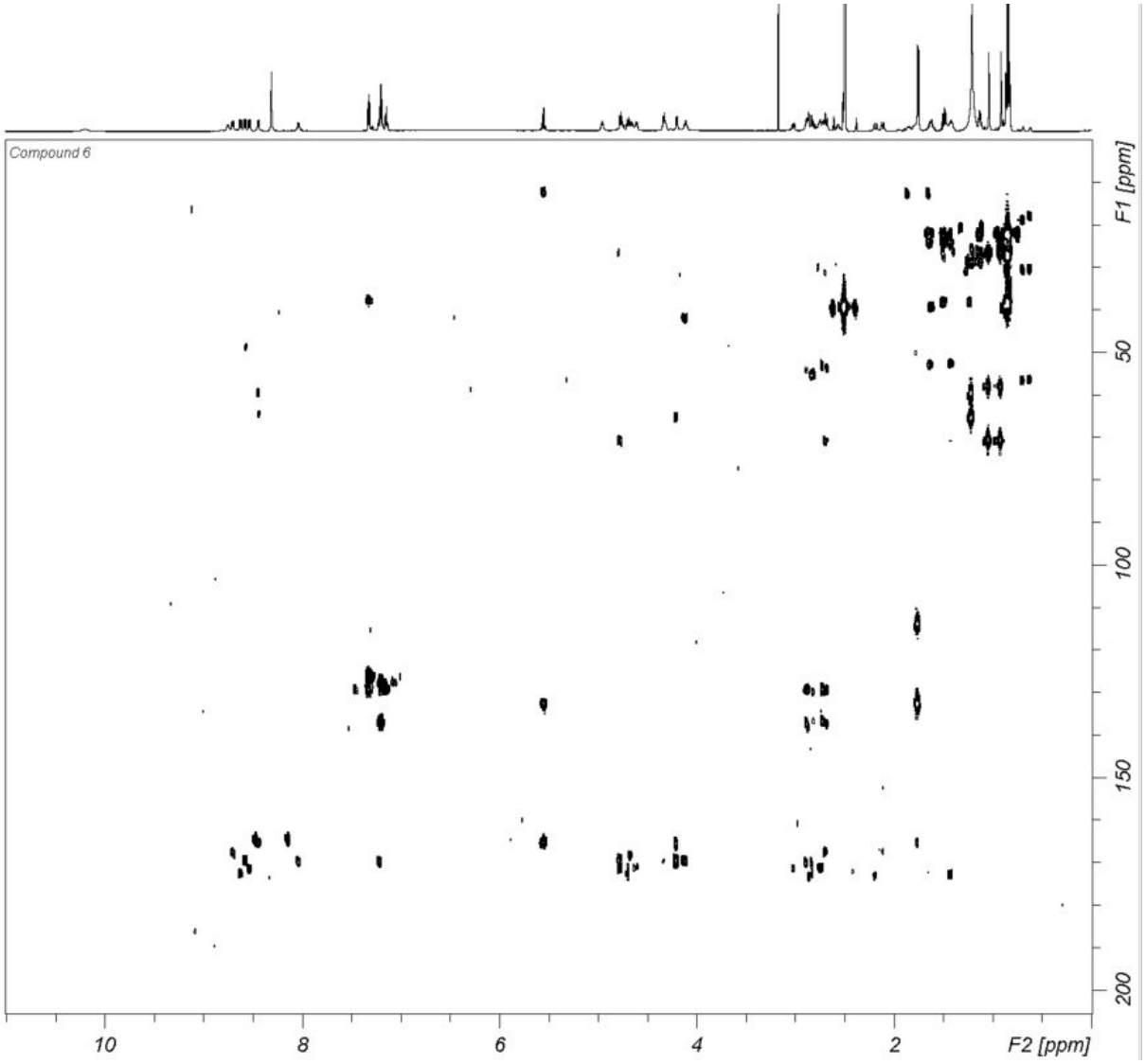

Figure S43. HMBC spectrum of compound **6** (DMSO-d_6, 600 MHz, 298 K).

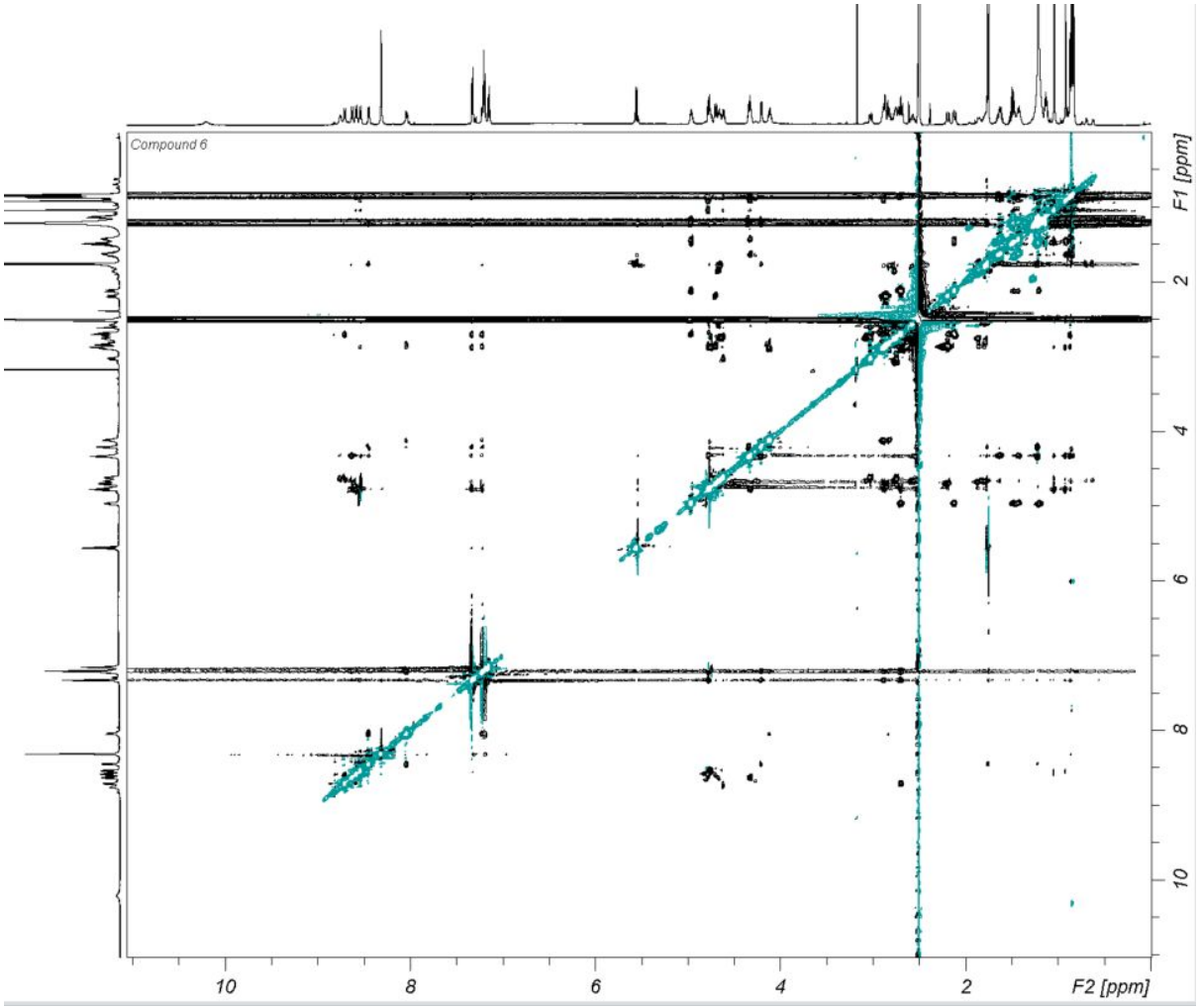

Figure S44. ROESY spectrum of compound **6** (DMSO-d_6, 600 MHz, 298 K).

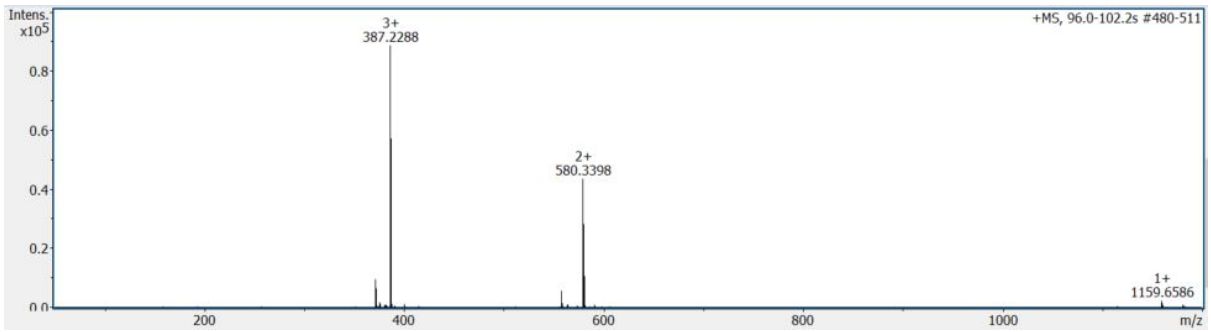

Figure S45. HRMS spectrum of compound **6**.

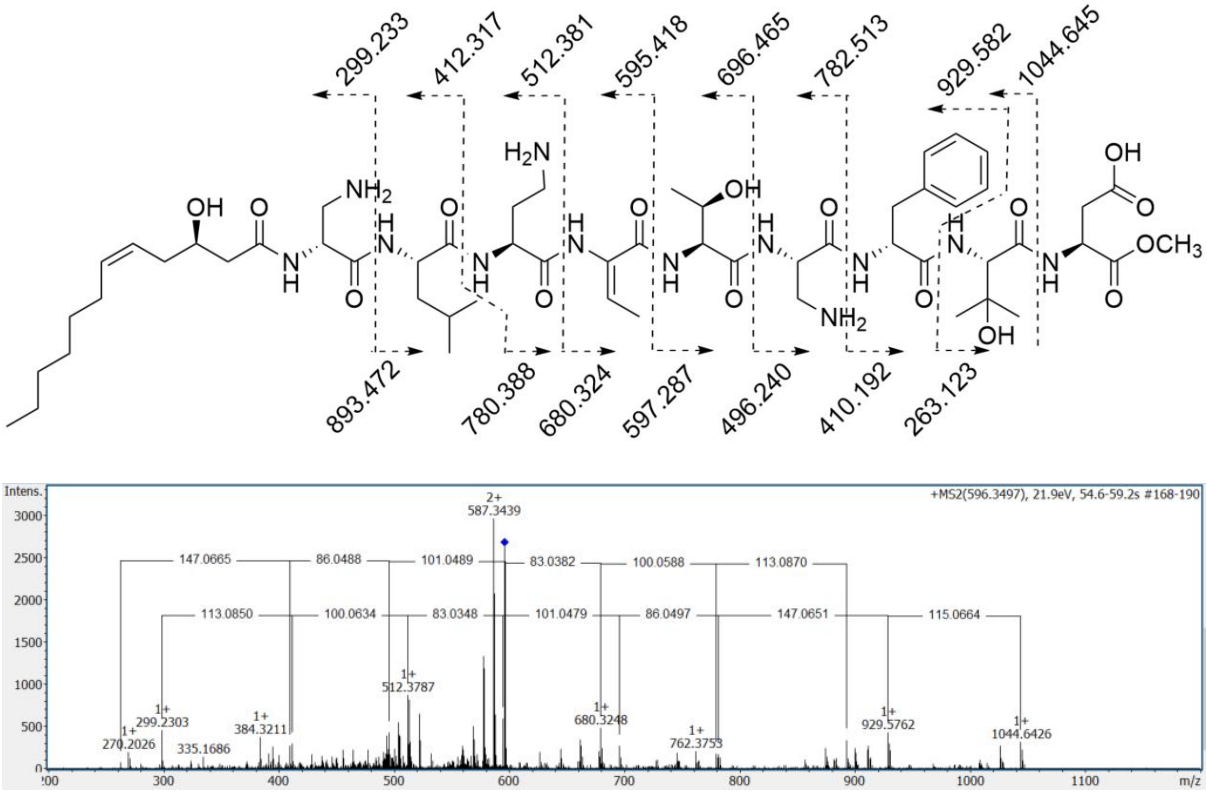

Figure S46. MSMS spectrum of compound **6** after treatment with NaOMe in MeOH. Mass differences between Y-series ions (top) and B-series ions (bottom) are shown in the mass spectrum. Theoretical m/z-values for the observed B- and Y-series ions are shown in the structure on top.

Table S7. ^{1}H and ^{13}C NMR-data (600 and 150 MHz, resp) for compound **7** (DMSO-d_6, 30°C)

Pos.	^{13}C	^{1}H	Mult (*J*, Hz)
3OHFA			
1	167.5	-	-
2	39.4	2.71	obsc
		2.16	br d (13.4)
3	70.5	4.96	m
4	30.8	1.50	obsc
5	38.0	1.17	m
6	24.2	1.95	obsc
7	129.7	5.31	m (11)
8	128.5	5.24	m (11)
9	25.9	1.93	obsc
10	25.0	1.25	obsc
11	26.8	1.51	obsc
12	22.0	0.86	d (6.6)
13	22.0	0.86	d (6.6)
DAPA1			
NH	-	8.65	d (8.9)
1	170.9	-	-
2	50.2	4.77	m
3	44.0	3.20	br d (13.4, 4.8)
		2.96	br d (13.4)
Leu			
NH	-	8.92	br s
1	173.2	-	-
2	53.0	4.29	m
3	39.2	1.64	m
		1.51	m
4	24.1	1.70	m
5	22.0	0.91	d (6.5)
6	22.0	0.86	d (6.7)
DABA			
NH	-	8.67	d (9.6)
1	168.1	-	-
2	49.5	4.63	m
3	29.0	1.78	obsc
4	35.5	2.72	obsc
		2.60	obsc
ABA			
NH	-	10.23	br s
1	165.4	-	-
2	132.6	-	-
3	114.4	5.58	q (7.3)
4	12.5	1.77	d (7.3)
Thr			
NH	-	8.45	d (7.4)
1	169.8	-	-
2	59.6	4.20	dd (7.7, 2.4)
3	65.0	4.35	dq (2.5, 6.5)
4	20.5	1.23	d (6.5)
DAPA2			
NH	-	8.19	d (8.6)
1	169.2	-	-
2	53.3	4.25	obsc
3	40.7	3.05	br d (12.7)
		2.87	obsc
Phe			
NH	-	7.25	d (8.7)
1	170.6	-	-
2	53.3	4.76	obsc
3	37.8	2.83	obsc
		2.72	obsc
4	137.0	-	-
5/9	129.2	7.30	m
6/8	127.6	7.20	m
7	125.9	7.15	m
Val			
NH	-	8.58	d (9.7)
1	169.6	-	-
2	56.3	4.59	m
3	30.6	1.78	obsc
4	17.7	0.68	d (6.9)
5	18.6	0.61	d (6.7)
Asp			
NH	-	8.48	d (9.7)
1	169.7	-	-
2	48.4	4.72	obsc
3	40.8	2.86	obsc
		2.23	br dd (15.7, 4.1)
4	n.d.	-	-

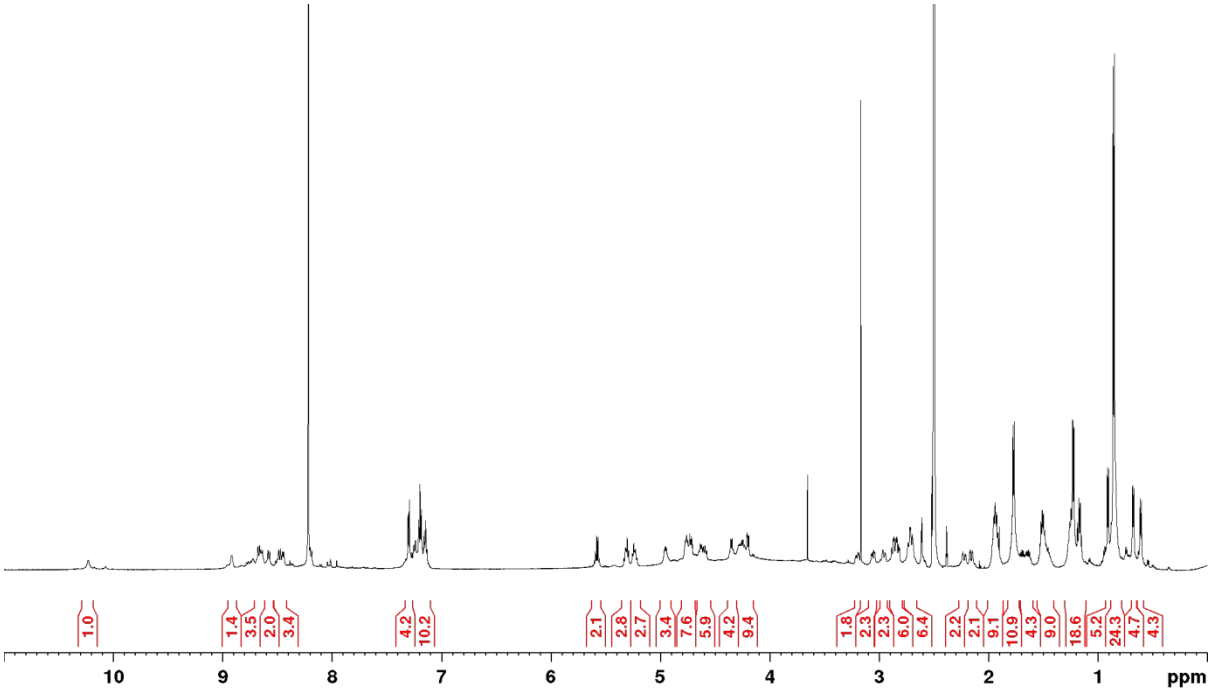

Figure S47. ^{1}H-NMR spectrum of compound **7** (DMSO-d_6, 600 MHz, 298 K).

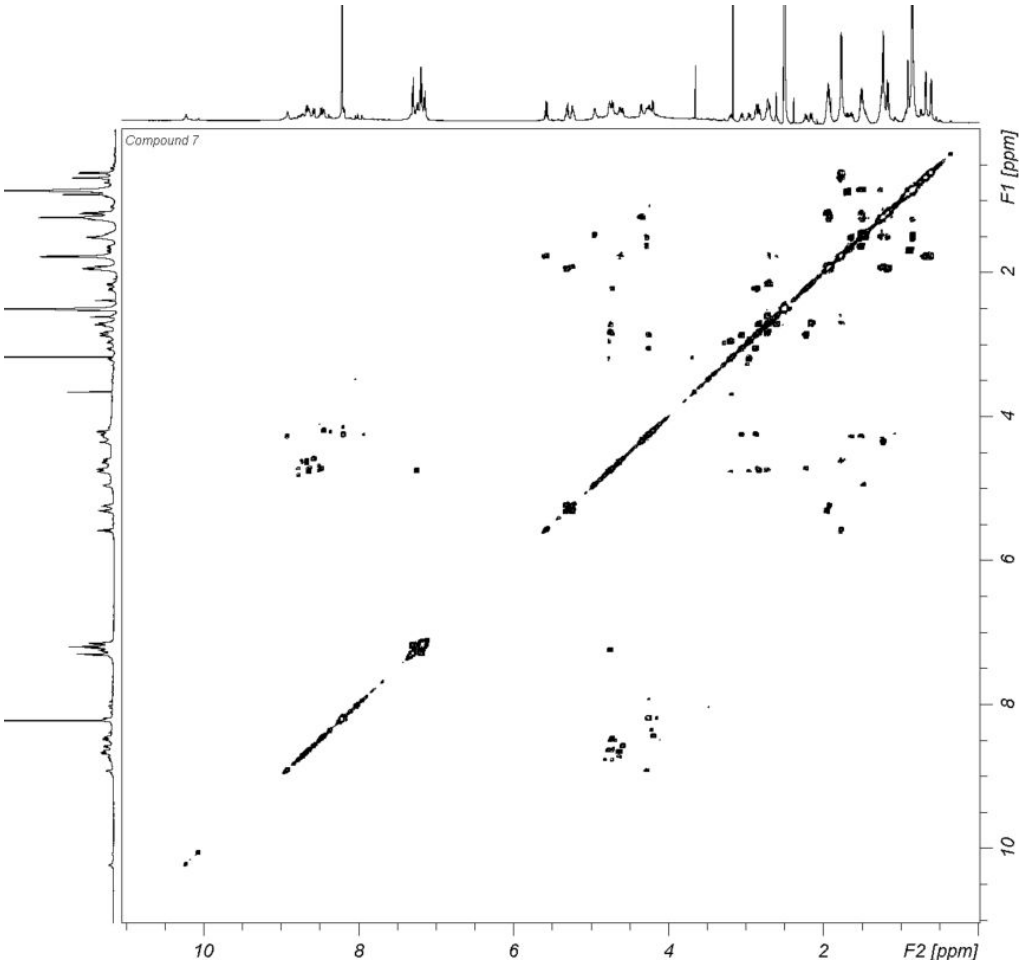

Figure S48. COSY spectrum of compound **7** (DMSO-d_6, 600 MHz, 298 K).

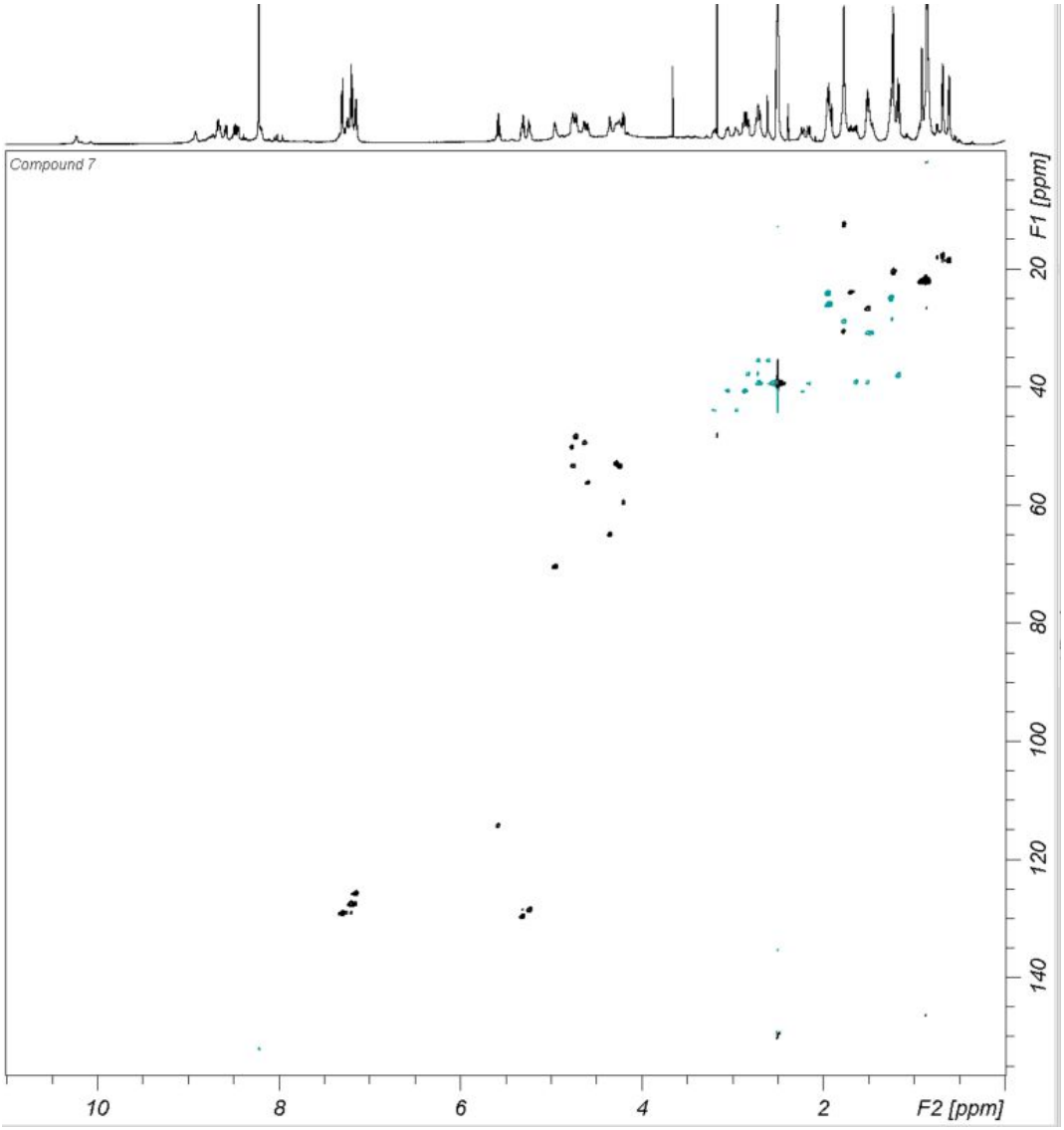

Figure S49. HSQC spectrum of compound **7** (DMSO-d_6, 600 MHz, 298 K).

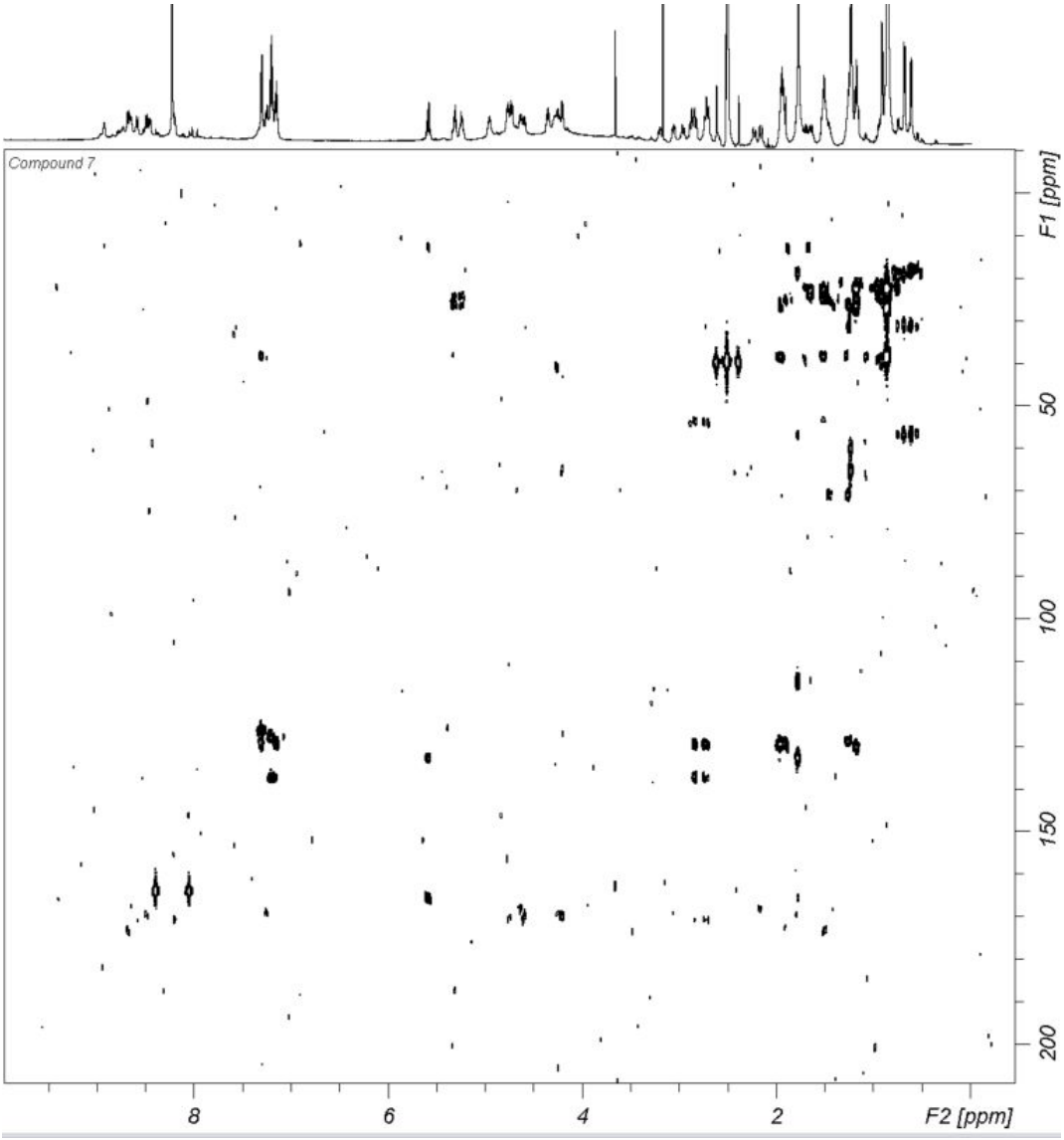

Figure S50. HMBC spectrum of compound **7** (DMSO-d_6, 600 MHz, 298 K).

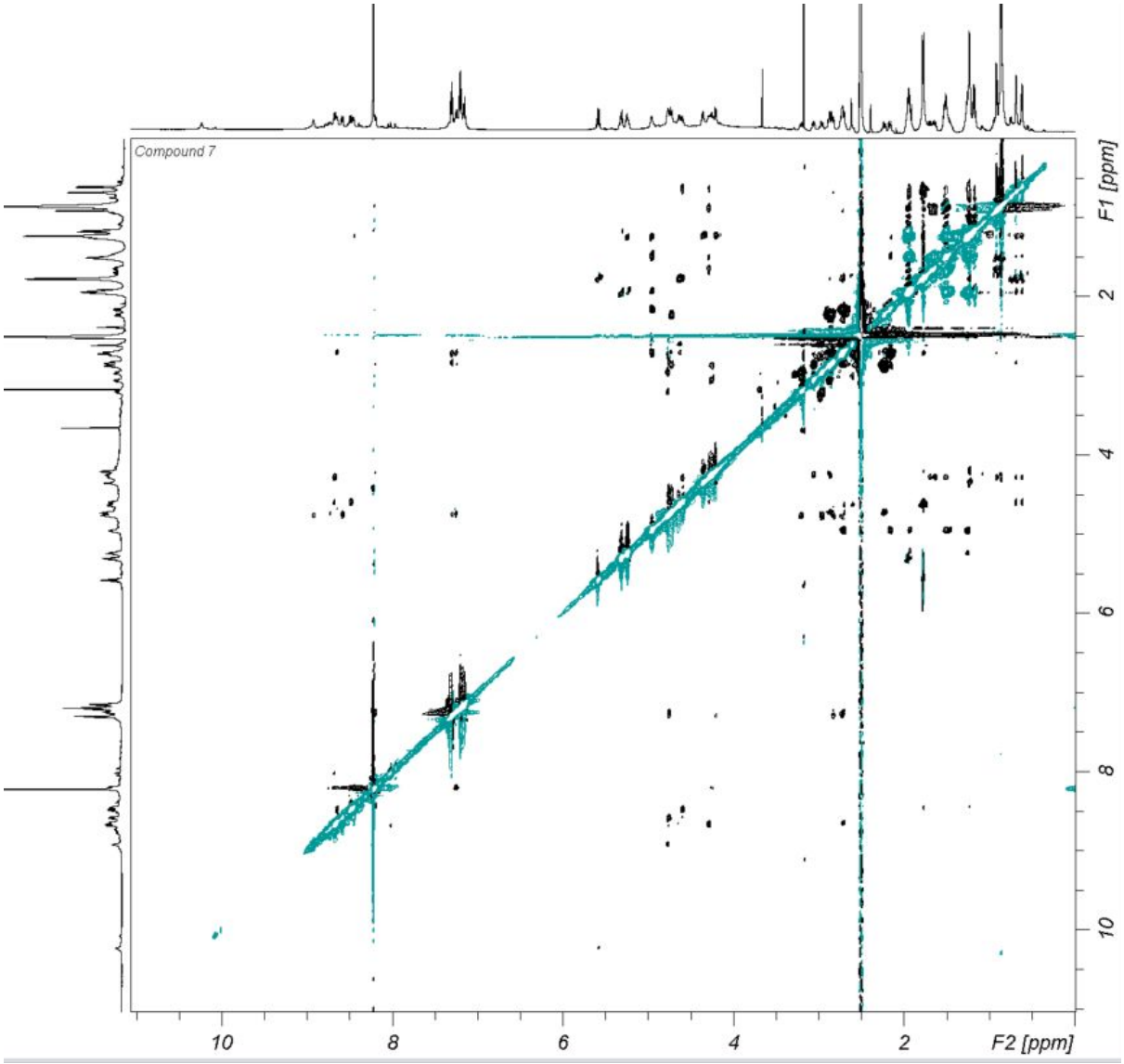

Figure S51. ROESY spectrum of compound **7** (DMSO-d_6, 600 MHz, 298 K).

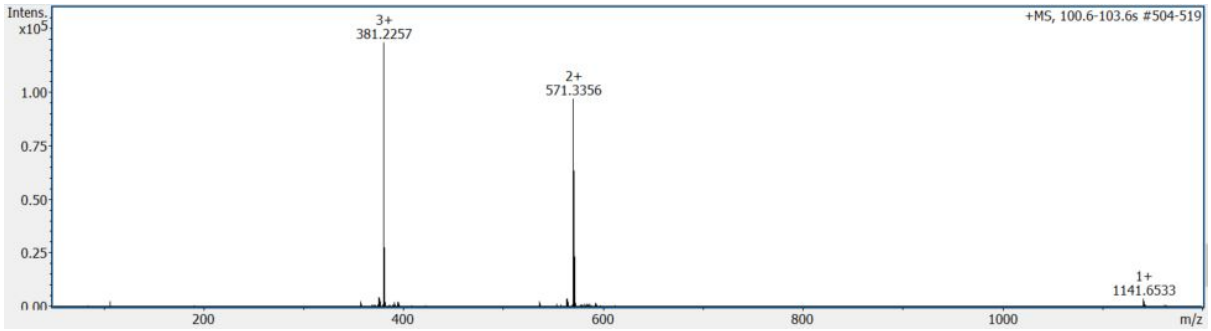

Figure S52. HRMS spectrum of compound **7**.

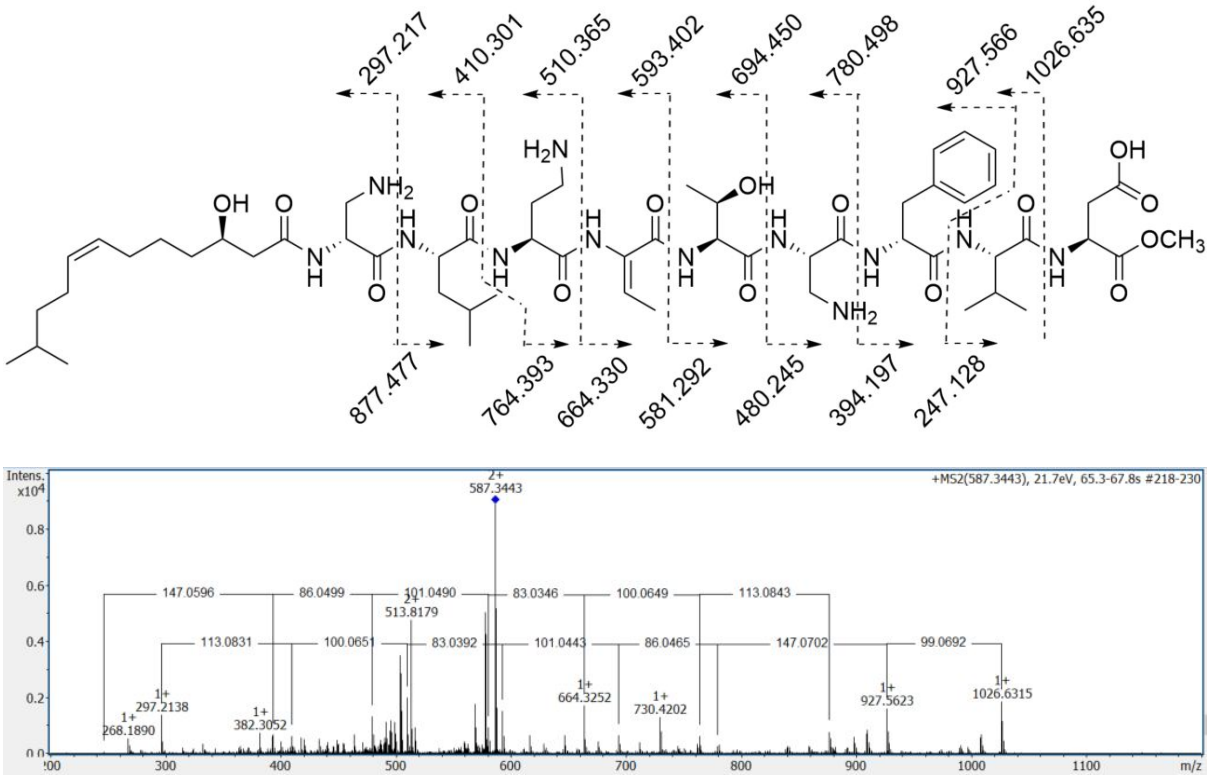

Figure S53. MSMS spectrum of compound **7** after treatment with NaOMe in MeOH. Mass differences between Y-series ions (top) and B-series ions (bottom) are shown in the mass spectrum. Theoretical m/z-values for the observed B- and Y-series ions are shown in the structure on top.

Table S8. ^{1}H and ^{13}C NMR-data (600 and 150 MHz, resp) for compound **8** (DMSO-d_6, 30°C)

Pos.	^{13}C	^{1}H	Mult (*J*, Hz)
3OHFA			
1	n.d.	-	-
2	38.7	2.66	br dd (14.0, 4.0)
		2.23	br d (14.0)
3	70.6	4.93	m
4	29.2	2.34	m
		2.17	m
5	124.0	5.24	m (11)
6	131.9	5.42	m (11)
7	26.5	1.96	m
8	28.7	1.25	m
9	26.0	1.23	obsc
10	37.9	1.12	m
11	27.1	1.49	m
12	22.1	0.84	d (6.6)
13	22.1	0.84	d (6.6)
DAPA1			
NH	-	8.61	obsc
1	n.d.	-	-
2	50.1	4.77	m
3	43.6	3.23	br d (12.0)
		2.98	br d (12.0)
Leu			
NH	-	8.93	br s
1	172.8	-	-
2	52.9	4.29	m
3	39.2	1.63	m
		1.50	obsc
4	24.0	1.68	m
5	22.0	0.90	d (6.4)
6	21.8	0.85	d (7.0)
DABA			
NH	-	8.67	d (9.6)
1	n.d.	-	-
2	49.4	4.63	m
3	29.1	1.78	obsc
4	35.6	2.72	obsc
		2.61	obsc
ABA			
NH	-	10.24	br s
1	165.8	-	-
2	132.6	-	-
3	114.2	5.58	q (7.3)
4	12.5	1.77	d (7.3)

Pos.	^{13}C	^{1}H	Mult (*J*, Hz)
Thr			
NH	-	8.45	d (7.6)
1	170.1	-	-
2	59.5	4.20	dd (7.7, 2.4)
3	65.0	4.35	dq (2.4, 6.5)
4	20.5	1.23	d (6.5)
DAPA2			
NH	-	8.19	d (8.4)
1	n.d.	-	-
2	53.2	4.25	m
3	40.6	3.06	br d (12.4)
		2.86	obsc
Phe			
NH	-	7.25	d (8.8)
1	n.d.	-	-
2	53.4	4.74	obsc
3	37.8	2.82	obsc
		2.72	obsc
4	137.2	-	-
5/9	129.1	7.30	m
6/8	127.5	7.20	m
7	125.8	7.15	m
Val			
NH	-	8.60	obsc
1	n.d.	-	-
2	56.4	4.57	m
3	30.4	1.78	obsc
4	17.9	0.65	d (6.7)
5	18.6	0.65	d (6.7)
Asp			
NH	-	8.48	d (9.6)
1	n.d.	-	-
2	48.4	4.74	obsc
3	40.8	2.85	obsc
		2.23	obsc
4	n.d.	-	-

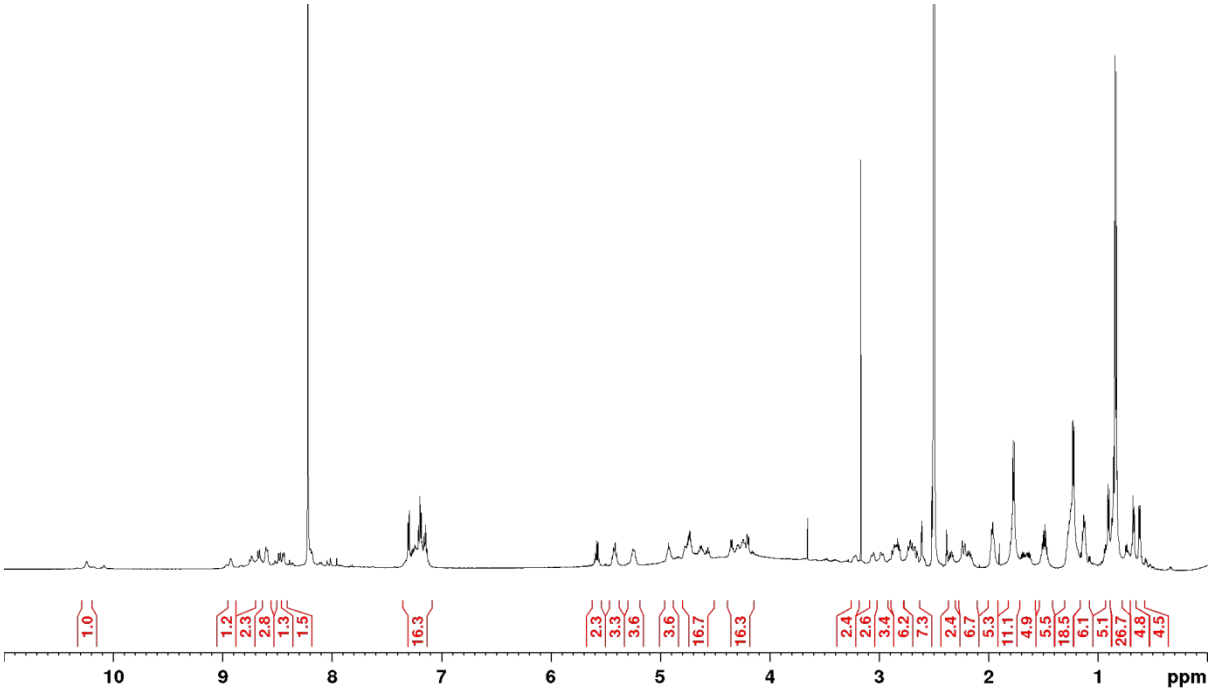

Figure S54. ^{1}H-NMR spectrum of compound **8** (DMSO-d_6, 600 MHz, 298 K).

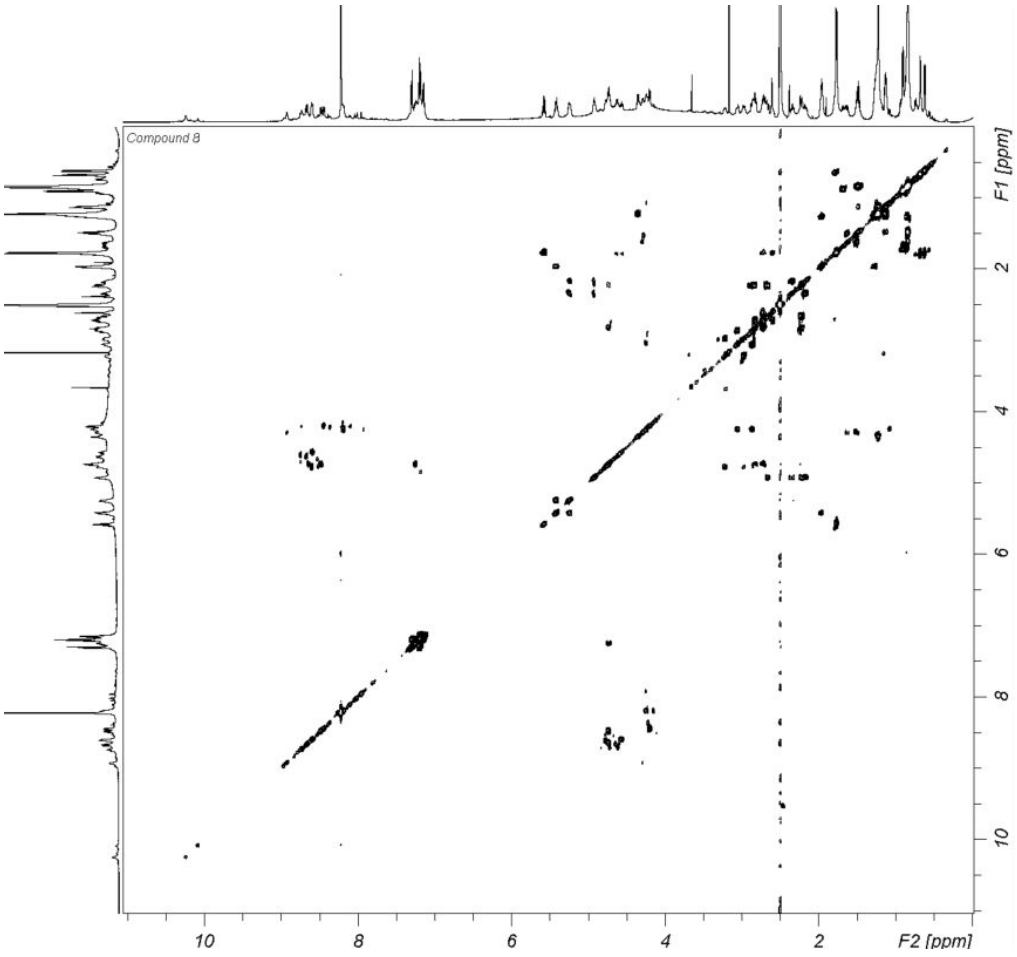

Figure S55. COSY spectrum of compound **8** (DMSO-d_6, 600 MHz, 298 K).

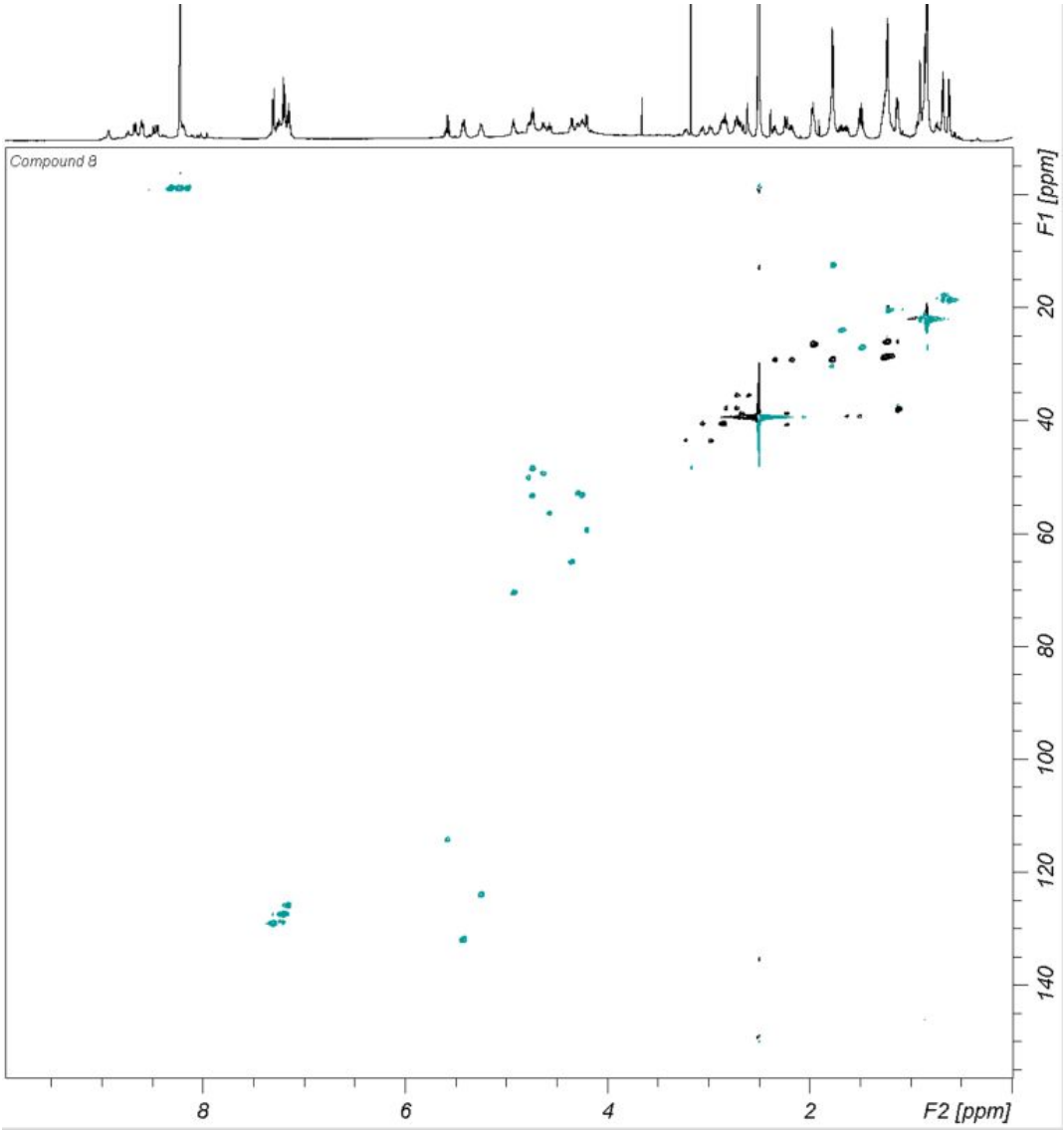

Figure S56. HSQC spectrum of compound **8** (DMSO-d_6, 600 MHz, 298 K).

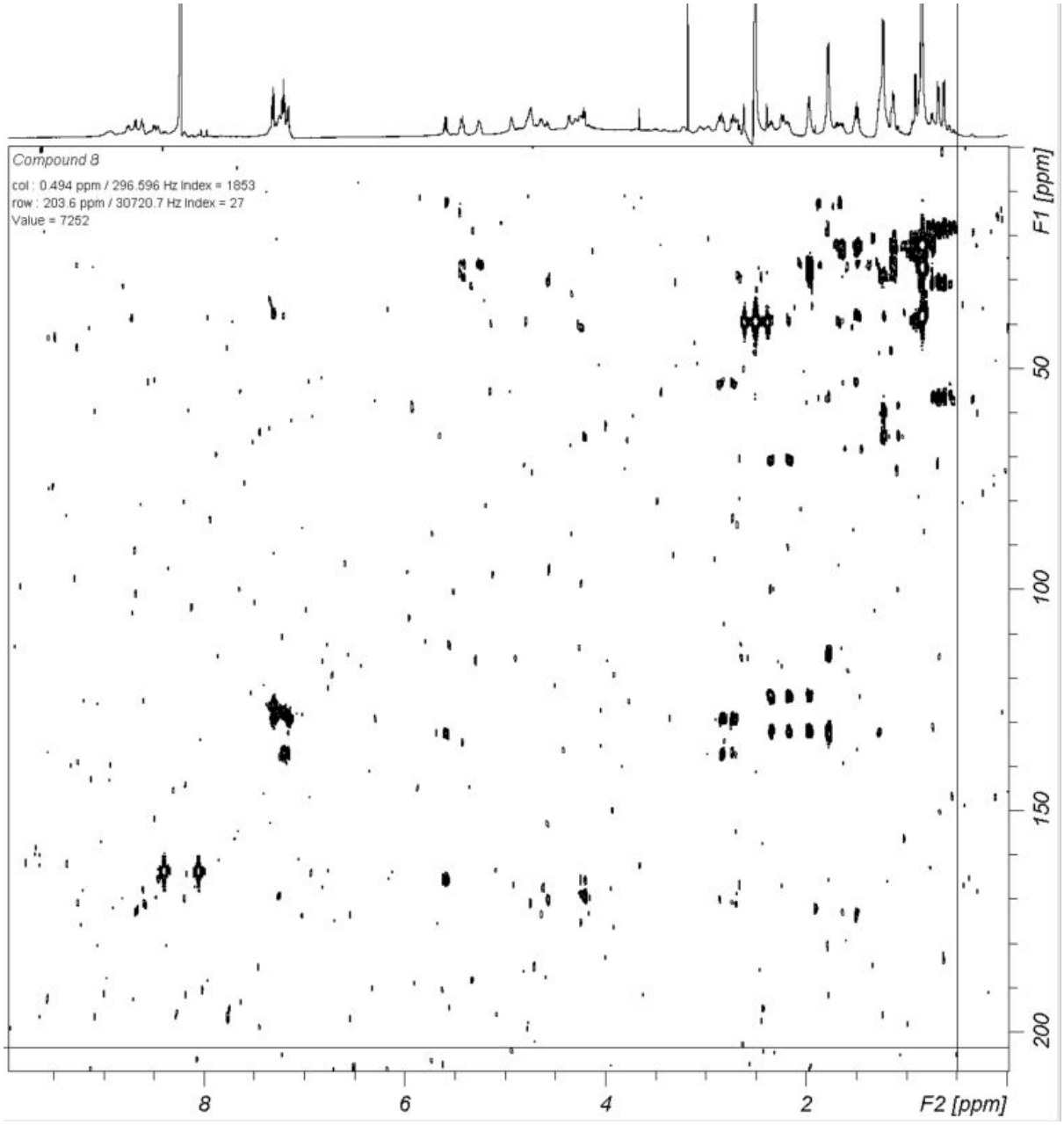

Figure S57. HMBC spectrum of compound **8** (DMSO-d_6, 600 MHz, 298 K).

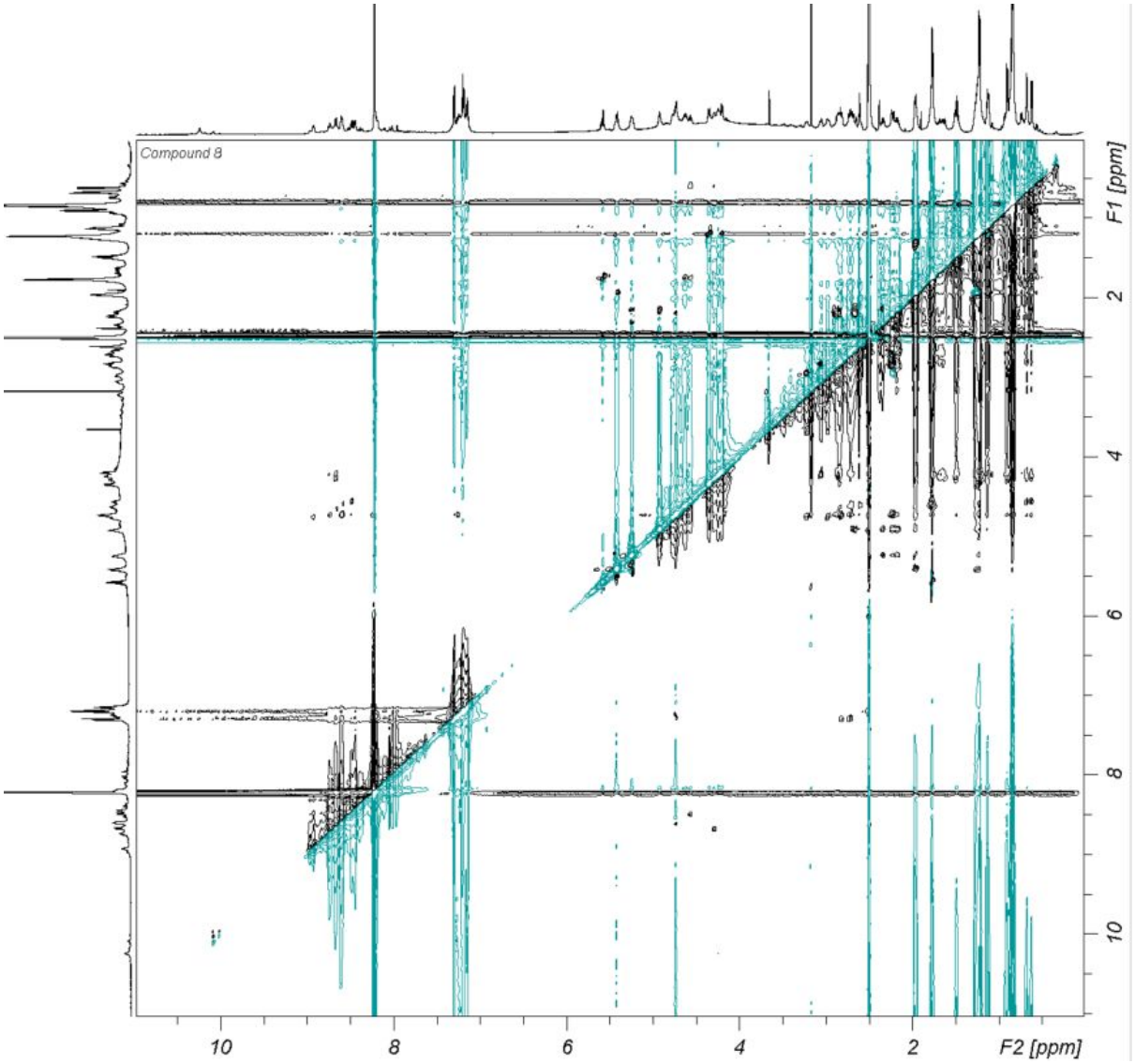

Figure S58. ROESY spectrum of compound **8** (DMSO-d_6, 600 MHz, 298 K).

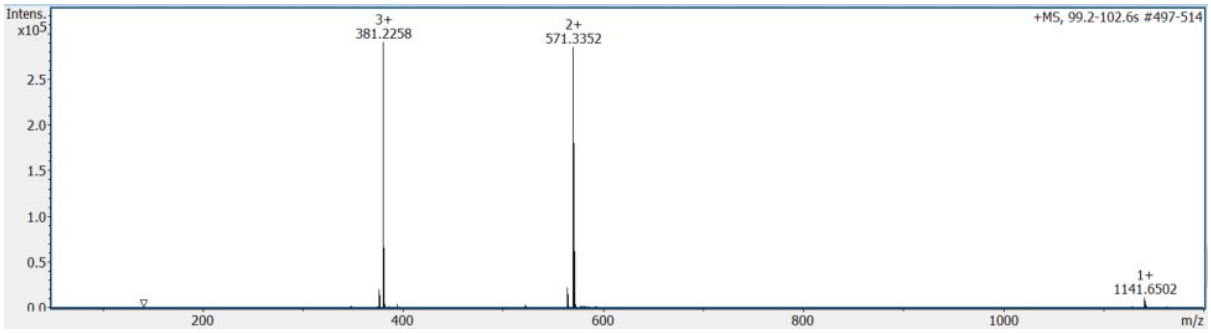

Figure S59. HRMS spectrum of compound **8**.

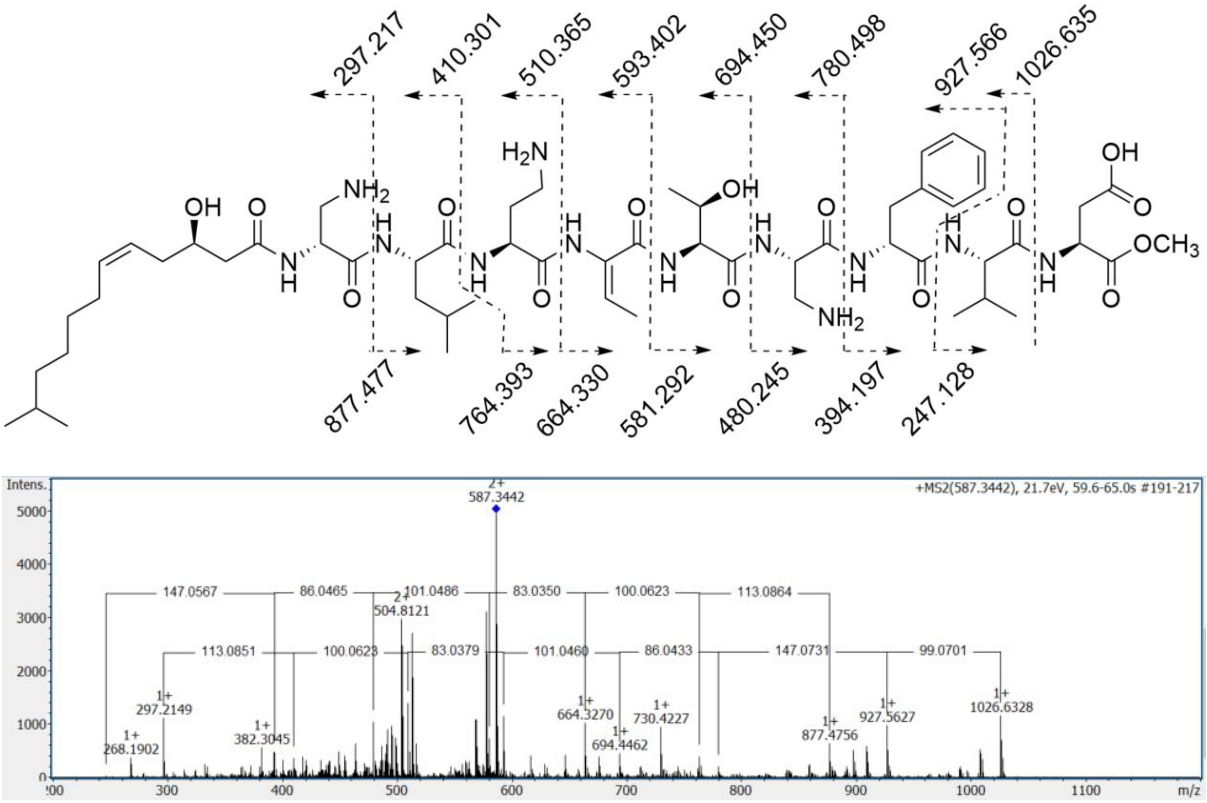

Figure S60. MSMS spectrum of compound **8** after treatment with NaOMe in MeOH. Mass differences between Y-series ions (top) and B-series ions (bottom) are shown in the mass spectrum. Theoretical m/z-values for the observed B- and Y-series ions are shown in the structure on top.

Table S9. Retention times from advanced Marfey's analysis of compounds **1–8**.

	Retention times (s) for L-FDLA derivatives																	
	References[a]		**Isolated compounds**															
	L	**D**	**1**	***epi.***[b]	**2**	***epi.***	**3**	***epi.***	**4**	***epi.***	**5**	***epi.***	**6**	***epi.***	**7**	***epi.***	**8**	***epi.***
Asp	33	38	33	-	32	-	32	-	34	-	32	-	32	-	33	-	33	-
DAPA	190	204	190	*204*	190	*204*	190	*204*	190	*204*	190	*204*	190	*203*	191	*203*	190	*204*
DABA	196	220	196	-	196	-	196	-	196	-	196	-	196	-	196	-	196	-
OHVal	36	69	37	-	36	-	36	-	-	-	-	-	36	-	-	-	-	-
Val	76	145	-	-	-	-	-	-	76	-	76	-	-	-	76	-	76	-
Leu	104	186	104	-	103	-	104	-	104	-	104	-	104	-	104	-	104	-
Phe	107	172	171	*107*	172	*106*	172	*107*	172	-	172	-	172	*107*	172	-	172	-
Thr	31	58	32	-	31	-	31	-	32	-	31	-	31	-	31	-	31	-
allo-Thr	35	46	-	-	-	-	-	-	-	-	-	-	-	-	-	-	-	-

[a]L-Amino acids were derivatized in two ways: 1) with L-FDLA and 2) with D/L-FDLA. The D-FDLA derivatives of L-amino acids are chromatographically equivalent to the L-FDLA derivatives of D-amino acids.
[b]The alternative isomer formed by epimerization during sample preparation, as observed by incorporation of deuterium when the hydrolysis was performed in 6 M DCl.